PROGRESS REPORT TO THE NATIONAL AERONAUTICS

AND SPACE ADMINISTRATION

Research Grant NsG 239-62

August, 1965

Prepared by the
Texas Engineering Experiment Station
Space Technology Division

TEXAS A&M UNIVERSITY 1876

Texas A&M University

College Station, Texas

PROGRESS REPORT TO THE NATIONAL AERONAUTICS
AND SPACE ADMINISTRATION

Research Grant No. NsG 239-62

August, 1965

Report submitted by

ORIGINAL SIGNED BY
H. E. WHITMORE

Harry E. Whitmore
Head, Space Technology Division

Prepared by the

Texas Engineering Experiment Station
Space Technology Division

Texas A&M University
College Station, Texas

Preliminary Every Board of Governors

INDEX

SUMMARY

Research at Texas A&M University under NASA Grant NsG 239-62 now consists of ten major projects which are covered in this report. Of the ten projects, eight were being pursued at the time of the last semi-annual report i.e., Projects 3, 5, 7, 8, 9, 10, 11, and 13. Project 2 concerning a Biological Waste Utilization System was discontinued when it was determined that NASA has no real interest in this area. Project 12 on the Effects of Irradiation on the Heart was also discontinued due to the loss of the principal investigator. Projects 14 and 15 have been originated since the last report.

A supplement to this report, on project #8, is being provided as a separate document. The supplement is on the subject of Linear Elastic Shell Theory and should prove valuable to persons interested in that field.

This report contains only a technical presentation on the various projects. The fiscal report is submitted quarterly on NASA forms 1030 and 1031.

Of interest is the fact that construction is underway on the new Space Research Complex at Texas A&M. The new complex will be completed in the summer of 1966 and will provide approximately 70,000 square feet of space for space research and related activities.

SPACE TECHNOLOGY PROJECT NO. 3

RADIAL HEAT TRANSFER FROM A PLASMA STREAM

N65-33656

RADIAL HEAT TRANSFER FROM A PLASMA STREAM

Project Investigators :

Dr. P. T. Eubank, Department of Chemical Engineering

Mr. J. R. Johnson, Graduate Assistant

This report concerns an experimental heat transfer apparatus previously constructed and calibrated for the calorimetric determination of heat transfer coefficients. Heat from a plasma flame flowing in a circular tube at atmospheric pressure is passed to the inside pipe walls, which are maintained at a low temperature with water as the coolant. The modes of forced convection (h_{cv}), radiation (h_R), and conduction (h_{cD}) have been studied using electrically-generated plasmas of helium, argon, and nitrogen at temperatures to 15,000 °K. Apparatus variables including average plasma temperature ($\overline{T}_p$), the gas used in generation of the plasma, longitudinal distance from the point of plasma generation (L), orifice to tube ratio$_X$ (R_o/R), configuration of the plasma generation section or nozzle, and mass flow rate of the plasma stream (W_p) are known to affect the total heat transfer coefficient (h_T), where

$$h_T = h_{cv} + h_R + h_{cD} \qquad (1)$$

It is estimated that the data has an accuracy of 5%.

Progress to Date

All experimental data for the first stage of this project has been obtained. Approximately seventy experimental runs for each of the three gases have been obtained over variable W_p and power input, which is closely related, of course, to $\overline{T}_p$. Values of the physical parameters--viscosity (μ), thermal conductivity (k), heat capacity (C_p), and free electron density (N_e)--were found in the literature over the temperature range desired. These results are shown in part by Table I where E is the input voltage, I the input amperage, T_w the inner tube wall temperature, T_2 the outlet cooling water temperature, T_1 the inlet cooling water temperature, W the water flow rate, Q the rate of heat transfer per cooling chamber, H_p the inlet average plasma enthalpy to each chamber, $\overline{H}_p$ the average plasma enthalpy for each chamber, $\overline{T}_p$ the corresponding temperature, and h_T the total heat transfer coefficient.

Theory

From Equation (1) and the theory of heat transfer rates by the individual modes, it may be found that

$$h_T = C_1 \; (2R/L)^{C_2} \, \overline{T}_p^{\,C_3} \, W_p^{\,C_4} + \frac{Q' R_p^{\,2}}{2R\overline{T}_p} + \frac{\int_{T_w}^{\overline{T}_p} k\,dt}{(\overline{T}_p - T_w)\; R \,\ln(R/R_p)} \qquad (2)$$

where R is the tube inner radius, C_1, C_2, C_3, C_4 are arbitrary constants, and

$$Q' = 1.4 \times 10^{-34} N_e^{\,2} \left[e^{-\frac{840}{\overline{T}_p}} - e^{-\frac{53,800}{\overline{T}_p}} \right] \quad (3)$$

according to the Kramers model for radiation.

Initially, Equation (3) together with photographs of the plasma flame, Figure 1, were used to predict radiant and conductive heat transfer by a "simple hot core" model. The entire plasma enthalpy was assumed to be contained in the core defined by the photographs. Within the core the temperature profile was assumed to be flat at $\overline{T}_p$.

An improved model for prediction of the temperature in the radial direction at a fixed longitudinal distance has been developed assuming the gas at the hot core interface is at its ionization temperature (T_i). Experimental temperature profiles of Grey[1] have been made dimensionless and similarity assumed with the present work. If, for example, a parabola is indicated, the two constants are adjusted until in agreements with the macroscopic measurements of this work.

The second term on the RHS of Equation (2) is then computed for each differential cylinder or sleeve-like element within the hot core. Similarly, the conduction term is modified and Equation (2) becomes

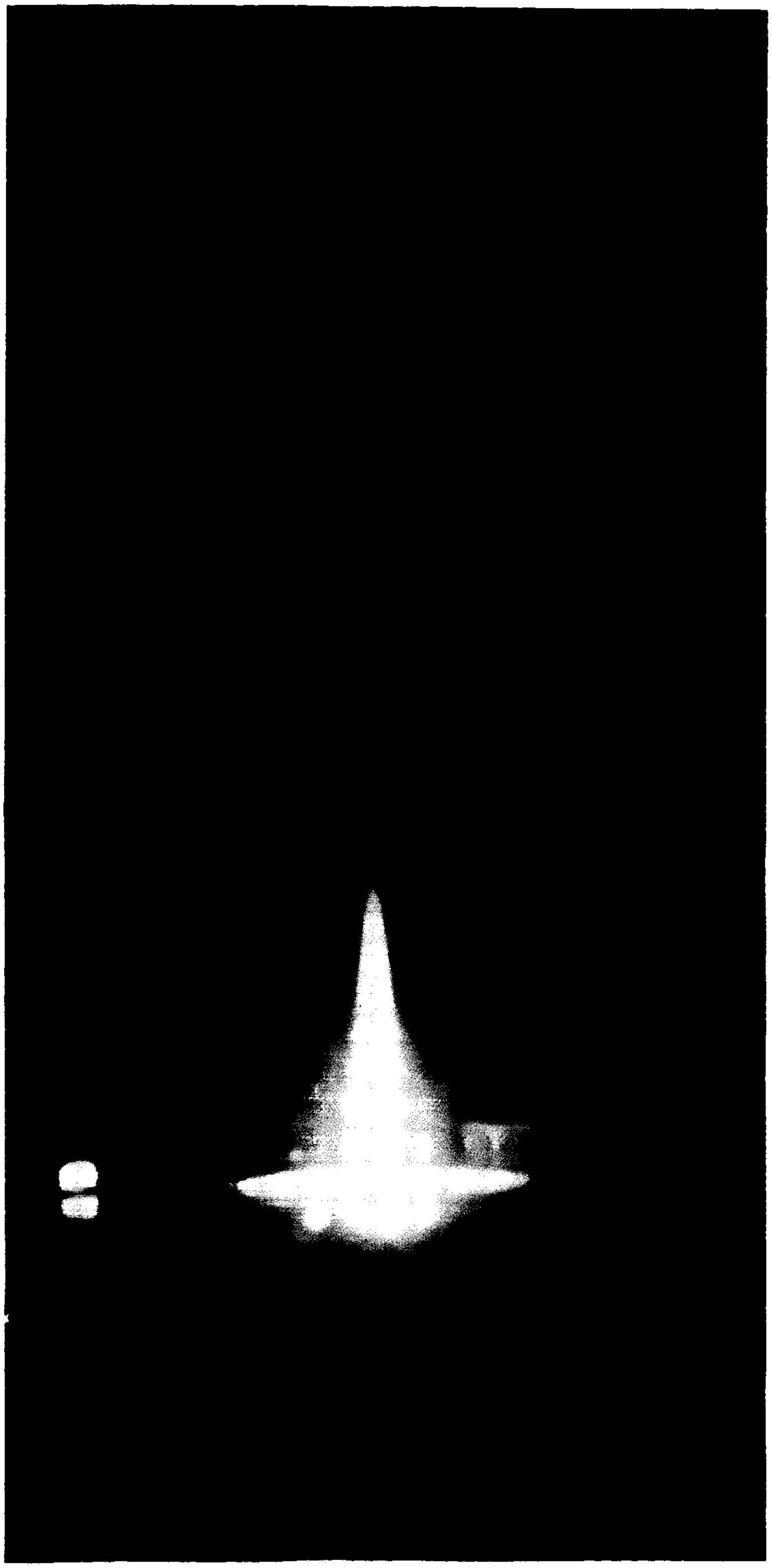

Fig. 1a. Helium

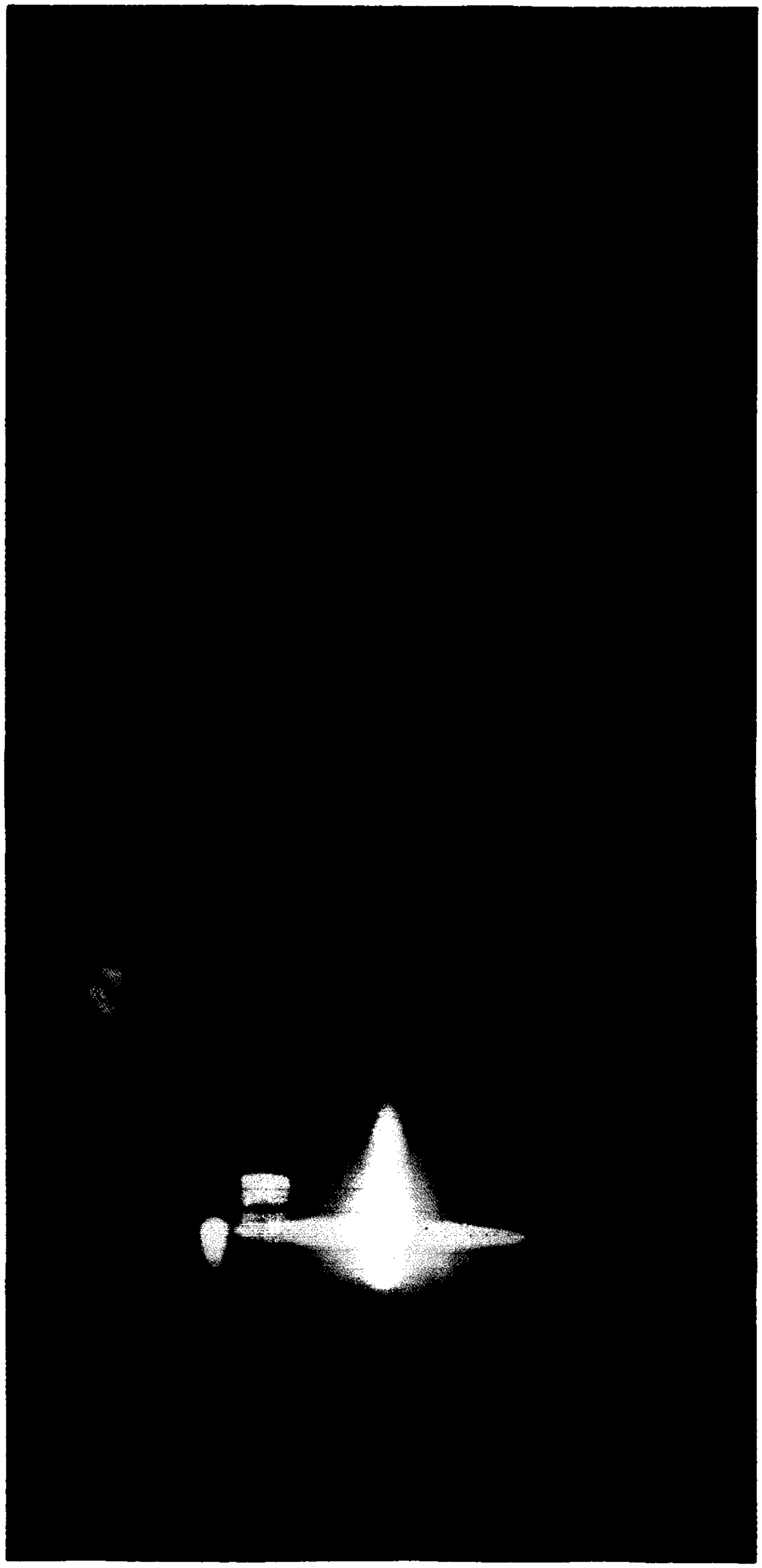

Fig. 1b. Argon

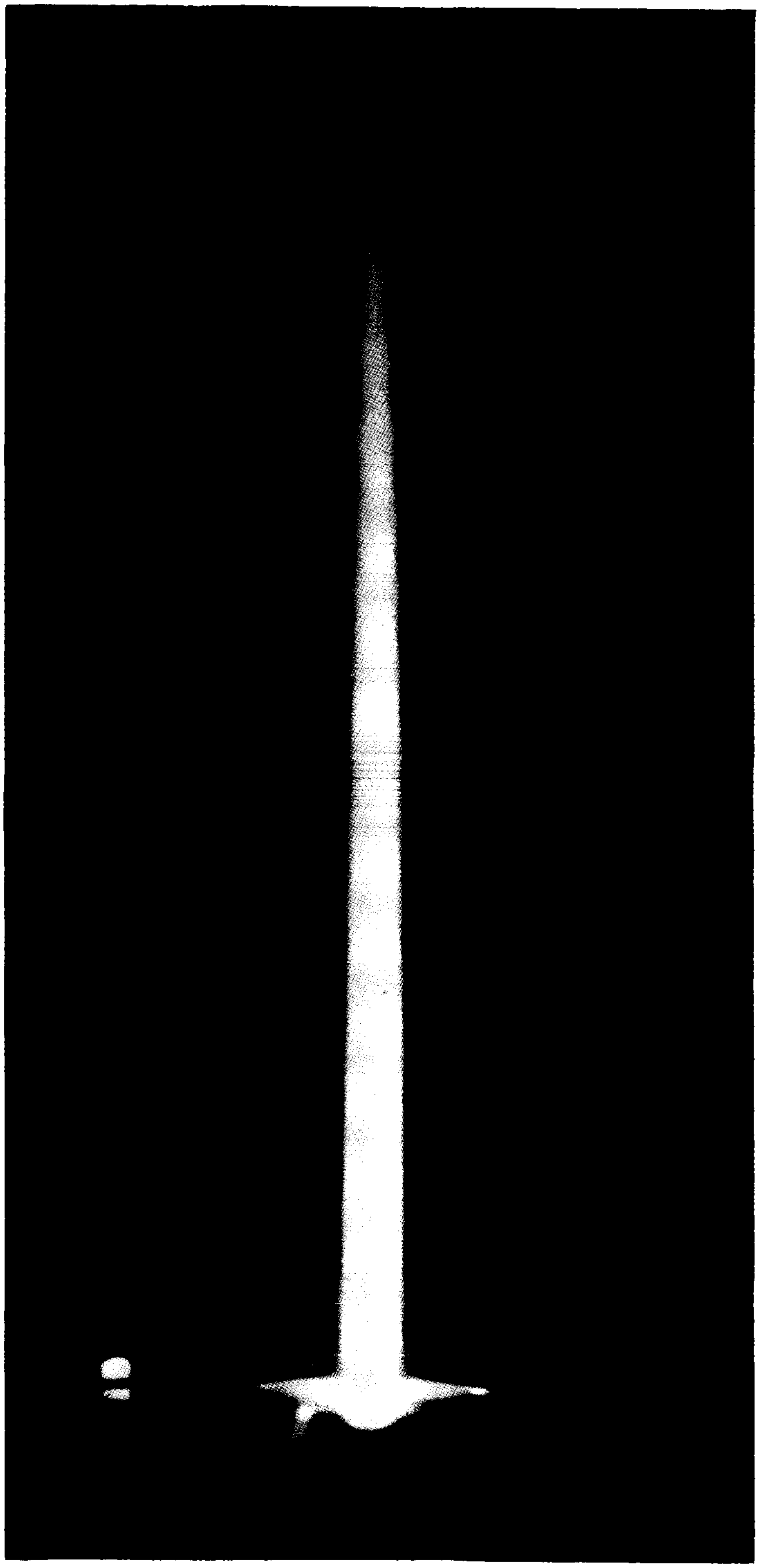

Fig. 1c. Nitrogen

$$h_T = C_1 \ (2R/L)^{C_2} \ \bar{T}_p^{\,C_3} \ W_p^{\,C_4} + \sum_j \frac{Q'_j r_j (\Delta r_j)}{R T_{pj}}$$

$$+ \frac{\int_{T_w}^{T_i} k \, dT}{(T_i - T_w) R \ln \frac{R}{R_p}} \qquad (5)$$

where $Q'_j = 1.4 \times 10^{-34} \ N_{e\,j}^{\,2} \ \left[e^{-(840/T_{pj})} - e^{-(53,800/T_{pj})}\right]$

Conclusions

Analysis of the experimental data with the model presented above results in the following generalizations:

1. Radiation and conduction are not important at the temperature levels investigated, but promise to become so at slightly higher values.

2. The dependence of the forced convection heat transfer coefficient (now equal to h_T) on the average plasma temperature is nil.

3. A clear dependence of the coefficient on W_p, (2R/L), and the gas physical properties is apparent.

---

1 ISA Transactions: 4(102-115) 1965.

Equation (4) may then be simplified for this work to

$$h_T = h_{cv} = C_5 \ (2R/L)^{C_2} \ W_p^{\ C_4} \tag{6}$$

where the constants C_5, C_2, and C_4 are understood to depend on the gas. Correlation of these constants with the experimental results, which is near completion, will terminate the initial phase of this project.

A second phase is planned as the Ph.D. research for Mr. J. R. Johnson. After slight modification of the apparatus and purchase of a much larger generator, similar data will be obtained at temperatures to 100,000°K. Also, studies of energy drain from the plasma by external magnetic fields and the effect on heat transfer rates and control of the plasma stream are planned.

TABLE I

A Sample of Experimental Results

I. Argon	E, Volts	I, Amp.	lb./hr.	Chamber	°F	T_2	T_1	W, lb./hr.	Q Btu./hr.	Hp Btu./lb.	$\overline{Hp}$,	Tp, °F	h_T, Btu./hr.ft^2°F
A. Run 8	21.0	90.0	5.430	1	81.2	77.5	77.0	544.2	272	550	525	4772	2.94
				2	90.8	78.7	77.0	432.6	756	500	431	4010	10.02
				3	88.1	78.2	77.0	450.2	562	362	310	3034	10.36
				4	85.1	77.5	77.0	438.8	219	258	238	2459	5.26
				5	81.0	77.25	77.0	423.5	106	218	208	2215	2.90
				6						198			
B. Run 9:	19.6	87.0	6.118	1	81.0	77.2	77.0	544.2	136	442	431	4009	1.79
				2	90.4	78.5	77.0	432.6	648	420	377	3494	10.09
				3	87.8	78.0	77.0	450.2	450	315	278	2772	9.27
				4	85.0	77.5	77.0	438.8	219	241	223	2322	5.62
				5	80.9	77.0	77.0	423.5	0	205	205	2188	0
				6						205			
C. Run 14:	21.5	154.0	4.117	1	90.6	78.5	76.5	429.9	859	1067	961	8264	5.10
				2	106.0	79.5	76.5	456.2	1370	856	690	6091	11.34
				3	93.5	78.0	76.5	444.3	665	525	444	4107	8.59
				4	87.2	77.0	76.5	424.6	212	364	338	3250	3.60
				5	81.7	77.0	76.5	456.2	218	312	284	2821	4.58
				6						257			
D. Run 20	24.2	185.0	6.136	1	94.9	80.0	77.5	462.5	1158	1176	1081	9234	6.10
				2	121.7	82.0	77.5	450.3	2025	987	821	7151	14.11
				3	108.7	80.5	77.5	447.2	1342	656	545	4946	14.03
				4	99.0	78.5	77.5	441.7	442	435	401	3779	6.28
				5	87.9	78.0	77.5	438.3	219	366	348	3346	3.59
				6						331			

	E	I	Wp	Chamber	Tw	T_2	T_1	W	Q	Hp	$\overline{Hp}$	$\overline{Tp}$	h
E. Run 22:	23.4	197.0	5.991	1	95.4	80.0	77.5	462.5	1158	1282	1185	10,055	5.57
				2	122.4	82.0	77.5	450.3	2025	1088	951	7,921	12.64
				3	109.0	80.5	77.5	447.2	1342	815	670	5,663	12.06
				4	98.9	78.5	77.5	441.7	442	526	489	4,467	5.17
				5	88.1	78.0	77.5	438.3	219	452	434	4,024	2.89
				6						416			
F. Run 23:	22.0	209.0	4.099	1	90.9	80.0	77.5	462.5	1158	1662	1521	11,026	5.05
				2	121.2	82.0	77.5	450.3	2025	1380	1182	8,349	11.94
				3	105.8	80.0	77.5	447.2	1118	885	748	5,704	9.96
				4	96.7	78.5	77.5	441.7	442	612	553	4,392	5.27
				5	86.1	78.0	77.5	438.3	219	505	478	3,836	3.05
				6						451			
II. Helium													
A. Run 9:	37.2	137.0	1.079	1	98.5	74.5	74.5	274.8	0	4130	4130	3,869	0
				2	95.4	75.5	74.5	273.3	273	4130	4005	3,767	3.90
				3	87.9	76.0	74.5	263.6	395	3880	3695	3,517	6.10
				4	85.9	77.0	74.5	261.4	653	3510	3210	3,126	11.60
				5	79.9	77.0	74.5	254.2	635	2910	2615	2,645	13.82
				6						2320			
B. Run 10:	35.0	180.0	1.079	1	105.1	75.0	74.5	272.0	136	5080	5010	4,578	1.55
				2	99.4	75.5	74.5	273.3	273	4940	4820	4,425	3.24
				3	89.8	76.5	74.5	260.6	521	4700	4455	4,129	6.67
				4	87.6	77.5	74.5	250.0	750	4210	3865	3,654	11.05
				5	81.0	78.0	74.5	254.2	890	3520	3110	3,043	16.28
				6						2700			

		E	I	Wp	Chamber	Tw	T_2	T_1	W	Q	Hp	$\overline{Hp}$	$\overline{Tp}$	h
C.	Run 11:	34.7	206.0	0.865	1	83.9	74.7	74.5	269.3	54	4900	4865	4453	0.79
					2	83.5	75.5	74.5	273.3	273	4830	4670	4295	3.34
					3	81.1	75.5	74.5	257.7	258	4510	4360	4048	3.36
					4	80.2	75.5	74.5	244.3	244	4210	4065	3814	3.41
					5	77.9	75.5	74.5	257.2	257	3920	3770	3580	3.87
					6						3620			
D.	Run 12:	35.7	210.0	1.291	1	119.1	75.0	74.5	255.7	128	5800	5755	5178	1.27
					2	114.5	76.5	74.5	270.3	541	5710	5500	4970	5.63
					3	99.7	78.0	74.5	248.8	870	5290	4955	4530	10.04
					4	96.0	80.0	74.5	238.5	1312	4620	4110	3849	18.24
					5	85.1	80.0	74.5	254.2	1399	3600	3060	3004	26.03
					6						2520			
E.	Run 13:	36.5	208.0	1.499	1	124.4	75.5	74.5	253.0	253	5510	5425	4908	2.68
					2	123.4	77.0	74.5	267.4	668	5340	5115	4660	7.51
					3	111.0	79.5	74.5	248.8	1247	4890	4475	4147	15.92
					4	105.8	81.5	74.5	235.7	1650	4060	3515	3370	26.93
					5	89.8	80.0	74.5	245.3	1350	2970	2520	2565	30.65
					6						2070			
F.	Run 15:	37.7	240.0	1.977	1	110.5	77.5	74.5	263.9	791	5450	5250	4769	8.63
					2	124.9	83.0	74.5	270.3	2300	5050	4465	4140	29.59
					3	144.6	87.5	74.5	239.9	3120	3880	3100	3037	58.69
					4	143.2	83.0	74.5	232.8	1982	2320	1816	1999	64.89
					5	110.2	78.75	74.5	248.3	1057	1313	1047	1382	59.54
					6						781			
III. Nitrogen														
A.	Run 5:	65.0	134.0	4.604	1	110.2	84.0	76.0	252.9	2020	3250	3030	9063	10.91
					2	112.5	91.0	76.0	246.6	3700	2810	2405	7869	23.21
					3	135.5	86.0	76.0	230.9	2309	2000	1753	6126	19.11
					4	164.6	81.5	76.0	235.6	1297	1507	1365	4862	14.00
					5	151.0	80.5	76.0	233.3	1050	1223	1109	3991	14.22
					6						996			

SPACE TECHNOLOGY PROJECT NO. 5

COMPUTATIONAL METHODS IN THE SOLUTIONS OF ATOMIC AND SOLID STATE PHYSICS PROBLEMS

N65-33657

COMPUTATIONAL METHODS IN THE SOLUTIONS OF ATOMIC AND SOLID STATE PHYSICS PROBLEMS

Project Investigators

Dr. E. R. Keown, Professor of Mathematics

Mr. D. L. Hardcastle, Graduate Assistant

Mr. D. R. Wiff, Graduate Assistant

I. Introduction

This is a report on the continuation of Project 5, previously entitled "A Mathematical Investigation of the Structure of the Light Metals." The same mathematical techniques are being used with the semi-conducting crystalline solids as were used in investigating the band structures of beryllium. The Augmented Plane Wave technique is now being applied to other solids. First, to crystals with diamond symmetry, and later, it is anticipated, to crystals with zinc-blende symmetry. This report consists of two parts: The first is a discussion of D. R. Wiff on his energy band calculations for germanium and the second is a discussion of D. L. Hardcastle of his calculations on atomic lithium.

Computer runs involved in this research are not included in this report but are available at Texas A&M.

II. Preliminary Energy Bands of Germanium (D.R. WIFF)

This section of the report contains a discussion of the preliminary investigation which will eventually result in theoretical band calculations for Germanium and Silicon crystals. These crystals have a diamond crystalline structure. Also involved are crystals of the zinc-blende type which have diamond-like translational symmetry, but do have the same rotational symmetry as do diamond-like crystals.

III. Details of the Calculation

A successful energy band calculation for Carbon with diamond crystalline structure has been carried out by Dr. E. R. Keown, using the Augmented Plane Wave Method of J. C. Slater by means of a program coded by J. H. Wood with minor revisions by C. Nielson to permit running under Fortran Monitor control. This work has been fully reported in PROGRESS REPORT TO THE NATIONAL AERONAUTICS AND SPACE ADMINISTRATION, August 1964. Due to the success of this calculation by the Augmented Plane Wave Method, an investigation of Germanium was begun. The Germanium crystal was chosen due to the voluminous experimental data available and the lack of a precise theoretical band calculation.

This investigation[#] was begun using the basic crystal potential obtained from the $(1s)^2$ $(2s)^2$ $(2p)^6$ $(3s)^2$ $(3p)^6$ $(3d)^{10}$ $(4s)^2$ $(4p)^2$ configuration of the germanium atom. This potential was calculated by the Herman-Skillman program[1] as modified by L. F. Mattheiss to include superposition of potentials from neighboring sites. The result of this calculation with an average potential of 0.332708

[#] All numerical values are in Atomic Units unless otherwise stated.

between the APW spheres is presented graphically in figure 2, with the notation indicated in figure 1. From physical reasoning and the results of F. Bassani and M. Yoshime[2] in their Orthogonal Plane Wave calculations of germanium, the points 2' and 25' should be reversed. When the average potential between the APW spheres was 1.670000, the points 2' and 25' are in the correct order, but as can be seen in figure 3, the calculations show germanium to be a conductor, not a semiconductor. As a result of this and due to the fact that the potential, which proved successful for carbon, was available, it was decided to scale the carbon potential by the formulas of Herman and Skillman so as to apply to the germanium atom. Having done this one could obtain various potentials to investigate what effect changing the potential would have on the band structure of germanium. This was done using fourteen different potentials none of which gave satisfactory results. A sample of the results is given in figure 4, for an average potential between APW spheres 0.000000. To see how the points 15, 2', and 25' varied with the different potentials used, the reader is referred to figure 5, which was calculated using an average potential between the APW spheres as 0.475000.

IV. Present Research Program

As a result of the calculations for germanium, it was felt that the very small energy gap between the conduction and valence bands

FIRST BRILLOUIN ZONE GERMANIUM

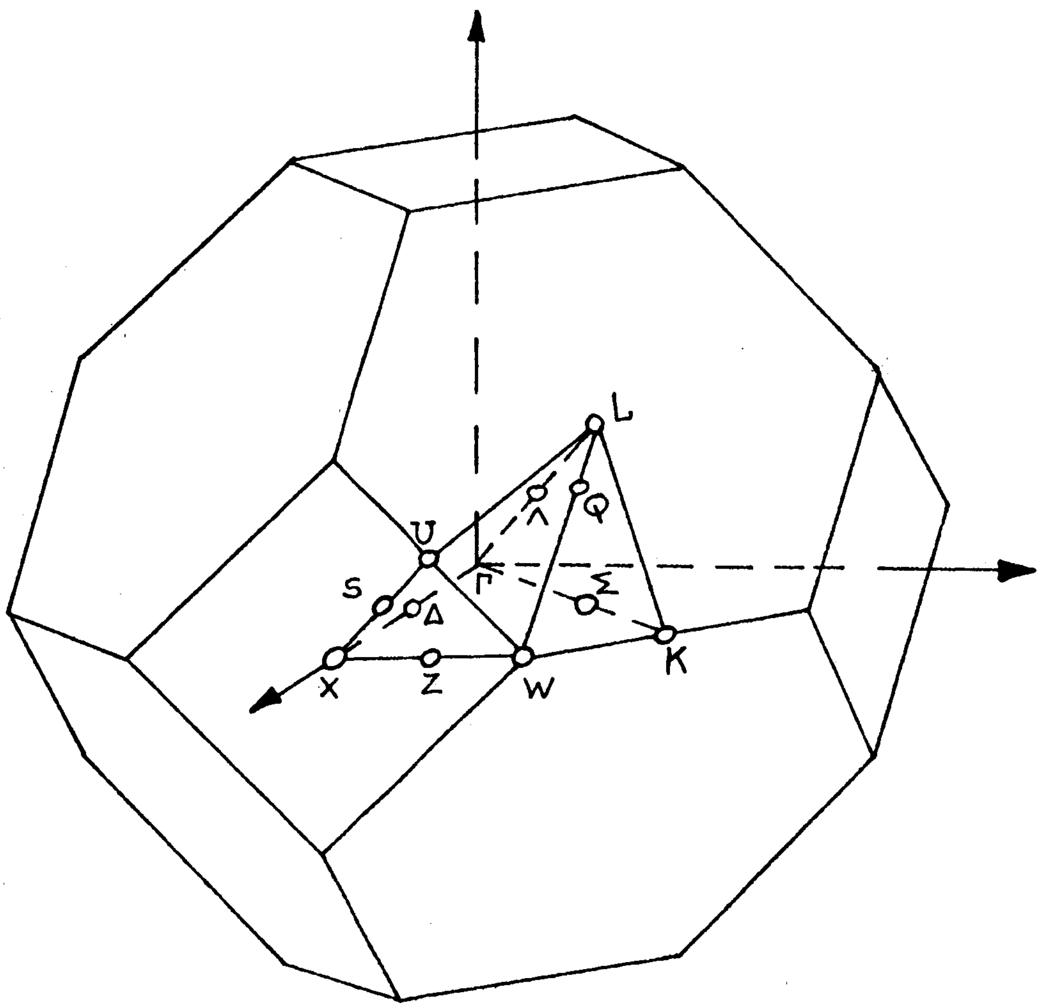

Figure 1.

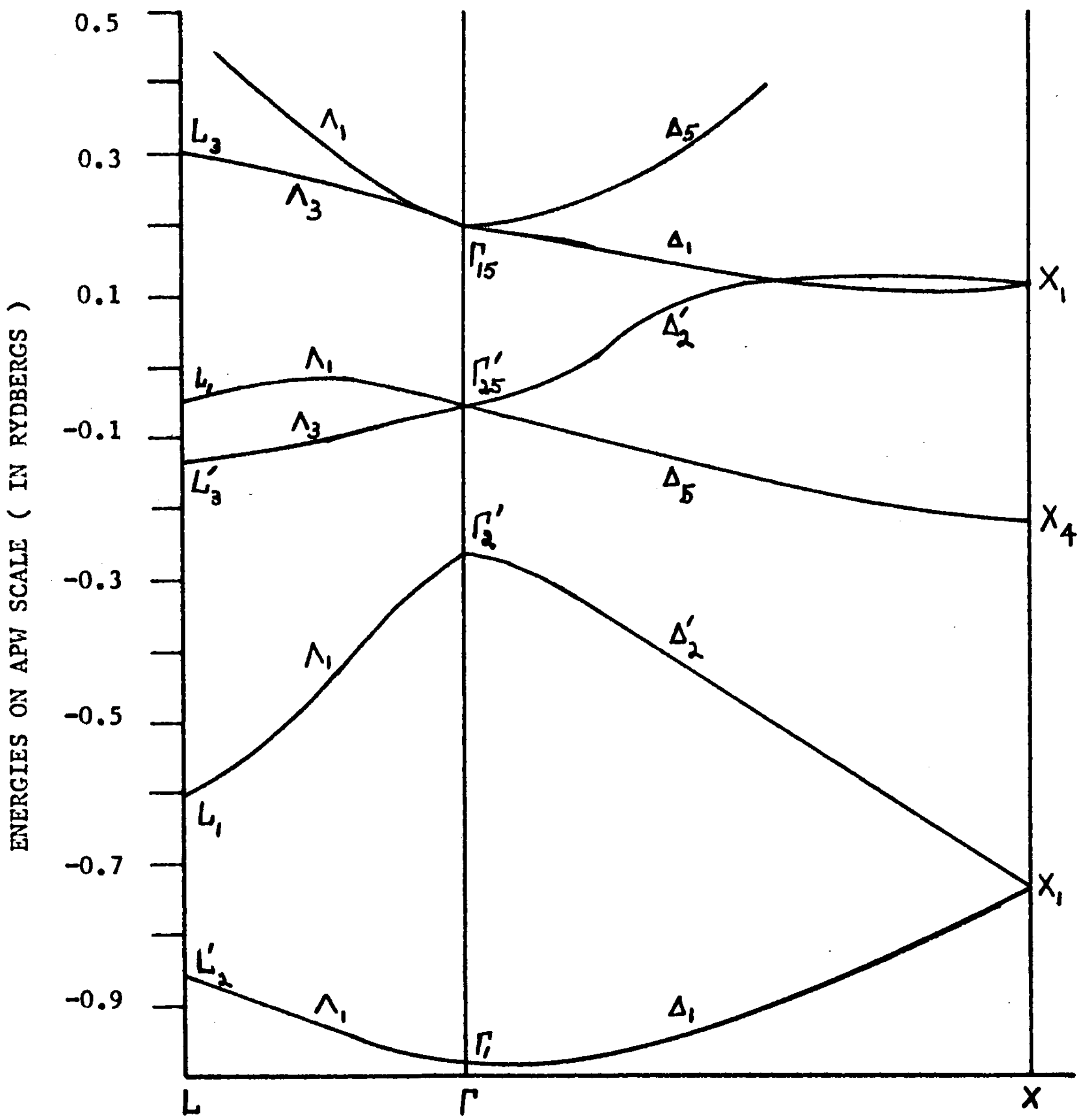
ENERGIES ON APW SCALE (IN RYDBERGS)
0.5
0.3
0.1
-0.1
-0.3
-0.5
-0.7
-0.9
L_3
Λ_1
Λ_3
Δ_5
Γ_{15}
Δ_1
X_1
Δ_2'
L_1
Λ_1
Γ_{25}'
Λ_3
L_3'
Δ_5
X_4
Γ_2'
Λ_1
Δ_2'
L_1
X_1
L_2'
Λ_1
Δ_1
Γ_1
L
Γ
X

Figure 2.

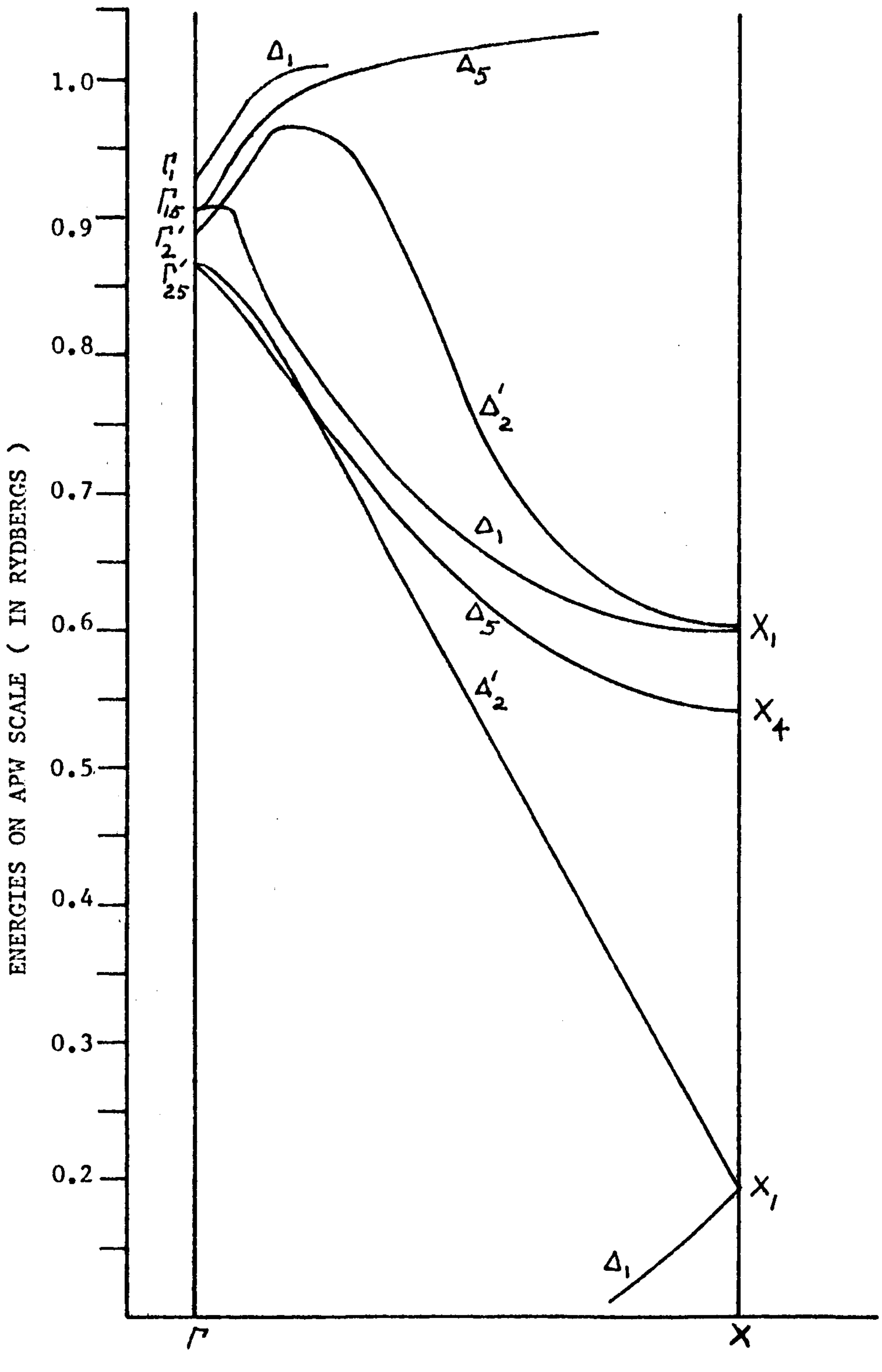
ENERGIES ON APW SCALE (IN RYDBERGS)
1.0
0.9
0.8
0.7
0.6
0.5
0.4
0.3
0.2
Δ1
Δ5
Γ1
Γ15
Γ2'
Γ25'
Δ2'
Δ1
Δ5
Δ2'
X1
X4
X1
Δ1
Γ
X

Figure 3.

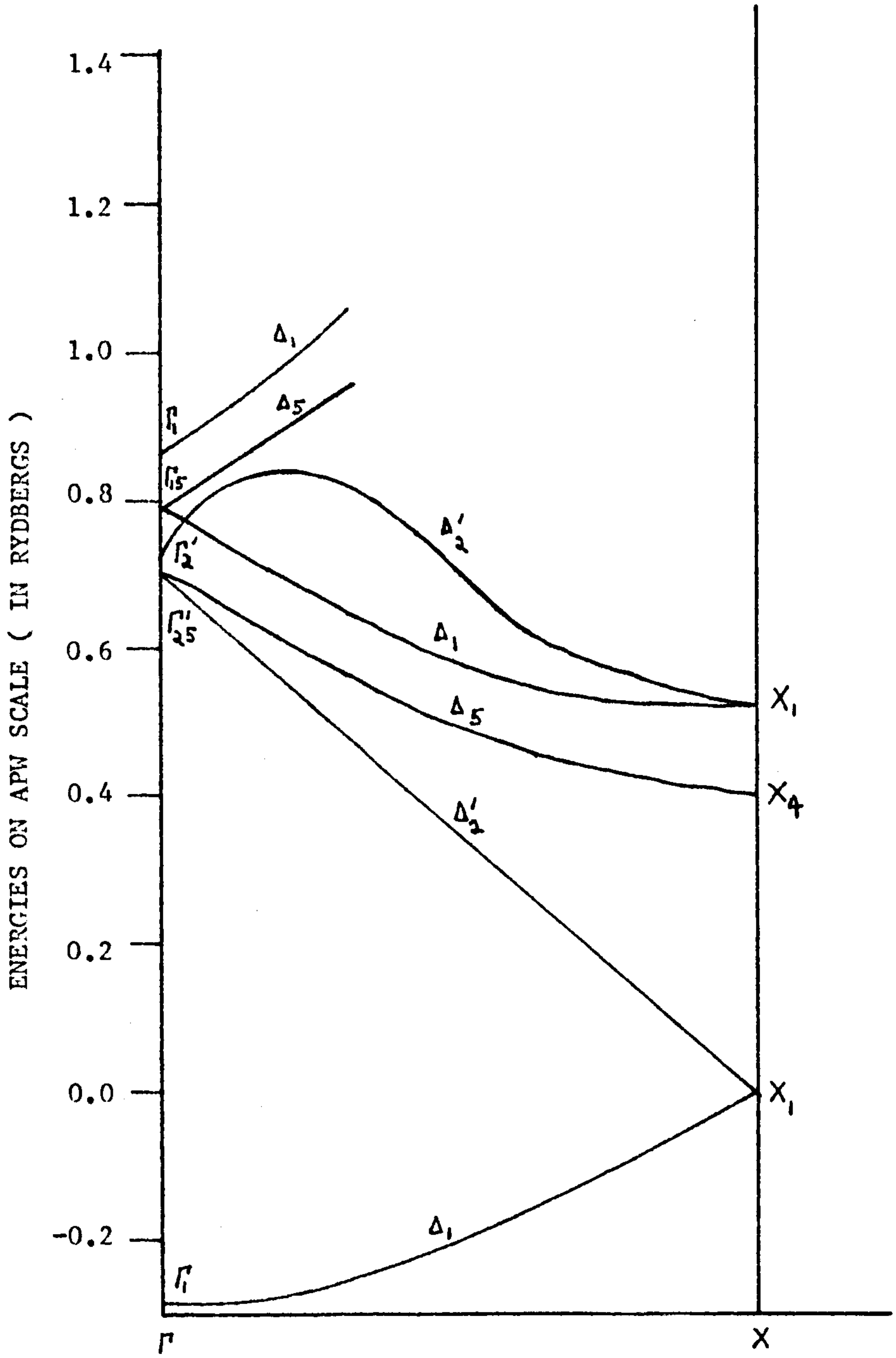

1.4
1.2
1.0
0.8
0.6
0.4
0.2
0.0
-0.2
ENERGIES ON APW SCALE (IN RYDBERGS)
Γ_1
Γ_{15}
Γ_2'
Γ_{25}'
Γ_1
Δ_1
Δ_5
Δ_2'
Δ_1
Δ_5
Δ_2'
Δ_1
X_1
X_4
X_1
Γ
X

Figure 4.

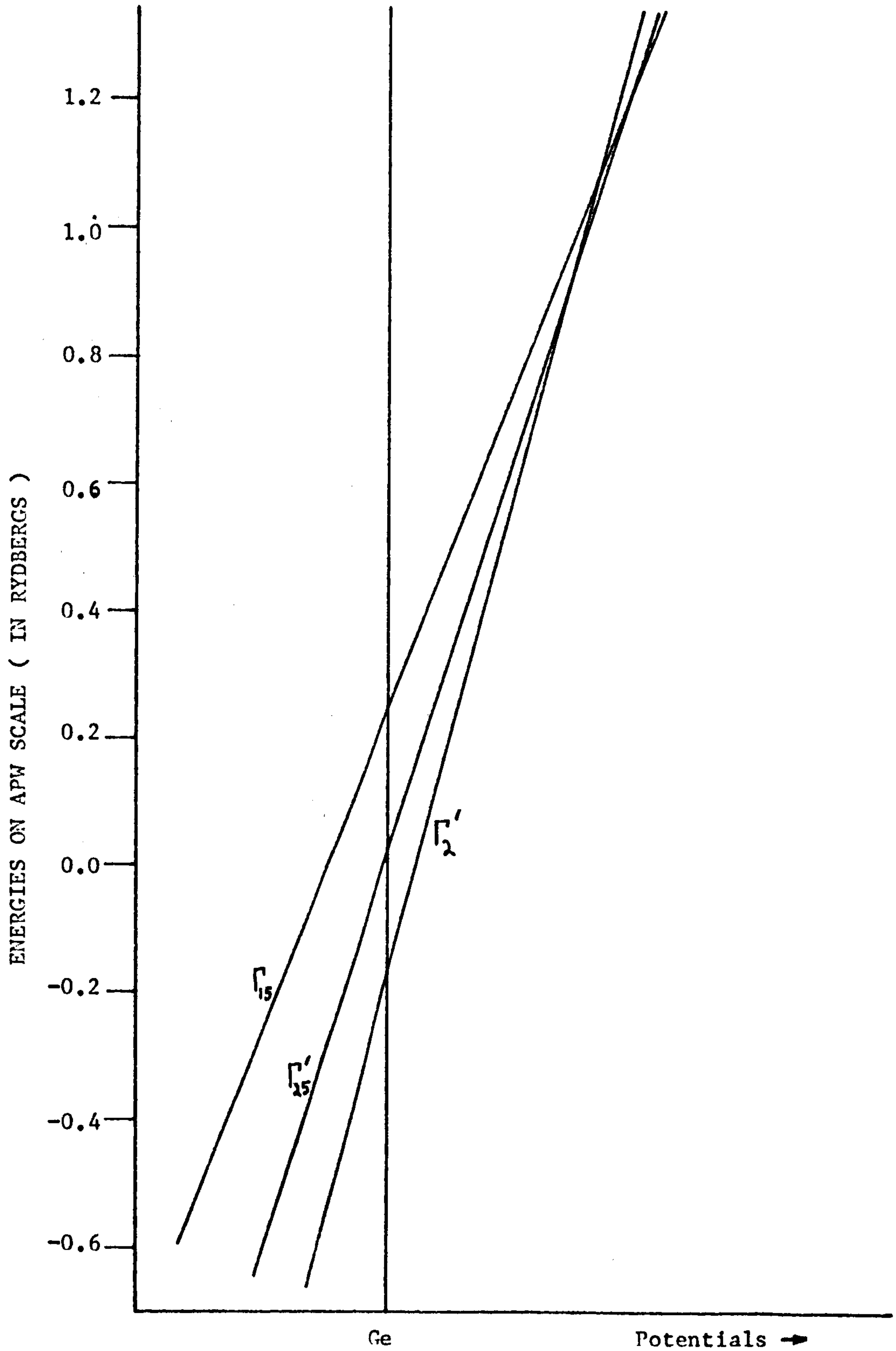

1.2
1.0
0.8
0.6
0.4
0.2
0.0
-0.2
-0.4
-0.6
ENERGIES ON APW SCALE (IN RYDBERGS)
Γ_{15}
Γ_{25}'
Γ_2'
Ge
Potentials

Figure 5.

as a beginning calculation tended to misrepresent the basic reliability of the Augmented Plane Wave Method to be applied to crystals with covalent bonding. Therefore the present research is four fold:

1) The need for a subroutine to calculate more accurately the starting values of the radial wave function, which are put initially into the Augmented Plane Wave program was demanding. The theory for this has been worked out and the subroutine is being coded.

2) Since the energy gap for germanium is 0.74eV and that for Silicon is 1.12eV,[3] new calculations are being started for Silicon because of the larger energy gap. It is hoped that these calculations will agree with experimental results and calculations by other methods.

3) Assuming the affirmative for silicon, calculations for germanium will then be resumed.

4) A thorough study of the Augmented Plane Wave Method theory is being made to convert the existing programs to be able to handle the diamond type lattice when one has two different types of atoms composing the crystal.

REFERENCES

1. F. Herman and S. Skillman, Atomic Structure Calculations, Prentice-Hall, Inc., (1963).
2. F. Bassani and M. Yoshime, Phys. Rev. 130, 20 (1963).
3. F. Seitz and D. Turnbull, Solid State Physics, Vol. 1, Academic Press Inc., (1955).

N65-33658

V. Hyperfine Structure of Lithium (D.L. HARDCASTLE)

Under the supervision of Dr. John L. Gammel, Mr. D. L. Hardcastle has developed the differential equations that are to be solved in carrying out the calculations of the hyperfine structure of lithium.[1] Dr. E. R. Keown has written two subprograms that will be used in the calculations. The first subprogram entitled UNHFE generates an initial set of wave functions that will be used in starting the iterative process by which the differential equations are solved. It is written using the results obtained by Sachs[2] and Roothaan, et. al.[3] The second subprogram entitled COEF calculates all of the coefficients appearing in the differential equation and is now being checked for errors by Mr. Hardcastle. The subprogram to solve the differential equations is now being written by Mr. Hardcastle.

The wave function for the atom is constructed from space and spin parts. The space parts are constructed from three independent functions and the spin parts from the two orthogonal one electron spin functions. The wave function for the atom is then found by mixing the above space and spin parts and requiring it to be antisymmetric in the interchange of any two particle, an eigenfunction of the total spin operator S^2, and an eigenfunction of the z component of the spin S_z. Using the resulting wave function and the variational principle[4] three differential equations are found. By specifying the state of the atom the angular part of the integral may be carried out. For the $1S^2 2S$ state the resulting equations are:

Equation I. $\iint P_2P_3\ (H'-\lambda)\ P\ P_1P_2P_3\ dr\ dr' = 0$

Equation II. $\iint P_1P_3\ (H'-\lambda)\ P\ P_1P_2P_3\ dr\ dr' = 0$

Equation III. $\iint P_1P_2\ (H'-\lambda)\ P\ P_1P_2P_3\ dr\ dr' = 0$

where P is the particle exchange operator

$$P = \left[2 + 2P\ (12) - P\ (13) - P\ (23) - P\ (13)\ P\ (12) - P(23)\ P(12)\right]$$

The integrals have the form

$$(P_i,\ P_j) = \int_0^\infty P_i\ (r)\ P_j\ (r)\ dr$$

$$(P_i,\ hP_j) = \int_0^\infty P_i(r)\ \left(-\frac{n^2}{2m}\frac{d^2}{dr^2} - \frac{3e^2}{r}\right)\ P_j\ (r)\ dr$$

$$(P_i,\ V'_{jk}P_\ell) = \int_0^\infty P_i(r')\ \frac{e^2}{r_>}\ P_j\ (r')\ dr'$$

$$(P_iP_j,\ V'_{k\ell}P_mP_n) = \int_0^\infty \int_0^\infty P_i(r)\ P_j(r')\ \frac{e^2}{r_>}\ P_m(r)\ P_n(r')\ dr\ dr'$$

where $r_>$ is the greater of the two variables and r and r' and where

$$H' = \sum_{i=1}^{3} H'_i + \sum_{i>j}^{3} V'_{ij}$$

$$h_i = H'_i = -\frac{n^2}{2m}\ \frac{d^2}{dr_i^2} - \frac{3e^2}{r_i}$$

and $V'_{ij} = \dfrac{e^2}{r_{>ij}}$.

EQUATION I

$$2h\ P_1\ (P_2,\ P_2)\ (P_3,\ P_3) + 2h\ P_2\ (P_2,\ P_1)\ (P_3,\ P_3)$$
$$-h\ P_3\ (P_2,\ P_2)\ (P_3,\ P_1) - h\ P_1\ (P_2,\ P_3)\ (P_3,\ P_2)$$
$$-h\ P_3\ (P_2,\ P_1)\ (P_3,\ P_2) - h\ P_2\ (P_2,\ P_3)\ (P_3,\ P_1)$$

$$+2\ P_1\ (P_2,\ hp_2)\ (P_3,\ P_3) + 2\ P_2\ (P_2,\ hP_1)\ (P_3,\ P_3)$$
$$-\ P_3\ (P_2,\ hP_2)\ (P_3,\ P_1) - P_1\ (P_2,\ hP_3)\ (P_3,\ P_2)$$
$$-\ P_3\ (P_2,\ hp_1)\ (P_3,\ P_2) - P_2\ (P_2,\ hP_3)\ (P_3,\ P_1)$$

$$+2\ P_1\ (P_2,\ P_2)\ (P_3,\ hP_3) + 2\ P_2\ (P_2,\ P_1)\ (P_3,\ hP_3)$$
$$-\ P_3\ (P_2,\ P_2)\ (P_3,\ hP_1) - P_1\ (P_2,\ P_3)\ (P_3,\ hP_2)$$
$$-\ P_3\ (P_2,\ P_1)\ (P_3,\ hP_2) - P_2\ (P_2,\ P_3)\ (P_3,\ hP_1)$$

$$+2\ P_1\ (P_2,\ V'_{12}\ P_2)\ (P_3,\ P_3) + P_2\ (P_2,\ V'_{12}\ \ P_1)\ (P_3,\ P_3)$$
$$-\ P_3\ (P_2,\ V'_{12}\ P_2)\ (P_3,\ P_1) - P_1\ (P_2,\ V'_{12}\ P_3)\ (P_3,\ P_2)$$
$$-\ P_3\ (P_2,\ V'_{12}\ P_1)\ (P_3,\ P_2) - (P_2,\ V'_{12}\ P_3)\ (P_3,\ P_1)$$

$$+2\ P_1\ (P_2,\ P_2)\ (P_3,\ V'_{13},\ P_3) + 2\ P_2\ (P_2,\ P_1)\ (P_3,\ V'_{13}\ P_3)$$
$$-\ P_3\ (P_2,\ P_2)\ (P_3,\ V'_{13}\ P_1)\ - P_1\ (P_2,\ P_3)\ (P_3,\ V'_{13}\ P_2)$$
$$-\ P_3\ (P_2,\ P_1)\ (P_3,\ V'_{13}\ P_2)\ - P_2\ (P_2,\ P_3)\ (P_3,\ V'_{13}\ P_1)$$

$$+2\ P_1\ (P_2P_3,\ V'_{23}\ P_2P_3) + 2\ P_2\ (P_2P_3,\ V'_{23}\ P_1P_3)$$
$$-\ P_3\ (P_2P_3,\ V'_{23}\ P_2P_1) - P_1\ (P_2P_3,\ V'_{23}\ P_3P_2)$$
$$-\ P_3\ (P_2P_3,\ V'_{23}\ P_1P_2) - P_2\ (P_2P_3,\ V'_{23}\ P_3P_1)$$

EQUATION I CONTINUED

$$= \lambda \Big[2 P_1 (P_2, P_2) (P_3, P_3) + 2 P_2 (P_2, P_1) (P_3, P_3)$$
$$- P_3 (P_2, P_2) (P_3, P_1) - P_1 (P_2, P_3) (P_3, P_2)$$
$$- P_3 (P_2, P_1) (P_3, P_2) - P_2 (P_2, P_3) (P_3, P_1) \Big]$$

EQUATION II

$$2\,(P_1,\ h\,P_1)\,P_2\,(P_3,\ P_3) + (P_1,\ h\,P_2)\,P_1\,(P_3,\ P_3)$$
$$-\,(P_1,\ h\,P_3)\,P_2\,(P_3,\ P_1) - (P_1,\ h\,P_1)\,P_3\,(P_3,\ P_2)$$
$$-\,(P_1,\ h\,P_2)\,P_3\,(P_3,\ P_1) - (P_1,\ h\,P_3)\,P_1\,(P_3,\ P_2)$$

$$+2\,(P_1,\ P_1)\,hP_2\,(P_3,\ P_3) +2\,(P_1,\ P_2)\,h\,P_1\,(P_3,\ P_3)$$
$$-\,(P_1,\ P_3)\,hP_2\,(P_3,\ P_1) - (P_1,\ P_1)\,h\,P_3\,(P_3,\ P_2)$$
$$-\,(P_1,\ P_2)\,hP_3\,(P_3,\ P_1) - (P_1,\ P_3)\,h\,P_1\,(P_3,\ P_2)$$

$$+2\,(P_1,\ P_1)\,P_2\,(P_3,\ h\,P_3) + 2\,(P_1,\ P_2)\,P_1\,(P_3,\ h\,P_3)$$
$$-\,(P_1,\ P_3)\,P_2\,(P_3,\ h\,P_1) - (P_1,\ P_1)\,P_3\,(P_3,\ h\,P_2)$$
$$-\,(P_1,\ P_2)\,P_3\,(P_3,\ h\,P_1) - (P_1,\ P_3)\,P_1\,(P_3,\ h\,P_2)$$

$$+2\,(P_1,\ V_{12}'\,P_1)\,P_2\,(P_3,\ P_3) +2\,(P_1,\ V_{12}'\,P_2)\,P_1\,(P_3,\ P_3)$$
$$-\,(P_1,\ V_{12}'\,P_3)\,P_2\,(P_3,\ P_1) - (P_1,\ V_{12}'\,P_1)\,P_3\,(P_3,\ P_2)$$
$$-\,(P_1,\ V_{12}'\,P_2)\,P_3\,(P_3,\ P_1) - (P_1,\ V_{12}'\,P_3)\,P_1\,(P_3,\ P_2)$$

$$+2\,P_2^{\,2}\,(P_1P_3,\ V_{13}'\,P_1P_3) +2\,P_1^{\,2}\,(P_1P_3,\ V_{13}'\,P_2P_3)$$
$$-P_2^{\,2}\,(P_1P_3,\ V_{13}'\,P_3P_1) - P_3^{\,2}\,(P_1P_3,\ V_{13}'\,P_1P_2)$$
$$-P_3^{\,2}\,(P_1P_3,\ V_{13}'\,P_2P_1) - P_1^{\,2}\,(P_1P_3,\ V_{13}'\,P_3P_2)$$

$$+2\,(P_1,\ P_1)\,P_2\,(P_3,\ V_2{}'_3\,P_3) +2\,(P_1,\ P_2)\,P_1\,(P_3,\ V_2{}'_3\,P_3)$$
$$-\,(P_1,\ P_3)\,P_2\,(P_3,\ V_2{}'_3\,P_1) - (P_1,\ P_1)\,P_3\,(P_3,\ V_2{}'_3\,P_2)$$
$$-\,(P_1,\ P_2)\,P_3\,(P_3,\ V_2{}'_3\,P_1) - (P_1,\ P_3)\,P_1\,(P_3,\ V_2{}'_3\,P_2)$$

EQUATION II CONTINUED

$$
\begin{aligned}
= \lambda \Big[& 2\,(P_1, P_1)\, P_2\, (P_3, P_3) + 2\,(P_1, P_2)\, P_1\, (P_3, P_3) \\
- & (P_1, P_3)\, P_2\, (P_3, P_1) - (P_1, P_1)\, P_3\, (P_3, P_2) \\
- & (P_1, P_2)\, P_3\, (P_3, P_1) - (P_1, P_3)\, P_1\, (P_3, P_2) \Big]
\end{aligned}
$$

EQUATION III

$$2\,(P_1, hP_1)\,(P_2, P_2)\,P_3 + 2\,(P_1, hP_2)\,(P_2, P_1)\,P_3$$
$$-\,(P_1, hP_3)\,(P_2, P_2)\,P_1 - (P_1, hP_1)\,(P_2, P_3)\,P_2$$
$$-\,(P_1, hP_3)\,(P_2, P_1)\,P_2 - (P_1, hP_2)\,(P_2, P_3)\,P_1$$

$$+2\,(P_1, P_1)\,(P_2, hP_2)\,P_3 + 2\,(P_1, P_2)\,(P_2, hP_1)\,P_3$$
$$-\,(P_1, P_3)\,(P_2, hP_2)\,P_1 - (P_1, P_1)\,(P_2, hP_3)\,P_2$$
$$-\,(P_1, P_3)\,(P_2, hP_1)\,P_2 - (P_1, P_2)\,(P_2, hP_3)\,P_1$$

$$+2\,(P_1, P_1)\,(P_2, P_2)\,h\,P_3 + 2\,(P_1, P_2)\,(P_2, P_1)\,h\,P_3$$
$$-\,(P_1, P_3)\,(P_2, P_2)\,h\,P_1 - (P_1, P_1)\,(P_2, P_3)\,h\,P_2$$
$$-\,(P_1, P_3)\,(P_2, P_1)\,h\,P_2 - (P_1, P_2)\,(P_2, P_3)\,h\,P_1$$

$$+2\,(P_1P_2, V'_{12}\,P_1P_2)\,P_3 + 2\,(P_1P_2, V'_{12}\,P_2P_1)\,P_3$$
$$-\,(P_1P_2, V'_{12}\,P_3P_2)\,P_1 - (P_1P_2, V'_{12}\,P_1P_3)\,P_2$$
$$-\,(P_1P_2, V'_{12}\,P_3P_1)\,P_2 - (P_1P_2, V'_{12}\,P_2P_3)\,P_1$$

$$+2\,(P_1, V'_{13}\,P_1)\,(P_2, P_2)\,P_3 + 2\,(P_1, V'_{13}\,P_2)\,(P_2, P_1)\,P_3$$
$$-\,(P_1, V'_{13}\,P_3)\,(P_2, P_2)\,P_1 - (P_1, V'_{13}\,P_1)\,(P_2, P_3)\,P_2$$
$$-\,(P_1, V'_{13}\,P_3)\,(P_2, P_1)\,P_2 - (P_1, V'_{13}\,P_2)\,(P_2, P_3)\,P_1$$

$$+2\,(P_1, P_1)\,(P_2, V'_{23}\,P_2)\,P_3 + 2\,(P_1, P_2)\,(P_2, V'_{23}\,P_1)\,P_3$$
$$-\,(P_1, P_3)\,(P_2, V'_{23}\,P_2)\,P_1 - (P_1, P_1)\,(P_2, V'_{23}\,P_3)\,P_2$$
$$-\,(P_1, P_3)\,(P_2, V'_{23}\,P_1)\,P_2 - (P_1, P_2)\,(P_2, V'_{23}\,P_3)\,P_1$$

EQUATION III CONTINUED

$$= \lambda \Big[2 \, (P_1, P_1)(P_2, P_2) P_3 + 2 \, (P_1, P_2)(P_2, P_1) P_3$$
$$- (P_1, P_3)(P_2, P_2) P_1 - (P_1, P_1)(P_2, P_3) P_2$$
$$- (P_1, P_3)(P_2, P_1) P_2 - (P_1, P_2)(P_2, P_3) P_1 \Big]$$

BIBLIOGRAPHY

1. Progress Report to the National Aeronautics and Space Administration, Texas A&M University, February 1965.
2. L. M. Sachs, Phys. Rev. 117, 1505 (1960).
3. C. C. J. Roothaan, L. M. Sachs and A. W. Weiss, Rev. Modern Phys. 32, 186 (1960).
4. L. I. Schiff, Quantum Mechanics, 2d ed., p. 171 (McGraw-Hill New York, 1955).

SPACE TECHNOLOGY PROJECT # 7

COSMIC RAY MUONS

COSMIC RAY MUONS

Project Investigators

Dr. N. M. Duller, Principal Investigator, Associate Professor of Physics

Mr. K. W. Bull, Graduate Research Assistant

Mr. W. G. Cantrell, Graduate Research Assistant

Mr. A. V. Jelinek, Graduate Research Assistant

Mr. J. R. Sharber, Graduate Research Assistant

Mr. E. L. Walker, Graduate Research Assistant

Mr. J. D. Winningham, Graduate Research Assistant

I. Review of the Work of the Past Period

Reliable and easily operated muon detectors of high efficiency have now been developed and are now being assembled in large arrays for intensity measurements.

The large flow-type Geiger counters described in the preceding progress report have proved especially useful. They are being arranged as primary trigger and coincidence detectors for the large spark chambers being set up in conjunction with the solid-iron magnet spectrometer previously described. During the past period Mr. K. W. Bull completed his Master's thesis on the development and characteristics of the large flow counters.

A notable advance in the spark chamber work has been the development of large-gap (interelectrode) chambers and a modified

Marx impulse generator* to provide the high-voltage pulses required for efficient operation of the chambers. An example of a five-stage Marx generator built in this laboratory and used to power several large-gap chambers is shown in Figure 1. A typical picture of a muon track in a three-inch double-gap modular spark chamber is shown in Figure 2. The gases tried and found to be successful for even fairly large-angle traversal of the muon tracks are commercial helium-isobutane mixtures and pure argon. Both of these are routinely available and inexpensive. Using the full capability of the five-stage generator shown in Figure 1, 100-kilovolt pulses have been applied to chambers with six-inch gaps. Essentially perfect track forming efficiencies are obtained even for simultaneous multiple tracks.

One complete "H-frame" solid-iron magnet is now assembled with coils. Measurements of the internal magnetic fields and tests of uniformity under saturated conditions are now being made. A photograph of the separate iron components of the magnet are shown before final installation of the coils in Figure 3.

The Cerenkov detector described in a previous report is being modified to bring the efficiency up from about 75% for fast muons so as to make the instrument more directly useful as an energy-biased detector for fast particles. Design objectives include higher total

---

* (see J. D. Craggs and J. M. Meek, High Voltage Laboratory Technique, Butterworths, London, 1954, p. 116.)

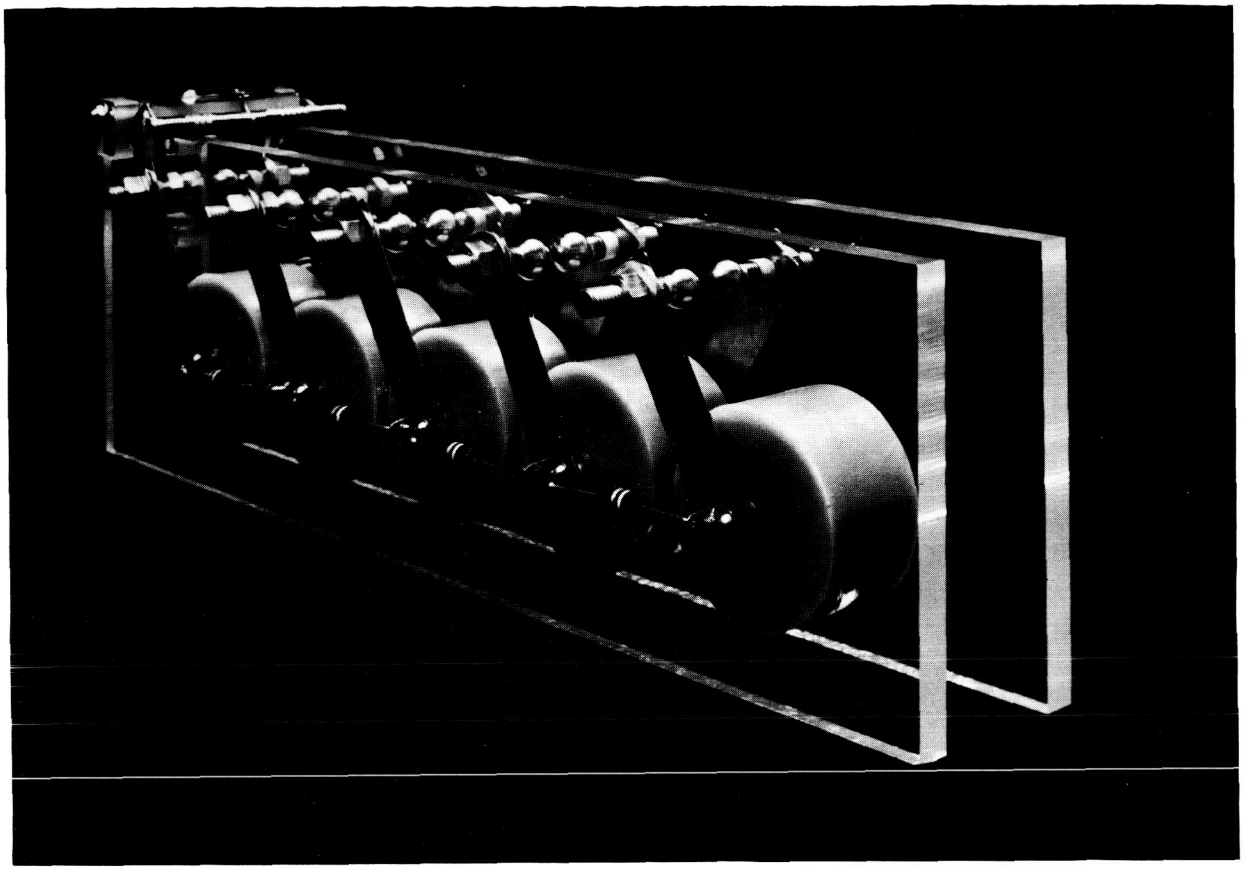

Figure 1. A five-stage modified Marx generator capable of providing randomly triggered 100-kilovolt pulses for actuating the large-gap spark chambers. The cylinders mounted within the Plexiglas frame are potted 30-kilovolt low-inductance capacitors of the "doorknob" type and are 2 ½" in diameter. Five spark gaps are clearly visible; these effectively short circuit when fired and connect the capacitors in series for the total output.

Figure 2. A typical muon track at an oblique angle in a three-inch-gap spark chamber module.

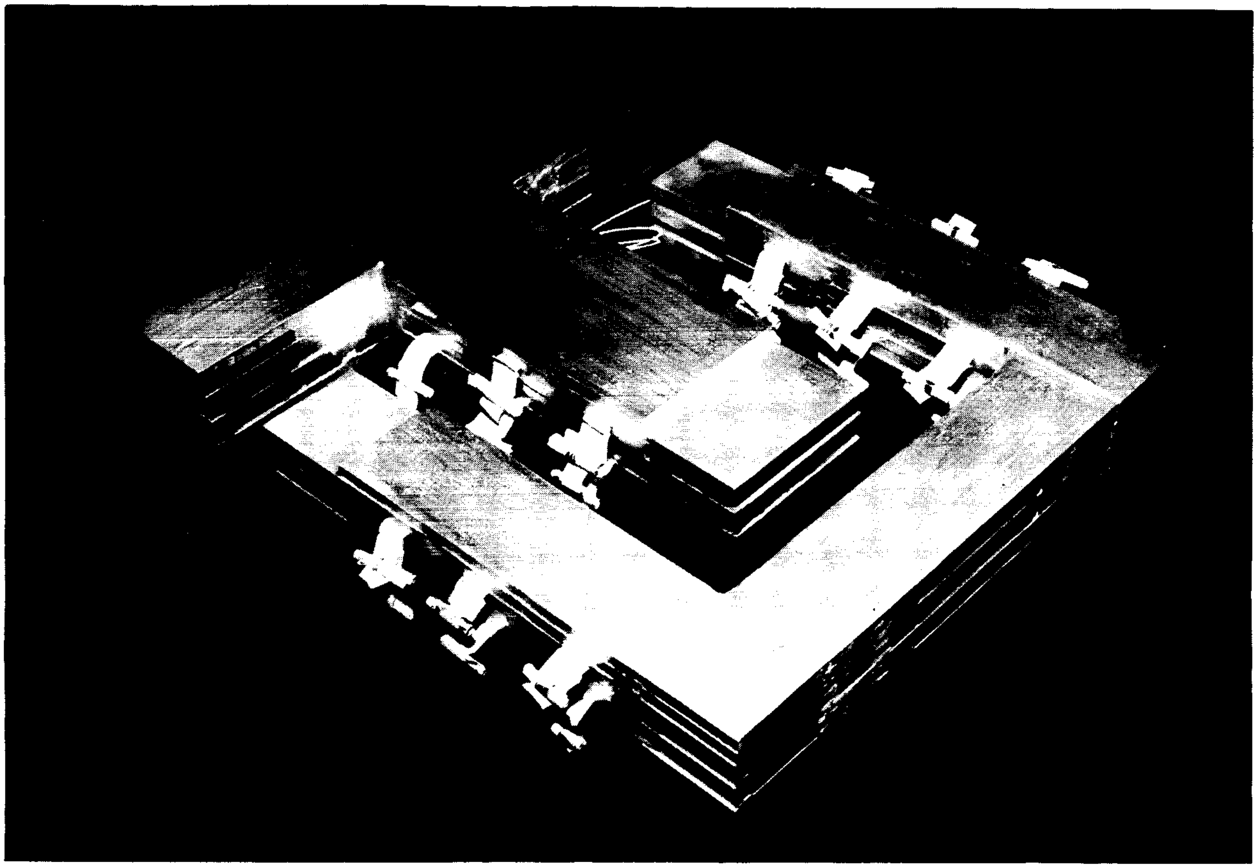

Figure 3. The separate iron components of the H-frame solid-iron magnet before assembly with coils. The coils slide onto the vertical arms of the "U" part of the magnet; the laminations of the "T" and "U" parts are then forced gently together. The "curlers" support and protect loop wires which have been inserted between laminations for magnetic tests and measurements.

gain in the photomultiplier channels and more accurately controlled delays in each light detector channel. It is hoped that this detector will be put into use with large concrete absorbers as energy discriminators in an experiment entirely separate from the magnetic spectrometer work.

Measurements of intensities will be in progress during the next period.

SPACE TECHNOLOGY PROJECT NO. 8

SPACE STRUCTURES

SPACE STRUCTURES

Project Investigators

Principal Investigator:

Dr. Charles H. Samson, Jr., Professor and Head, Department of Civil Engineering

Shell Research:

Dr. Thomas J. Kozik, Associate Professor of Mechanical Engineering

Dr. Harry J. Sweet, Assistant Professor of Aerospace Engineering and of Civil Engineering

Mr. Danny R. Tidwell, Assistant Professor of Aerospace Engineering and of Civil Engineering

Impact Attenuation Research:

Dr. William B. Ledbetter, Assistant Professor of Civil Engineering and of Aerospace Engineering

Mr. V. O. Bennett, Graduate Research Assistant

Mr. B. R. Smith, Graduate Research Assistant

Mr. P. A. Gibson, Graduate Research Assistant

1. This project is concerned with two areas of research:

    1. Behavior of Isotropic and Anisotropic Shells

    2. Impact Attenuation Devices

The objectives of the shell research are specified in five phases as follows:

a. Development of a general set of thin shell equations for an orthotropic material.

b. Development of a general set of equations for a material exhibiting plane anisotropy.

c. Development of a general set of equations for a shell exhibiting plane anisotropy whereby the elastic constants do not exhibit diagonal symmetry.

d. Development of a general structural analysis of thin shells using the finite-element approach.

e. Limited testing of the various structurally anisotropic materials when applied to different shell configurations to determine the degree of compliance between theory and test.

The impact attenuation research has involved the development and evaluation of various energy absorption devices which rely on the failure of a structural member as the energy absorption medium.

This report covers the work accomplished from January, 1965 through July, 1965.

II. Progress on Shell Research

Part (a) has been completed and was included in the August, 1964 progress report. Part (b) is complete and a final report on this portion is included in this progress report (see Enclosure 1). Work on part (c) has continued. Work has just begun on part (d).

During the reporting period, Dr. Kozik wrote a rather detailed paper covering the fundamentals of thin shell theory. This work will be provided as a supplement to this report.

III. Progress on Impact Attenuation Research

An experimental program has been formulated and research is underway to determine the dynamic impact attenuation of selected frangible aluminum tubes through the use of the Texas A&M Structural Research drop-test facility (see July, 1964 progress report for details of this facility).

The drop test facility was further modified to yield more nearly reproducible impact loadings. The instrumentation necessary to record the dynamic loads and tube deformations has been developed.

As of the writing of this progress report the following variables are being investigated:

a. Die machining tolerances (two)

b. Tube geometry (four)

c. Type of test (one static and one dynamic)

Typical results being obtained, together with the description of the test variables and parameters, are described in greater detail in Enclosure 2. It is emphasized that the results reported are progress results and premature conclusions should not be drawn.

N65-33659

A GENERAL THEORY OF THIN ELASTIC SHELLS OF PLANE ANISOTROPIC MATERIALS*

By

HARRY J. SWEET

DEPARTMENT OF AEROSPACE ENGINEERING

TEXAS A&M UNIVERSITY

* The material presented here was extracted from a dissertation having the above title which was submitted by the author in partial fulfillment of the requirements for the degree of Doctor of Philosophy at Texas A&M University.

ENCLOSURE 1

NOMENCLATURE

A, B	Lamè parameters of shell middle surface
a_{ij}	Elastic constants
E	Young's modulus
e_1, e_2	Normal strains of the shell middle surface in the directions of tangents to the principal curvilinear coordinate lines
e_{12}	Shearing strain at the middle surface
e_α, e_β, e_γ	Normal strains of an equidistant surface element in directions tangent and normal to that surface
$e_{\alpha\beta}$	Shearing strain at an equidistant surface
H	Average value of the middle surface curvatures
K	Product of the middle surface curvatures
k_i	Middle surface curvature changes
k_1, k_2	Principal middle surface curvatures
L	Half the difference of the middle surface curvatures
U, V, W	Middle surface displacement components
U_α, U_β, U_γ	Displacement components of a point off the middle surface
X, Y, Z	Body force components
α, β	Principal coordinate lines on the shell middle surface
γ	Coordinate normal to the shell middle surface
Δ	Volume dilitation
δ	Shell thickness
τ_α, τ_β, $\tau_{\alpha\gamma}$ $\tau_{\beta\gamma}$, $\tau_{\alpha\gamma}'$, $\tau_{\beta\gamma}'$	Plane-anisotropic material constants

$\mu_\alpha, \mu_\beta, \mu_{\alpha\beta}$	Plane-anisotropic material constants
ν	Poisson's ratio
$\sigma_\alpha, \sigma_\beta, \sigma_\gamma$	Normal stresses
$\sigma_{\alpha\beta}$	Shear stress
$\varkappa$	Rotation of an element lying on an equidistant surface

A GENERAL THEORY OF THIN ELASTIC SHELLS OF PLANE ANISOTROPIC MATERIALS

Harry J. Sweet[2]

ABSTRACT

This paper is concerned with the development of general thin shell equations for plane anisotropic materials. The equations are derived and presented in terms of the three components of the middle surface displacement of the shell.

A complete set of equations is given for the determination of the solution to the shell problem for any shell shape.

I. Definitions and Assumptions

A shell can be defined as a body bounded by two curved surfaces, the distance between the surfaces being small in comparison with the other dimensions. The curved surface which lies at equal distances from these two surfaces at all points is defined as the middle surface. The thickness of the shell is defined as the length of a normal to the middle surface intercepted by the shell surfaces.

---

[1] The work here reported was done under NASA research grant NsG 239-62

[2] Assistant Professor of Aerospace Engineering, Texas A&M University, College Station, Texas.

Shells are normally classified according to their thickness, their material properties, and the relative magnitudes of the deflections. The material properties determine the degree of anisotropy and whether the material behaves elastically or plastically. This paper is concerned with thin elastic shells of plane anisotropic materials which undergo small displacements.

The derivation is based on a modified form of the Kirchoff-Love hypotheses. These hypotheses are normally stated in the following manner:

(a) Straight fibers which are perpendicular to the middle surface before deformation remain so after deformation and do not change their length.

(b) The normal stresses acting on planes parallel to the middle surface may be neglected in comparison with the other stresses.

These assumptions are generalizations of the basic assumptions used in deriving the beam bending formula and are subject to the same types of inaccuracies and limitations. With this approach, it is not possible to take into account the effects of transverse shearing stresses on deflections and the results will not apply to shells in the neighborhood of highly concentrated normal loads. Fortunately, there are a large number of practical problems where the inherent inaccuracies of the Kirchoff-Love hypotheses are negligible. In general, the inaccuracies can be expected to be of order δ k, where δ is the thickness and k is a middle surface curvature.

There is an obvious contradiction in the Kirchoff hypotheses because of the fact that a state of plane strain is specified in part (a) while a state of plane stress is specified in part (b). Actually the specification of plane stress is an assumption, while the specification of plane strain is an approximation that is generally completely justified unless the equilibrium equations in terms of displacements are obtained by the application of the generalized Hooke's law. To avoid contradictions, the work that follows is based on the assumptions that straight fibers that are perpendicular to the middle surface before deformation will remain so after deformation and that normal stresses acting on planes parallel to the middle surface are negligible. No restrictions are placed on the stretching of the normal fibers and, as a matter of fact, the equations which describe this stretching are developed.

It is also assumed that the tangential displacement components have a negligible effect on curvature changes and twist. It has been found that, for isotropic shells, this assumption limits the application of the resulting equations to cases in which the maximum stresses due to bending are of the same or greater magnitude than those due to stretching of the middle surface.

II. Fundamental Relationships

A. Curvilinear Coordinates

Any space surface can be represented in terms of two parameters, α and β, such that

$$x = x(\alpha, \beta)$$

$$y = y(\alpha, \beta)$$

$$z = z(\alpha, \beta)$$

where x, y, and z are the cartesian coordinates of some point on the surface. These parameters form a set of coordinate lines on the surface and are called the curvilinear coordinates of the surface.

An infinite number of curvilinear coordinates can be drawn for any given surface. It does not follow, however, that all the possible sets are equally convenient. If the principal curvilinear coordinates are used, certain simplifications result which are not possible for other sets of coordinates. Also, since lines of principal curvature are orthogonal, the principal curvilinear coordinates are also orthogonal.

A line segment of length ds lying on a surface can be expressed in terms of components in the principal coordinate directions as

$$ds^2 = A^2 d\alpha^2 + B^2 d\beta^2 \qquad (1)$$

where the coefficients A and B are the lamè parameters or scale factors. For the special case where the length ds coincides with an α coordinate curve, the length is given by

$$ds = A d\alpha \qquad (2)$$

while if it coincides with the β coordinate curve, it is given by

$$ds = B d\beta \qquad (3)$$

The two previous equations can be taken as the definitions of the coefficients A and B.

Letting k_1 and k_2 represent the respective curvatures of the surface in the α and β directions, the relation between the Lamè parameters and the curvatures must satisfy the two following conditions:

a) Conditions of Codazzi

$$\frac{\partial}{\partial \alpha}(k_2 B) = k_1 \frac{\partial B}{\partial \alpha}, \qquad \frac{\partial}{\partial \beta}(k_1 A) = k_2 \frac{\partial A}{\partial \beta} \qquad (4)$$

b) Condition of Gauss

$$\frac{\partial}{\partial \alpha}\left(\frac{1}{A}\frac{\partial B}{\partial \alpha}\right) + \frac{\partial}{\partial \beta}\left(\frac{1}{B}\frac{\partial A}{\partial \beta}\right) = -ABk_1 k_2 \qquad (5)$$

The conditions stated above, sometimes called the Peterson-Codazzi-Gauss conditions, result from the requirement of continuity of the surface up to the second derivative and are useful in the simplification of shell equations. These definitions and expressions form a basis for the development of shell theory. Further information on surfaces and curvilinear coordinates may be found in References 1 and 2.

B. Shell Surfaces

The analysis that follows is limited to the case of shells of constant thickness. For convenience, point locations and displacements are referenced to the middle surface of the shell. The principal curvilinear coordinates of the middle surface are designated as α and β, while the coordinate measuring distances normal to the middle surface is designated as γ. The α, β, γ coordinate systems are established according to the right-hand rule as shown in Figure 1. The positive γ direction can therefore be determined from the vector equation $\bar{e}_\gamma = \bar{e}_\alpha \times \bar{e}_\beta$ where $\bar{e}_\alpha$, $\bar{e}_\beta$, and $\bar{e}_\gamma$ are unit vectors in the positive α, β, and γ directions, respectively.

Consider some equidistant surface lying a distance γ from the middle surface and within the shell as shown in Figure 2. The curvilinear coordinates of this surface correspond to those of the middle surface. An element of length ds on this equidistant surface is given by

$$ds^2 = \frac{1}{h_1^2} d\alpha^2 + \frac{1}{h_2^2} d\beta^2 \qquad (6)$$

where the coefficients $\frac{1}{h_1}$ and $\frac{1}{h_2}$ are the Lamé parameters of this equi-

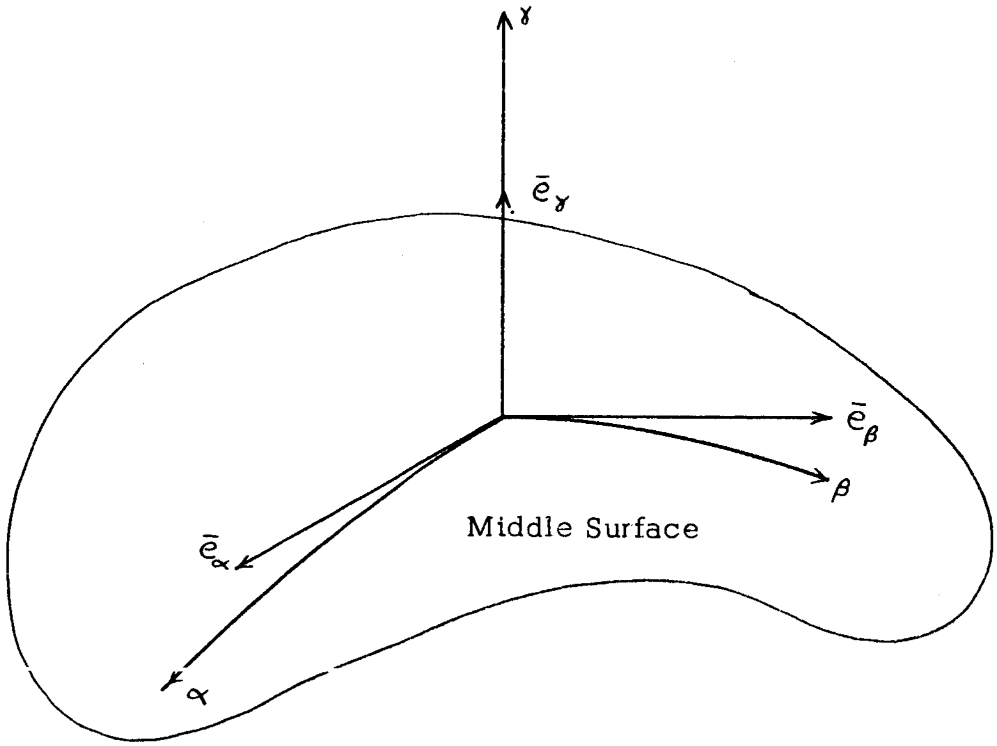

Figure 1. Orthonormal Triad of Vectors on the Shell Middle Surface.

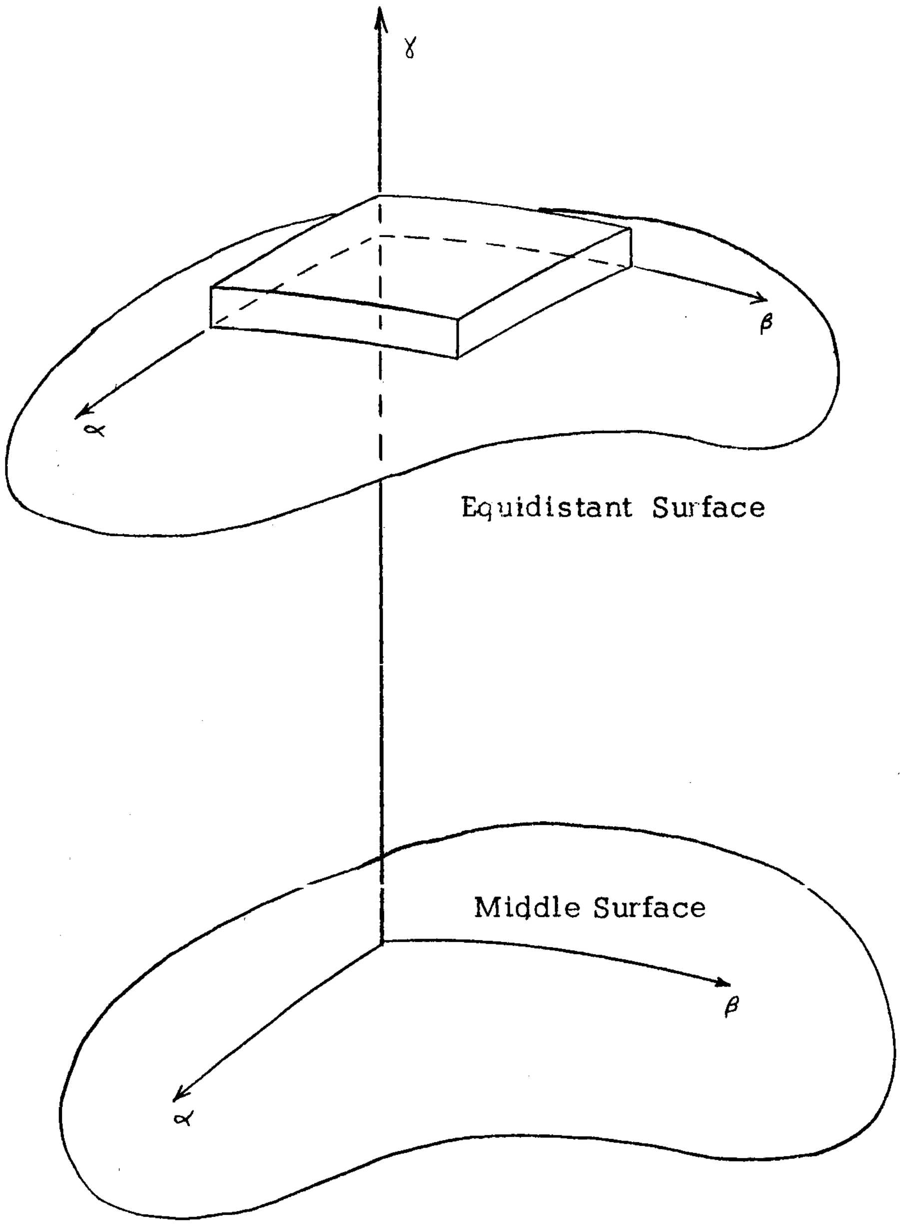

Figure 2. Element Located at a Distance γ Above the Middle Surface.

distant surface. For increments of length in the α and β directions,

$$ds = \frac{d\alpha}{h_1}$$
$$ds = \frac{d\beta}{h_2} \tag{7}$$

The quantities h_1 and h_2 are related to the Lamé parameters and principal curvatures by the following relationships:

$$h_1 = \frac{1}{A(1 + k_1 \gamma)}$$
$$h_2 = \frac{1}{B(1 + k_2 \gamma)} \tag{8}$$

If a coordinate γ', normal to an equidistant surface, is constructed at some point on the surface, it will coincide with the γ coordinate constructed at the corresponding point on the middle surface, and therefore

$$d\gamma' = d\gamma \tag{9}$$

The equations of Codazzi and Gauss, written for an equidistant surface, are given by[3]

$$h_1 \frac{\partial h_2^{-1}}{\partial \alpha} = \frac{1}{A}\frac{\partial B}{\partial \alpha}, \quad h_1 \frac{\partial h_2^{-1}}{\partial \alpha}\frac{\partial h_1^{-1}}{\partial \gamma} = \frac{\partial^2 h_2^{-1}}{\partial \alpha \partial \gamma}$$

$$h_2 \frac{\partial h_1^{-1}}{\partial \beta} = \frac{1}{B}\frac{\partial A}{\partial \beta}, \quad h_2 \frac{\partial h_1^{-1}}{\partial \beta}\frac{\partial h_2^{-1}}{\partial \gamma} = \frac{\partial^2 h_2^{-1}}{\partial \beta \partial \gamma}$$

$$\frac{\partial}{\partial \alpha}\left(h_1 \frac{h_2^{-1}}{\partial \alpha}\right) + \frac{\partial}{\partial \beta}\left(h_2 \frac{\partial h_1^{-1}}{\partial \beta}\right) = -k_1 k_2 AB \tag{10}$$

C. Strain-Displacement Relationships

Let U_α, U_β, and U_γ be the displacement components in the α, β, and γ directions, respectively, of a point lying on some equidistant

---

3 Numerical superscripts refer to corresponding items in the list of references.

surface. From theory of elasticity, the expressions for the three normal strains e_α, e_β, and e_γ and the shearing strain $e_{\alpha\beta}$ are found to be given by[4].

$$e_\alpha = h_1 \frac{\partial U_\alpha}{\partial \alpha} + h_1 h_2 \frac{\partial h_1^{-1}}{\partial \beta} U_\beta + h_1 \frac{\partial h_1^{-1}}{\partial \gamma} U_\gamma$$

$$e_\beta = h_2 \frac{\partial U_\beta}{\partial \beta} + h_1 h_2 \frac{\partial h_2^{-1}}{\partial \alpha} U_\alpha + h_2 \frac{\partial h_2^{-1}}{\partial \gamma} U_\gamma \tag{11}$$

$$e_\gamma = \frac{\partial U_\gamma}{\partial \gamma}$$

$$e_{\alpha\beta} = \frac{h_1}{h_2} \frac{\partial}{\partial \alpha} (h_2 U_\beta) + \frac{h_2}{h_1} \frac{\partial}{\partial \beta} (h_1 U_\alpha)$$

The displacements U_α and U_β are related to the middle surface displacements U, V and W by the following relationships:

$$U_\alpha = (1 + k_1 \gamma) U - \frac{\gamma}{A} \frac{\partial W}{\partial \alpha} \tag{12}$$

$$U_\beta = (1 + k_2 \gamma) V - \frac{\gamma}{B} \frac{\partial W}{\partial \beta}$$

The above expressions are a direct consequence of the Kirchoff-Love hypotheses. The displacement component U_γ will be determined during the course of the derivation of the shell equations.

D. Equilibrium Conditions

A free body diagram of a typical shell element is shown in Figure 3. Stresses and dimensions are shown only for positive faces and for lengths displaced from the α, β, γ coordinates since this is a standard representation and the remaining stresses and dimensions are not needed for clarification. Summing forces in the α, β and γ directions, the following three equations of equilibrium result:[5]

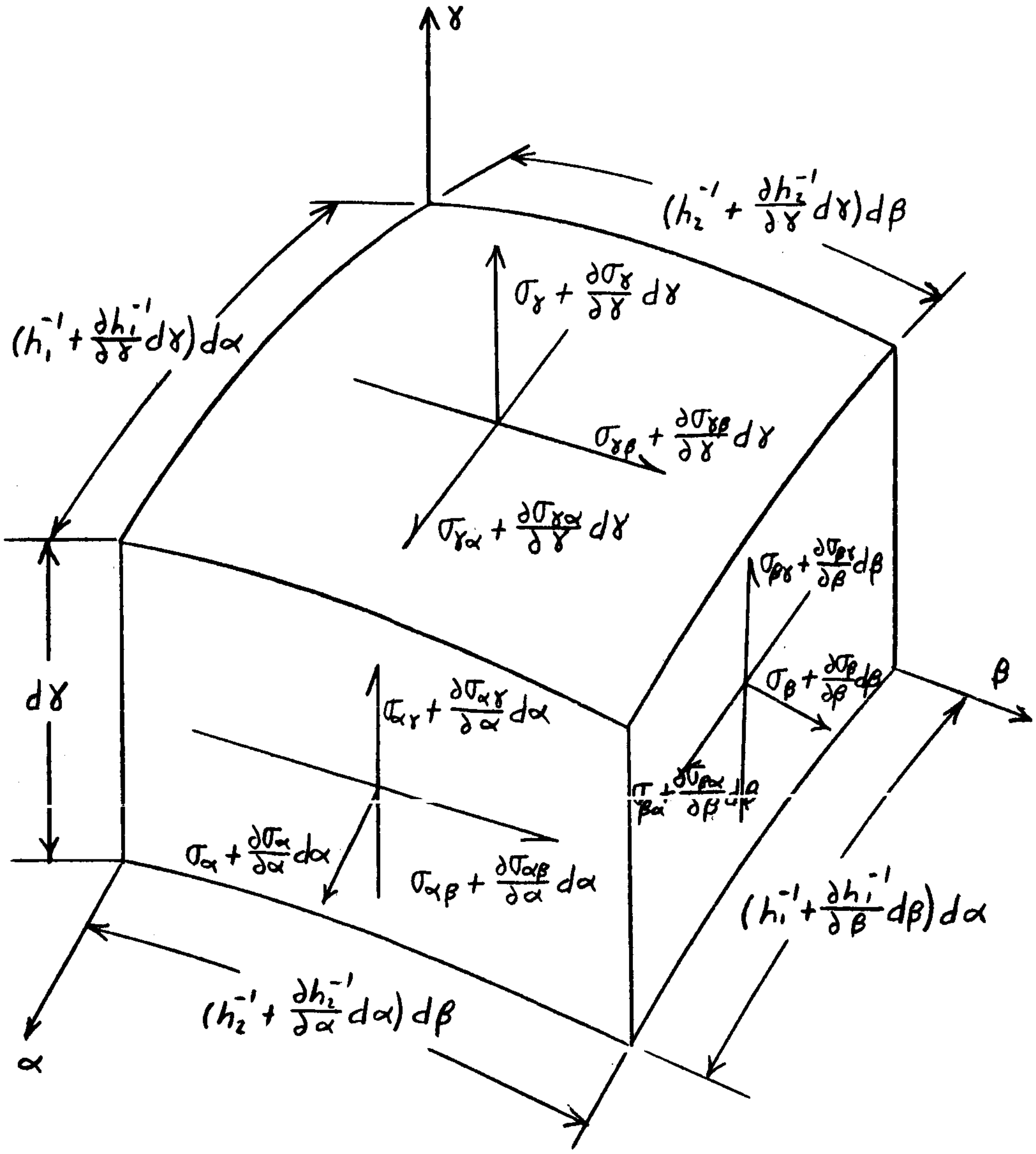

Figure 3. General Stress Condition of a Shell Element.

$$\frac{\partial}{\partial\alpha}\left(\frac{\sigma_\alpha}{h_2}\right) - \frac{\partial h_2^{-1}}{\partial\alpha}\sigma_\beta + h_1\frac{\partial}{\partial\beta}\left(\frac{\sigma_{\alpha\beta}}{h_1^2}\right) + h_1\frac{\partial}{\partial\gamma}\left(\frac{\sigma_{\alpha\gamma}}{h_1^2 h_2}\right) + \frac{Pa}{h_1h_2} = 0$$

$$\frac{\partial}{\partial\beta}\left(\frac{\sigma_\beta}{h_1}\right) - \frac{\partial h_1^{-1}}{\partial\beta}\sigma_\alpha + h_2\frac{\partial}{\partial\alpha}\left(\frac{\sigma_{\alpha\beta}}{h_1^2}\right) + h_2\frac{\partial}{\partial\gamma}\left(\frac{\sigma_{\beta\gamma}}{h_2^2 h_1}\right) + \frac{P_\beta}{h_1h_2} = 0$$

$$-\frac{1}{h_2}\frac{\partial h_1^{-1}}{\partial\gamma}\sigma_\alpha - \frac{1}{h_1}\frac{\partial h_2^{-1}}{\partial\gamma}\sigma_\beta + \frac{\partial}{\partial\alpha}\left(\frac{\sigma_{\alpha\gamma}}{h_2}\right) + \frac{\partial}{\partial\beta}\left(\frac{\sigma_{\beta\gamma}}{h_1}\right) \tag{13}$$

$$+\frac{\partial}{\partial\gamma}\left(\frac{\sigma_\gamma}{h_1h_2}\right) + \frac{P_\gamma}{h_1h_2} = 0$$

E. Stress-Strain Relationships

According to the generalized Hooke's law, the normal and shearing strains at a point are related to the associated normal and shearing stresses by equations of the following form:

$$\begin{aligned}
e_\alpha &= a_{11}\sigma_\alpha + a_{12}\sigma_\beta + a_{13}\sigma_\gamma + a_{14}\sigma_{\beta\gamma} + a_{15}\sigma_{\alpha\gamma} + a_{16}\sigma_{\alpha\beta} \\
e_\beta &= a_{21}\sigma_\alpha + a_{22}\sigma_\beta + \cdots\cdots\cdots\cdots a_{26}\sigma_{\alpha\beta} \\
&\cdots\cdots\cdots\cdots\cdots\cdots\cdots\cdots\cdots\cdots \qquad (14) \\
e_{\alpha\beta} &= a_{61}\sigma_\alpha + a_{62}\sigma_\beta + \cdots\cdots\cdots\cdots a_{66}\sigma_{\alpha\beta}
\end{aligned}$$

where a_{ij} are the elastic constants of the material. An interrelation exists between the elastic constants such that $a_{ij} = a_{ji}$, so that there are actually 21 independent elastic constants. The stress-strain relationships for any homogeneous elastic material can be expressed in terms of the above elastic constants. Some special cases that are of importance in engineering applications are listed below.

1. Plane of Elastic Symmetry

If, at each point in a body, there is a plane possessing the property that any two directions which are symmetrical relative to this plane are equivalent with respect to their elastic constants, the material is said to possess the property of plane anisotropy. If the γ coordinate is perpendicular to that plane at each point in a shell, the equations of the generalized Hooke's law reduce to the following form:

$$
\begin{aligned}
e_{\alpha} &= a_{11}\sigma_{\alpha} + a_{12}\sigma_{\beta} + a_{13}\sigma_{\gamma} + a_{16}\sigma_{\alpha\beta} \\
e_{\beta} &= a_{12}\sigma_{\alpha} + a_{22}\sigma_{\beta} + a_{23}\sigma_{\gamma} + a_{26}\sigma_{\alpha\beta} \\
e_{\gamma} &= a_{13}\sigma_{\alpha} + a_{23}\sigma_{\beta} + a_{33}\sigma_{\gamma} + a_{36}\sigma_{\alpha\beta} \\
e_{\beta\gamma} &= a_{44}\sigma_{\beta\gamma} + a_{45}\sigma_{\alpha\gamma} \\
e_{\gamma\alpha} &= a_{45}\sigma_{\beta\gamma} + a_{55}\sigma_{\alpha\gamma} \\
e_{\alpha\beta} &= a_{16}\sigma_{\alpha} + a_{26}\sigma_{\beta} + a_{36}\sigma_{\gamma} + a_{66}\sigma_{\alpha\beta}
\end{aligned} \qquad (15)
$$

In taking this special case, the number of independent elastic constants has been reduced from 21 to 13.

2. <u>Three Planes of Elastic Symmetry</u>

If, at each point of a body, there are three mutually perpendicular planes of elastic symmetry, the material is said to possess the property of orthogonal anisotropy or orthotropy. If these planes are perpendicular to the corresponding orthogonal coordinate directions α, β, and γ at each point in a shell, the material is said to possess the property of curvilinear orthotropy and the equations of the generalized Hooke's law will further reduce to the following form:

$$
\begin{aligned}
e_{\alpha} &= a_{11}\sigma_{\alpha} + a_{12}\sigma_{\beta} + a_{13}\sigma_{\gamma} \\
e_{\beta} &= a_{12}\sigma_{\alpha} + a_{22}\sigma_{\beta} + a_{23}\sigma_{\gamma} \\
e_{\gamma} &= a_{13}\sigma_{\alpha} + a_{23}\sigma_{\beta} + a_{33}\sigma_{\gamma} \\
e_{\beta\gamma} &= a_{44}\sigma_{\beta\gamma} \\
e_{\gamma\alpha} &= a_{55}\sigma_{\gamma\alpha} \\
e_{\alpha\beta} &= a_{66}\sigma_{\alpha\beta}
\end{aligned} \qquad (16)
$$

The number of independent elastic constants has now been reduced to nine.

3. Complete Symmetry

If, at any point in a body, all planes through that point are planes of elastic symmetry the material is said to be isotropic. For an isotropic material, the elastic constants take on particular relative values such that

$$
\begin{aligned}
e_{\alpha} &= \frac{1}{E}\left[\sigma_{\alpha} - \nu(\sigma_{\beta} + \sigma_{\gamma})\right] \\
e_{\beta} &= \frac{1}{E}\left[\sigma_{\beta} - \nu(\sigma_{\alpha} + \sigma_{\gamma})\right] \\
e_{\gamma} &= \frac{1}{E}\left[\sigma_{\gamma} - \nu(\sigma_{\alpha} + \sigma_{\beta})\right] \\
e_{\beta\gamma} &= \frac{2(1+\nu)}{E}\,\sigma_{\beta\gamma} \\
e_{\gamma\alpha} &= \frac{2(1+\nu)}{E}\,\sigma_{\gamma\alpha} \\
e_{\alpha\beta} &= \frac{2(1+\nu)}{E}\,\sigma_{\alpha\beta}
\end{aligned}
\qquad (17)
$$

where E is Young's modulus and ν is Poisson's ratio. The number of independent elastic constants has now been reduced to two.

Obviously, each of the above situations is a special case of the one which preceded it so that any analysis that is valid for one case will be equally valid for the less complicated cases. This work will be carried out for the case of plane anisotropy, and the results will therefore apply to orthotropic and isotropic shells as well.

In the work that follows it will be necessary to express the stresses in terms of strains rather than the strains in terms of stresses as was done above. For isotropic materials this relationship is often given in the following form:

$$
\begin{aligned}
\sigma_\alpha &= (\Upsilon + 2\mu)\Delta - 2\mu\,(e_\beta + e_\gamma) \\
\sigma_\beta &= (\Upsilon + 2\mu)\Delta - 2\mu\,(e_\alpha + e_\gamma) \\
\sigma_\gamma &= (\Upsilon + 2\mu)\Delta - 2\mu\,(e_\alpha + e_\beta) \\
\sigma_{\beta\gamma} &= \mu e_{\beta\gamma} \\
\sigma_{\gamma\alpha} &= \mu e_{\gamma\alpha} \\
\sigma_{\alpha\beta} &= \mu e_{\alpha\beta}
\end{aligned}
\qquad (18)
$$

where Υ and μ are the Lamé coefficients of elasticity and are related to E and ν by the following equations:

$$
\begin{aligned}
\Upsilon &= \frac{E\nu}{(1+\nu)(1-2\nu)} \\
\mu &= \frac{E}{2(1+\nu)}
\end{aligned}
\qquad (19)
$$

The Lamé coefficients of elasticity have no meaning for anisotropic materials. It will be convenient, however, to express the stress-strain relationship in terms of coefficients that will reduce to the Lamé coefficients for the special case of isotropy.

For the case of plane stress, the plane-anisotropic stress-strain relationships reduce to:

$$
\begin{aligned}
e_\alpha &= a_{11}\sigma_\alpha + a_{12}\sigma_\beta + a_{16}\sigma_{\alpha\beta} \\
e_\beta &= a_{12}\sigma_\alpha + a_{22}\sigma_\beta + a_{26}\sigma_{\alpha\beta} \\
e_\gamma &= a_{13}\sigma_\alpha + a_{23}\sigma_\beta + a_{36}\sigma_{\alpha\beta} \\
e_{\beta\gamma} &= 0 \\
e_{\gamma\alpha} &= 0 \\
e_{\alpha\beta} &= a_{16}\sigma_\alpha + a_{26}\sigma_\beta + a_{66}\sigma_{\alpha\beta}
\end{aligned}
\qquad (20)
$$

These equations can be written in the form

$$
\sigma_\alpha = (\Upsilon_\alpha + 2\mu_\alpha)\Delta - 2\mu_\alpha(e_\beta + e_\gamma) + \Upsilon_{\alpha\gamma}\, e_{\alpha\beta}
$$

$$\sigma_\beta = (\tau_\beta + 2\mu_\beta)\,\Delta - 2\mu_\beta(e_\alpha + e_\gamma) + \tau_{\beta\gamma}\, e_{\alpha\beta} \tag{21}$$

$$\sigma_{\alpha\beta} = \mu_{\alpha\beta} e_{\alpha\beta} + \tau'_{\alpha\gamma} e_\alpha + \tau'_{\beta\gamma}\, e_\beta$$

where

$$\tau_\alpha = \frac{(a_{12}a_{66} - a_{16}a_{26})}{\left\{(a_{11}+a_{12}+a_{13})(a_{12}a_{66}-a_{16}a_{26}) - (a_{12}+a_{22}+a_{23})(a_{11}a_{66}-a_{16}^2) + (a_{16}+a_{26}+a_{36})(a_{11}a_{26}-a_{12}a_{16})\right\}}$$

$$\tau_\beta = \frac{(a_{12}a_{66} - a_{16}a_{26})}{\left\{(a_{12}+a_{22}+a_{23})(a_{12}a_{66}-a_{16}a_{26}) - (a_{11}+a_{12}+a_{13})(a_{22}a_{66}-a_{26}^2) + (a_{16}+a_{26}+a_{36})(a_{22}a_{16}-a_{12}a_{26})\right\}}$$

$$2\mu_\alpha = \frac{a_{26}(a_{16}+a_{26}+a_{36}) - a_{66}(a_{12}+a_{22}+a_{23})}{\left\{(a_{11}+a_{12}+a_{13})(a_{12}a_{66}-a_{16}a_{26}) - (a_{12}+a_{22}+a_{23})(a_{11}a_{66}-a_{16}^2) + (a_{16}+a_{26}+a_{36})(a_{11}a_{26}-a_{12}a_{16})\right\}}$$

$$2\mu_\beta = \frac{a_{66}(a_{11}+a_{12}+a_{13}) - a_{16}(a_{16}+a_{26}+a_{36})}{\left\{(a_{12}+a_{22}+a_{23})(a_{12}a_{66}-a_{16}a_{26}) - (a_{11}+a_{12}+a_{13})(a_{22}a_{66}-a_{26}^2) + (a_{16}+a_{26}+a_{36})(a_{22}a_{16}-a_{12}a_{26})\right\}}$$

$$\mu_{\alpha\beta} = \frac{a_{11}a_{22} - a_{12}^2}{a_{66}(a_{11}a_{22}-a_{12}^2) - a_{16}(a_{16}a_{22}-a_{12}a_{26}) + a_{26}(a_{16}a_{12}-a_{11}a_{26})}$$

$$\tau_{\alpha\gamma} = \frac{a_{16}(a_{22}+a_{23}) - a_{12}(a_{26}+a_{36})}{\left\{(a_{11}+a_{12}+a_{13})(a_{12}a_{66}-a_{16}a_{26}) - (a_{12}+a_{22}+a_{23})(a_{11}a_{66}-a_{16}^2) + (a_{16}+a_{26}+a_{36})(a_{11}a_{26}-a_{12}a_{16})\right\}}$$

$$\Upsilon_{\beta\gamma} = \frac{a_{26}(a_{11}+a_{13}) - a_{12}(a_{16}+a_{36})}{\{(a_{12}+a_{22}+a_{23})(a_{12}a_{66}-a_{16}a_{26}) - (a_{11}+a_{12}+a_{13})(a_{22}a_{66}-a_{26}^{2}) + (a_{16}+a_{26}+a_{36})(a_{22}a_{16}-a_{12}a_{26})\}}$$

$$\Upsilon'_{\alpha\gamma} = \frac{a_{26}a_{12}-a_{16}a_{22}}{a_{66}(a_{11}a_{22}-a_{12}^{2}) - a_{16}(a_{16}a_{22}-a_{12}a_{26}) + a_{26}(a_{16}a_{12}-a_{11}a_{26})}$$

$$\Upsilon'_{\beta\gamma} = \frac{a_{16}a_{12}-a_{11}a_{26}}{a_{66}(a_{11}a_{22}-a_{12}^{2}) - a_{16}(a_{16}a_{22}-a_{12}a_{26}) + a_{26}(a_{16}a_{12}-a_{11}a_{26})} \tag{22}$$

The above set of coefficients will be referred to as the modified Lamé coefficients. For the special case of isotropy,

$$\Upsilon_{\alpha} = \Upsilon_{\beta} = \Upsilon,$$

$$\mu_{\alpha} = \mu_{\beta} = \mu_{\alpha\beta} = \mu,$$

and

$$\Upsilon_{\alpha\gamma} = \Upsilon_{\beta\gamma} = \Upsilon'_{\alpha\gamma} = \Upsilon'_{\beta\gamma} = 0$$

and the equations reduce to the stress-strain relationships for the case of plane stress expressed in terms of Lamé coefficients of elasticity.

III. Shell Equations

A. Equilibrium of a Shell Element

The ultimate goal is the development of the governing differential equations in terms of middle surface displacement components. To accomplish this, Equations (11), (12), (13) and (21) are first combined to yield the following set of equilibrium equations in terms of middle surface displacement components:

$$\Big\{(\tau_\alpha + 2\mu_\alpha) B \frac{\partial \Delta_0}{\partial\alpha} - 2U_{\alpha\beta} A \frac{\partial \chi_0}{\partial\beta} + 2\mu_\alpha ABKU$$

$$+ \Big[(\tau_\alpha+2\mu_\alpha) - (\tau_\beta + 2\mu_\beta)\Big] \frac{\partial B}{\partial\alpha}\Delta_0 + 2(\mu_\alpha - \mu_{\alpha\beta}) \frac{\partial}{\partial\beta}\left(\frac{1}{B}\frac{\partial A}{\partial\beta}\right) U$$

$$-2(\mu_\alpha-\mu_\beta)\frac{1}{A}\frac{\partial B}{\partial\alpha}\frac{\partial U}{\partial\alpha} - 2(\mu_\alpha-\mu_{\alpha\beta})\frac{\partial^2 V}{\partial\alpha\partial\beta}$$

$$+2(\mu_\alpha-\mu_{\alpha\beta})\frac{1}{AB}\frac{\partial A}{\partial\beta}\frac{\partial B}{\partial\alpha}V + \tau'_{\alpha\gamma}(k_1+k_2)\frac{\partial A}{\partial\beta}U_\gamma + \tau'_{\alpha\gamma}Ak_1\frac{\partial U_\gamma}{\partial\beta}$$

$$+\tau'_{\beta\gamma}\frac{1}{B}\frac{\partial A}{\partial\beta}U_\gamma + \tau'_{\beta\gamma}\frac{\partial}{\partial\beta}(Ak_2U_\gamma) - \tau_{\alpha\gamma}\frac{\partial}{\partial\alpha}\left(\frac{1}{A}\frac{\partial A}{\partial\beta}\right)U + \tau_{\beta\gamma}\frac{1}{AB}\frac{\partial B}{\partial\alpha}\frac{\partial A}{\partial\beta}U$$

$$+\tau'_{\beta\gamma}\frac{1}{A}\frac{\partial}{\partial\beta}\left(\frac{A}{B}\frac{\partial B}{\partial\alpha}\right)U - (\tau_{\alpha\gamma}+\tau'_{\alpha\gamma})\frac{1}{A}\frac{\partial A}{\partial\beta}\frac{\partial U}{\partial\alpha} + (\tau'_{\beta\gamma}-\tau_{\beta\gamma})\frac{1}{B}\frac{\partial B}{\partial\alpha}\frac{\partial U}{\partial\beta}$$

$$+(\tau_{\alpha\gamma}+\tau'_{\alpha\gamma})\frac{\partial^2 U}{\partial\alpha\partial\beta} - \tau_{\alpha\gamma}\frac{\partial}{\partial\alpha}\left(\frac{1}{A}\frac{\partial B}{\partial\alpha}\right)V + \tau_{\beta\gamma}\frac{1}{AB}\left(\frac{\partial B}{\partial\alpha}\right)^2 V$$

$$+\tau'_{\alpha\gamma}\frac{1}{A}\frac{\partial}{\partial\beta}\left(\frac{A}{B}\frac{\partial A}{\partial\beta}\right)V - \tau_{\alpha\gamma}\frac{B}{A^2}\frac{\partial A}{\partial\beta}\frac{\partial V}{\partial\alpha} - \tau_{\beta\gamma}\frac{1}{A}\frac{\partial B}{\partial\alpha}\frac{\partial V}{\partial\alpha} + \tau'_{\alpha\gamma}\frac{1}{B}\frac{\partial A}{\partial\beta}\frac{\partial V}{\partial\beta}$$

$$+\tau'_{\beta\gamma}\frac{1}{A}\frac{\partial}{\partial\beta}\left(\frac{A^2}{B}\right)\frac{\partial V}{\partial\beta} + \tau_{\alpha\gamma}\frac{\partial^2 V}{\partial\alpha^2}\frac{B}{A} + \tau'_{\beta\gamma}\frac{A}{B}\frac{\partial^2 V}{\partial\beta^2}\Big\}$$

$$+\Big\{(\tau_\alpha+2\mu_\alpha)Bk_2\frac{\partial\Delta_0}{\partial\alpha} + (\tau_\alpha+2\mu_\alpha)B\frac{\partial\Delta_1}{\partial\alpha} - 2\mu_{\alpha\beta}Ak_1\frac{\partial\chi_0}{\partial\beta}$$

$$-2\mu_{\alpha\beta}A\frac{\partial\chi_1}{\partial\beta} + 2\mu_\alpha ABKk_1U - 2\mu_\alpha BK\frac{\partial W}{\partial\alpha}$$

$$+\Big[(\tau_\alpha+2\mu_\alpha)-(\tau_\beta+2\mu_\beta)\Big]k_1\frac{\partial B}{\partial\alpha}\Delta_0$$

$$+\Big[(\tau_\alpha+2\mu_\alpha)-(\tau_\beta+2\mu_\beta)\Big]\frac{\partial B}{\partial\alpha}\Delta_1 + 2(\mu_\alpha-\mu_{\alpha\beta})k_1\frac{\partial}{\partial\beta}\left(\frac{1}{B}\frac{\partial A}{\partial\beta}\right)U$$

$$-2(\mu_\alpha-\mu_{\alpha\beta})\frac{1}{A}\frac{\partial}{\partial\beta}\left(\frac{1}{B}\frac{\partial A}{\partial\beta}\right)\frac{\partial W}{\partial\alpha} - 2(\mu_\alpha-\mu_\beta)\frac{1}{A}\frac{\partial B}{\partial\alpha}\frac{\partial k_1U}{\partial\alpha}$$

$$+2(\mu_\alpha-\mu_\beta)\frac{1}{A}\frac{\partial B}{\partial\alpha}\frac{\partial}{\partial\alpha}\left(\frac{1}{A}\frac{\partial W}{\partial\alpha}\right) - 2(\mu_\alpha-\mu_{\alpha\beta})\frac{\partial^2}{\partial\alpha\partial\beta}(k_2V)$$

$$+2(\mu_\alpha-\mu_{\alpha\beta})\frac{\partial^2}{\partial\alpha\partial\beta}\left(\frac{1}{B}\frac{\partial W}{\partial\beta}\right) + 2(\mu_\beta-\mu_{\alpha\beta})\frac{k_2}{AB}\frac{\partial A}{\partial\beta}\frac{\partial B}{\partial\alpha}V$$

$$-2(\mu_\beta-\mu_{\alpha\beta})\frac{1}{AB^2}\frac{\partial A}{\partial\beta}\frac{\partial B}{\partial\alpha}\frac{\partial W}{\partial\beta}+\tau_{\beta\gamma}'Ak_2\frac{\partial}{\partial\beta}(2k_1-k_2)U_\gamma$$

$$-\tau_{\alpha\gamma}\frac{\partial^2 k_1}{\partial\alpha\partial\beta}U+\tau_{\beta\gamma}\frac{1}{B}\frac{\partial B}{\partial\alpha}\frac{\partial k_1}{\partial\beta}U-\tau_{\alpha\gamma}\frac{\partial k_1}{\partial\beta}\frac{\partial U}{\partial\alpha}-\tau_{\alpha\gamma}\frac{B}{A}\frac{\partial^2}{\partial\alpha^2}\left(\frac{1}{B}\frac{\partial W}{\partial\beta}\right)$$

$$+\tau_{\alpha\gamma}\frac{1}{A}\frac{\partial B}{\partial\alpha}\frac{\partial}{\partial\alpha}(k_1-k_2)V-\tau_{\alpha\gamma}\frac{\partial}{\partial\alpha}\left(\frac{B}{A}\frac{\partial k_2}{\partial\alpha}\right)V+\tau_{\beta\gamma}\frac{1}{A}\frac{\partial B}{\partial\alpha}\frac{\partial k_2}{\partial\alpha}V$$

$$+\tau_{\alpha\gamma}'\frac{1}{B}\frac{\partial A}{\partial\beta}\frac{\partial k_1}{\partial\beta}V-\tau_{\alpha\gamma}\frac{B}{A}\frac{\partial k_1}{\partial\alpha}\frac{\partial V}{\partial\alpha}+\tau_{\beta\gamma}'\frac{A}{B}\frac{\partial}{\partial\beta}(2k_1-k_2)\frac{\partial V}{\partial\beta}$$

$$+\tau_{\alpha\gamma}\frac{\partial}{\partial\alpha}\left(\frac{1}{A^2}\frac{\partial A}{\partial\beta}\frac{\partial W}{\partial\alpha}\right)-\tau_{\beta\gamma}\frac{1}{A^2B}\frac{\partial B}{\partial\alpha}\frac{\partial A}{\partial\beta}\frac{\partial W}{\partial\alpha}-\tau_{\beta\gamma}'\frac{A}{B}\frac{\partial^2}{\partial\beta^2}\left(\frac{1}{B}\frac{\partial W}{\partial\beta}\right)$$

$$-\tau_{\beta\gamma}'\frac{1}{A^2}\frac{\partial}{\partial\beta}\left(\frac{A}{B}\frac{\partial B}{\partial\alpha}\right)\frac{\partial W}{\partial\alpha}-\tau_{\alpha\gamma}'\frac{1}{A}\frac{\partial A}{\partial\beta}\frac{\partial}{\partial\alpha}\left(\frac{1}{A}\frac{\partial W}{\partial\alpha}\right)$$

$$-(\tau_{\beta\gamma}'-\tau_{\beta\gamma})\frac{1}{B}\frac{\partial B}{\partial\alpha}\frac{\partial}{\partial\beta}\left(\frac{1}{A}\frac{\partial W}{\partial\alpha}\right)-(\tau_{\alpha\gamma}+\tau_{\alpha\gamma}')\frac{\partial^2}{\partial\alpha\partial\beta}\left(\frac{1}{A}\frac{\partial W}{\partial\alpha}\right)$$

$$+\tau_{\alpha\gamma}\frac{\partial}{\partial\alpha}\left(\frac{1}{A}\frac{\partial B}{\partial\alpha}\right)\frac{1}{B}\frac{\partial W}{\partial\beta}-\tau_{\beta\gamma}\frac{1}{AB^2}\left(\frac{\partial B}{\partial\alpha}\right)^2\frac{\partial W}{\partial\beta}-\tau_{\alpha\gamma}'\frac{1}{AB}\frac{\partial}{\partial\beta}\left(\frac{A}{B}\frac{\partial A}{\partial\beta}\right)\frac{\partial W}{\partial\beta}$$

$$+\tau_{\alpha\gamma}\frac{B}{A^2}\frac{\partial A}{\partial\alpha}\frac{\partial}{\partial\alpha}\left(\frac{1}{B}\frac{\partial W}{\partial\beta}\right)+\tau_{\beta\gamma}\frac{1}{A}\frac{\partial B}{\partial\alpha}\frac{\partial}{\partial\alpha}\left(\frac{1}{B}\frac{\partial W}{\partial\beta}\right)$$

$$-\tau_{\alpha\gamma}'\frac{1}{B}\frac{\partial A}{\partial\beta}\frac{\partial}{\partial\beta}\left(\frac{1}{B}\frac{\partial W}{\partial\beta}\right)-\tau_{\beta\gamma}'\frac{1}{A}\frac{\partial}{\partial\beta}\left(\frac{A^2}{B}\right)\frac{\partial}{\partial\beta}\left(\frac{1}{B}\frac{\partial W}{\partial\beta}\right)\Big\}\gamma$$

$$+\Big\{(\tau_\alpha+2\mu_\alpha)Bk_2\frac{\partial\Delta_1}{\partial\alpha}-2\mu_{\alpha\beta}Ak_1\frac{\partial\chi_1}{\partial\beta}$$

$$+\Big[(\tau_\alpha+2\mu_\alpha)-(\tau_\beta+2\mu_\beta)\Big]k_1\frac{\partial B}{\partial\alpha}\Delta_1-\tau_{\alpha\gamma}\frac{\partial k_1}{\partial\beta}\frac{\partial k_1}{\partial\alpha}U$$

$$+\tau_{\beta\gamma}'\frac{1}{B}\frac{\partial B}{\partial\alpha}\frac{\partial}{\partial\beta}(2k_1-k_2)U$$

$$-\tau_{\alpha\gamma}\frac{B}{A}\frac{\partial k_2}{\partial\alpha}\frac{\partial}{\partial\alpha}(2k_2-k_1)V+\tau_{\alpha\gamma}\frac{\partial}{\partial\alpha}\left(\frac{1}{A}\frac{\partial k_1}{\partial\beta}\frac{\partial W}{\partial\alpha}\right)$$

$$-\tau_{\beta\gamma}\frac{1}{AB}\frac{\partial B}{\partial\alpha}\frac{\partial k_1}{\partial\beta}\frac{\partial W}{\partial\alpha}-\tau_{\alpha\gamma}\frac{1}{B}-\tau_{\alpha\gamma}\frac{1}{B}\frac{\partial}{\partial\alpha}\left(\frac{1}{A}(k_1-k_2)\frac{\partial B}{\partial\alpha}\right)\frac{\partial W}{\partial\beta}$$

$$+\tau_{\alpha\gamma}\frac{\partial}{\partial\alpha}\left(\frac{B}{A}\frac{\partial k_2}{\partial\alpha}\right)\frac{1}{B}\frac{\partial W}{\partial\beta}-\tau_{\beta\gamma}\frac{1}{AB}\frac{\partial B}{\partial\alpha}\frac{\partial k_2}{\partial\alpha}\frac{\partial W}{\partial\beta}$$

$$+\tau'_{\alpha\gamma}\frac{1}{B^2}\frac{\partial A}{\partial\beta}\frac{\partial k_1}{\partial\beta}\frac{\partial W}{\partial\beta}-\tau_{\alpha\gamma}\frac{B}{A^2}(k_1-k_2)\frac{\partial A}{\partial\alpha}\frac{\partial}{\partial\alpha}\left(\frac{1}{B}\frac{\partial W}{\partial\beta}\right)$$

$$+\tau_{\alpha\gamma}\frac{B}{A}\frac{\partial k_1}{\partial\alpha}\frac{\partial}{\partial\alpha}\left(\frac{1}{B}\frac{\partial W}{\partial\beta}\right)-\tau'_{\beta\gamma}\frac{A}{B}\frac{\partial}{\partial\beta}(2k_1-k_2)\frac{\partial}{\partial\beta}\left(\frac{1}{B}\frac{\partial W}{\partial\beta}\right)$$

$$-\tau'_{\beta\gamma}\frac{1}{AB}\frac{\partial B}{\partial\alpha}\frac{\partial}{\partial\beta}(2k_1-k_2)\frac{\partial W}{\partial\alpha}\Big\}\gamma^2$$

$$+\Big\{\tau_{\alpha\gamma}\frac{1}{B}\frac{\partial}{\partial\alpha}\left(\frac{B}{A}(2k_2-k_1)\frac{\partial k_2}{\partial\alpha}\right)\frac{\partial W}{\partial\beta}$$

$$+\tau_{\alpha\gamma}\frac{\partial k_1}{\partial\alpha}\frac{\partial k_1}{\partial\beta}\frac{1}{A}\frac{\partial W}{\partial\alpha}+\tau'_{\beta\gamma}\frac{1}{AB}k_1\frac{\partial B}{\partial\alpha}\frac{\partial}{\partial\beta}(2k_1-k_2)\frac{\partial W}{\partial\alpha}\Big\}\gamma^3$$

$$-2\mu_\alpha\frac{\partial}{\partial\gamma}\left(\frac{1}{h_2}\frac{\partial U_\gamma}{\partial\alpha}\right)-2(\mu_\alpha-\mu_\beta)\frac{\partial}{\partial\gamma}\left(U_\gamma\frac{\partial h_2^{-1}}{\partial\alpha}\right)$$

$$+h_1\frac{\partial}{\partial\gamma}\left(\frac{\sigma_{\gamma\alpha}}{h_1h_2^2}\right)+\frac{P_\gamma}{h_1h_2}=0 \tag{23}$$

$$\Big\{(\tau_\beta+2\mu_\beta)A\frac{\partial\Delta_o}{\partial\beta}+2\mu_{\alpha\beta}B\frac{\partial\chi_o}{\partial\alpha}+2\mu_\beta ABKV$$

$$+\left[(\tau_\beta+2\mu_\beta)-(\tau_\alpha+2\mu_\alpha)\right]\frac{\partial A}{\partial\beta}\Delta_o+2(\mu_\beta-\mu_{\alpha\beta})\frac{\partial}{\partial\alpha}\left(\frac{1}{A}\frac{\partial B}{\partial\alpha}\right)V$$

$$-2(\mu_\beta-\mu_\alpha)\frac{1}{B}\frac{\partial A}{\partial\beta}\frac{\partial V}{\partial\beta}-2(\mu_\beta-\mu_{\alpha\beta})\frac{\partial^2U}{\partial\alpha\partial\beta}$$

$$+\frac{2}{AB}(\mu_\beta-\mu_{\alpha\beta})\frac{\partial B}{\partial\alpha}\frac{\partial A}{\partial\beta}U+\tau'_{\beta\gamma}(k_1+k_2)\frac{\partial B}{\partial\alpha}U_\gamma+\tau'_{\beta\gamma}Bk_2\frac{\partial U_\gamma}{\partial\alpha}$$

$$+\tau'_{\alpha\gamma}\frac{1}{A}\frac{\partial B}{\partial\alpha}U_\gamma+\tau'_{\alpha\gamma}\frac{\partial}{\partial\alpha}(Bk_1U_\gamma)-\tau_{\beta\gamma}\frac{\partial}{\partial\beta}\left(\frac{1}{B}\frac{\partial B}{\partial\alpha}\right)V-\tau_{\alpha\gamma}\frac{1}{AB}\frac{\partial A}{\partial\beta}\frac{\partial B}{\partial\alpha}V$$

$$+\tau'_{\alpha\gamma}\frac{1}{B}\frac{\partial}{\partial\alpha}\left(\frac{B}{A}\frac{\partial A}{\partial\beta}\right)V-(\tau_{\beta\gamma}+\tau'_{\beta\gamma})\frac{1}{B}\frac{\partial B}{\partial\alpha}\frac{\partial V}{\partial\beta}+(\tau'_{\alpha\gamma}-\tau_{\alpha\gamma})\frac{1}{A}\frac{\partial A}{\partial\beta}\frac{\partial V}{\partial\alpha}$$

$$+(\tau_{\beta\gamma}+\tau'_{\beta\gamma})\frac{\partial^2V}{\partial\alpha\partial\beta}-\tau_{\beta\gamma}\frac{\partial}{\partial\beta}\left(\frac{1}{B}\frac{\partial A}{\partial\beta}\right)U+\tau_{\alpha\gamma}\frac{1}{AB}\left(\frac{\partial A}{\partial\beta}\right)^2U$$

$$+\tau'_{\beta\gamma}\frac{1}{B}\frac{\partial}{\partial\alpha}\left(\frac{B}{A}\frac{\partial B}{\partial\alpha}\right)U-\tau_{\beta\gamma}\frac{A}{B^2}\frac{\partial B}{\partial\alpha}\frac{\partial U}{\partial\beta}-\tau_{\alpha\gamma}\frac{1}{B}\frac{\partial A}{\partial\beta}\frac{\partial U}{\partial\beta}+\tau'_{\beta\gamma}\frac{1}{A}\frac{\partial B}{\partial\alpha}\frac{\partial U}{\partial\alpha}$$

$$+ \tau_{\alpha\gamma}' \frac{1}{B}\frac{\partial}{\partial\alpha}\left(\frac{B^2}{A}\right)\frac{\partial U}{\partial\alpha} + \tau_{\beta\gamma}\frac{A}{B}\frac{\partial^2 U}{\partial\beta^2} + \tau_{\alpha\gamma}'\frac{B}{A}\frac{\partial^2 U}{\partial\alpha^2}\Big\}$$

$$+\Big\{(\tau_\beta + 2\mu_\beta) A k_1 \frac{\partial\Delta_0}{\partial\beta} + (\tau_\beta+2\mu_\beta) A \frac{\partial\Delta_1}{\partial\beta} + 2\mu_{\alpha\beta} B k_2 \frac{\partial\chi_0}{\partial\alpha}$$

$$+2\mu_{\alpha\beta} B\frac{\partial\chi_1}{\partial\alpha} + 2\mu_\beta ABK k_2 V - 2\mu_\beta AK \frac{\partial W}{\partial\beta}$$

$$+\left[(\tau_\beta+2\mu_\beta) - (\tau_\alpha+2\mu_\alpha)\right] k_2 \frac{\partial A}{\partial\beta}\Delta_0$$

$$+\left[(\tau_\beta+2\mu_\beta)-(\tau_\alpha+2\mu_\alpha)\right]\frac{\partial A}{\partial\beta}\Delta_1 + 2(\mu_\beta-\mu_{\alpha\beta})k_2\frac{\partial}{\partial\alpha}\left(\frac{1}{A}\frac{\partial B}{\partial\alpha}\right)V$$

$$-2(\mu_\beta-\mu_{\alpha\beta})\frac{1}{B}\frac{\partial}{\partial\alpha}\left(\frac{1}{A}\frac{\partial B}{\partial\alpha}\right)\frac{\partial W}{\partial\beta} - 2(\mu_\beta-\mu_\alpha)\frac{1}{B}\frac{\partial A}{\partial\beta}\frac{\partial k_2 V}{\partial\beta}$$

$$+2(\mu_\beta-\mu_\alpha)\frac{1}{B}\frac{\partial A}{\partial\beta}\frac{\partial}{\partial\beta}\left(\frac{1}{B}\frac{\partial W}{\partial\beta}\right) - 2(\mu_\beta-\mu_{\alpha\beta})\frac{\partial^2}{\partial\alpha\partial\beta}(k_1 U)$$

$$+2(\mu_\beta-\mu_{\alpha\beta})\frac{\partial^2}{\partial\alpha\partial\beta}\left(\frac{1}{A}\frac{\partial W}{\partial\alpha}\right) + 2(\mu_\alpha-\mu_{\alpha\beta})\frac{k_1}{AB}\frac{\partial B}{\partial\alpha}\frac{\partial A}{\partial\beta}U$$

$$-2(\mu_\alpha-\mu_{\alpha\beta})\frac{1}{A^2B}\frac{\partial B}{\partial\alpha}\frac{\partial A}{\partial\beta}\frac{\partial W}{\partial\alpha} + \tau_{\alpha\gamma}' B k_1\frac{\partial}{\partial\alpha}(2k_2-k_1)U\gamma$$

$$-\tau_{\beta\gamma}\frac{\partial^2 k_2}{\partial\alpha\partial\beta}V + \tau_{\alpha\gamma}\frac{1}{A}\frac{\partial A}{\partial\beta}\frac{\partial k_2}{\partial\alpha}V - \tau_{\beta\gamma}\frac{\partial k_2}{\partial\alpha}\frac{\partial V}{\partial\beta}$$

$$+\tau_{\beta\gamma}\frac{1}{B}\frac{\partial A}{\partial\beta}\frac{\partial}{\partial\beta}(k_2-k_1)U - \tau_{\beta\gamma}\frac{\partial}{\partial\beta}\left(\frac{A}{B}\frac{\partial k_1}{\partial\beta}\right)U + \tau_{\alpha\gamma}\frac{1}{B}\frac{\partial A}{\partial\beta}\frac{\partial k_1}{\partial\beta}U$$

$$+\tau_{\beta\gamma}'\frac{1}{A}\frac{\partial B}{\partial\alpha}\frac{\partial k_2}{\partial\alpha}U - \tau_{\beta\gamma}\frac{A}{B}\frac{\partial k_2}{\partial\beta}\frac{\partial U}{\partial\beta} + \tau_{\alpha\gamma}'\frac{B}{A}\frac{\partial}{\partial\alpha}(2k_2-k_1)\frac{\partial U}{\partial\alpha}$$

$$+\tau_{\beta\gamma}\frac{\partial}{\partial\beta}\left(\frac{1}{B^2}\frac{\partial B}{\partial\alpha}\frac{\partial W}{\partial\beta}\right) - \tau_{\alpha\gamma}\frac{1}{AB^2}\frac{\partial A}{\partial\beta}\frac{\partial B}{\partial\alpha}\frac{\partial W}{\partial\beta}$$

$$-\tau_{\alpha\gamma}'\frac{1}{B^2}\frac{\partial}{\partial\alpha}\left(\frac{B}{A}\frac{\partial A}{\partial\beta}\right)\frac{\partial W}{\partial\beta} - \tau_{\beta\gamma}'\frac{1}{B}\frac{\partial B}{\partial\alpha}\frac{\partial}{\partial\beta}\left(\frac{1}{B}\frac{\partial W}{\partial\beta}\right)$$

$$-(\tau_{\alpha\gamma}'-\tau_{\alpha\gamma})\frac{1}{A}\frac{\partial A}{\partial\beta}\frac{\partial}{\partial\alpha}\left(\frac{1}{B}\frac{\partial W}{\partial\beta}\right) - (\tau_{\beta\gamma}+\tau_{\beta\gamma}')\frac{\partial^2}{\partial\alpha\partial\beta}\left(\frac{1}{B}\frac{\partial W}{\partial\beta}\right)$$

$$+\tau_{\beta\gamma}\frac{\partial}{\partial\beta}\left(\frac{1}{B}\frac{\partial A}{\partial\beta}\right)\frac{1}{A}\frac{\partial W}{\partial\alpha} - \tau_{\alpha\gamma}\frac{1}{A^2B}\left(\frac{\partial A}{\partial\beta}\right)^2\frac{\partial W}{\partial\alpha} - \tau_{\beta\gamma}'\frac{1}{AB}\frac{\partial}{\partial\alpha}\left(\frac{B}{A}\frac{\partial B}{\partial\alpha}\right)\frac{\partial W}{\partial\alpha}$$

$$+\tau_{\beta\gamma}\frac{A}{B^2}\frac{\partial B}{\partial\beta}\frac{\partial}{\partial\beta}\left(\frac{1}{A}\frac{\partial W}{\partial\alpha}\right)+\tau_{\alpha\gamma}\frac{1}{B}\frac{\partial A}{\partial\beta}\frac{\partial}{\partial\beta}\left(\frac{1}{A}\frac{\partial W}{\partial\alpha}\right)$$

$$-\tau_{\beta\gamma}'\frac{1}{A}\frac{\partial B}{\partial\alpha}\frac{\partial}{\partial\alpha}\left(\frac{1}{A}\frac{\partial W}{\partial\alpha}\right)-\tau_{\alpha\gamma}'\frac{1}{B}\frac{\partial}{\partial\alpha}\left(\frac{B^2}{A}\right)\frac{\partial}{\partial\alpha}\left(\frac{1}{A}\frac{\partial W}{\partial\alpha}\right)$$

$$-\tau_{\beta\gamma}\frac{A}{B}\frac{\partial^2}{\partial\beta^2}\left(\frac{1}{A}\frac{\partial W}{\partial\alpha}\right)-\tau_{\alpha\gamma}'\frac{B}{A}\frac{\partial^2}{\partial\alpha^2}\left(\frac{1}{A}\frac{\partial W}{\partial\alpha}\right)\Big\}\gamma$$

$$+\Big\{(\tau_\beta+2\mu_\beta)Ak_1\frac{\partial\Delta_1}{\partial\beta}+2\mu_{\alpha\beta}Bk_2\frac{\partial\chi_1}{\partial\alpha}$$

$$+\Big[(\tau_\beta-2\mu_\beta)-(\tau_\alpha+2\mu_\alpha)\Big]k_2\frac{\partial A}{\partial\beta}\Delta_1-\tau_{\beta\gamma}\frac{\partial k_2}{\partial\alpha}\frac{\partial k_2}{\partial\beta}V$$

$$+\tau_{\alpha\gamma}'\frac{1}{A}\frac{\partial A}{\partial\beta}\frac{\partial}{\partial\alpha}(2k_2-k_1)V-\tau_{\beta\gamma}\frac{A}{B}\frac{\partial k_1}{\partial\beta}\frac{\partial}{\partial\beta}(2k_1-k_2)U$$

$$+\tau_{\beta\gamma}\frac{\partial}{\partial\beta}\left(\frac{1}{B}\frac{\partial k_2}{\partial\alpha}\frac{\partial W}{\partial\beta}\right)-\tau_{\alpha\gamma}\frac{1}{AB}\frac{\partial A}{\partial\beta}\frac{\partial k_2}{\partial\alpha}\frac{\partial W}{\partial\beta}-\tau_{\beta\gamma}\frac{1}{A}\frac{\partial}{\partial\beta}\left(\frac{1}{B}(k_2-k_1)\frac{\partial A}{\partial\beta}\right)\frac{\partial W}{\partial\alpha}$$

$$+\tau_{\beta\gamma}\frac{\partial}{\partial\beta}\left(\frac{A}{B}\frac{\partial k_1}{\partial\beta}\right)\frac{1}{A}\frac{\partial W}{\partial\alpha}-\tau_{\alpha\gamma}\frac{1}{AB}\frac{\partial A}{\partial\beta}\frac{\partial k_1}{\partial\beta}\frac{\partial W}{\partial\alpha}$$

$$+\tau_{\beta\gamma}'\frac{1}{A^2}\frac{\partial B}{\partial\alpha}\frac{\partial k_2}{\partial\alpha}\frac{\partial W}{\partial\alpha}-\tau_{\beta\gamma}\frac{A}{B^2}(k_2-k_1)\frac{\partial B}{\partial\beta}\frac{\partial}{\partial\beta}\left(\frac{1}{A}\frac{\partial W}{\partial\alpha}\right)$$

$$+\tau_{\beta\gamma}\frac{A}{B}\frac{\partial k_2}{\partial\beta}\frac{\partial}{\partial\beta}\left(\frac{1}{A}\frac{\partial W}{\partial\alpha}\right)-\tau_{\alpha\gamma}'\frac{B}{A}\frac{\partial}{\partial\alpha}(2k_2-k_1)\frac{\partial}{\partial\alpha}\left(\frac{1}{A}\frac{\partial W}{\partial\alpha}\right)$$

$$-\tau_{\alpha\gamma}'\frac{1}{AB}\frac{\partial A}{\partial\beta}\frac{\partial}{\partial\alpha}(2k_2-k_1)\frac{\partial W}{\partial\beta}\Big\}\gamma^2$$

$$+\Big\{\tau_{\beta\gamma}\frac{1}{A}\frac{\partial}{\partial\beta}\left(\frac{A}{B}(2k_1-k_2)\frac{\partial k_1}{\partial\beta}\right)\frac{\partial W}{\partial\alpha}$$

$$+\tau_{\beta\gamma}\frac{\partial k_2}{\partial\beta}\frac{\partial k_2}{\partial\alpha}\frac{1}{B}\frac{\partial W}{\partial\beta}+\tau_{\alpha\gamma}'\frac{1}{AB}k_2\frac{\partial A}{\partial\beta}\frac{\partial}{\partial\alpha}(2k_2-k_1)\frac{\partial W}{\partial\beta}\Big\}\gamma^3$$

$$-2\mu_\beta\frac{\partial}{\partial\gamma}\left(\frac{1}{h_1}\frac{\partial U_\gamma}{\partial\beta}\right)-2(\mu_\beta-\mu_\alpha)\frac{\partial}{\partial\gamma}\left(U_\gamma\frac{\partial h_1^{-1}}{\partial\beta}\right)$$

$$+h_2\frac{\partial}{\partial\gamma}\left(\frac{\sigma_{\beta\gamma}}{h_1h_2^2}\right)+\frac{P_\beta}{h_1h_2}=0 \qquad (24)$$

$$\Big\{-\Big[(\tau_\alpha+2\mu_\alpha)+(\tau_\beta+2\mu_\beta)\Big]\ HAB\,\Delta_o + 2\mu_\alpha\frac{\partial}{\partial\alpha}(k_2BU)$$

$$+2\mu_\beta\frac{\partial}{\partial\beta}(k_1AV) - \Big[(\tau_\alpha+2\mu_\alpha)-(\tau_\beta+2\mu_\beta)\Big]\ LAB\Delta_o$$

$$-2(\mu_\alpha-\mu_\beta)k_2B\frac{\partial U}{\partial\alpha} - 2(\mu_\beta-\mu_\alpha)k_1A\frac{\partial V}{\partial\beta}$$

$$+\tau_{\alpha\gamma}k_1\frac{\partial A}{\partial\beta}U + \tau_{\beta\gamma}k_2\frac{\partial A}{\partial\beta}U + \tau_{\beta\gamma}k_2\frac{\partial B}{\partial\alpha}V + \tau_{\alpha\gamma}k_1\frac{\partial B}{\partial\alpha}V$$

$$-\tau_{\alpha\gamma}Ak_1\frac{\partial U}{\partial\beta} - \tau_{\beta\gamma}Ak_2\frac{\partial U}{\partial\beta} - \tau_{\beta\gamma}Bk_2\frac{\partial V}{\partial\alpha} - \tau_{\alpha\gamma}Bk_1\frac{\partial V}{\partial\alpha}\Big\}$$

$$+\Big\{-\Big[(\tau_\alpha+2\mu_\alpha)+(\tau_\beta+2\mu_\beta)\Big]AB\,(K\Delta_o+H\Delta_1)$$

$$+2\mu_\alpha\frac{\partial}{\partial\alpha}(KBU) - 2\mu_\alpha\frac{\partial}{\partial\alpha}\Big(\frac{B}{A}k_2\frac{\partial W}{\partial\alpha}\Big) + 2\mu_\beta\frac{\partial}{\partial\beta}(KAV)$$

$$-2\mu_\beta\frac{\partial}{\partial\beta}\Big(\frac{A}{B}k_1\frac{\partial W}{\partial\beta}\Big) - \Big[(\tau_\alpha+2\mu_\alpha)-(\tau_\beta+2\mu_\beta)\Big]\ LAB\Delta_1$$

$$-2(\mu_\alpha-\mu_\beta)k_2B\frac{\partial}{\partial\alpha}(k_1U) + 2(\mu_\alpha-\mu_\beta)k_2B\frac{\partial}{\partial\alpha}\Big(\frac{1}{A}\frac{\partial W}{\partial\alpha}\Big)$$

$$-2(\mu_\beta-\mu_\alpha)k_1A\frac{\partial}{\partial\beta}(k_2V) + 2(\mu_\beta-\mu_\alpha)k_1A\frac{\partial}{\partial\beta}\Big(\frac{1}{B}\frac{\partial W}{\partial\beta}\Big)$$

$$+\tau_{\alpha\gamma}Ak_1\frac{\partial k_1}{\partial\beta}U + \tau_{\beta\gamma}(k_1-k_2)k_2\frac{\partial A}{\partial\beta}U + \tau_{\beta\gamma}Ak_2\frac{\partial k_1}{\partial\beta}U$$

$$+\tau_{\alpha\gamma}k_1\frac{\partial A}{\partial\beta}\Big(k_1U-\frac{1}{A}\frac{\partial W}{\partial\alpha}\Big) + \tau_{\beta\gamma}k_2\frac{\partial A}{\partial\beta}\Big(k_1U-\frac{1}{A}\frac{\partial W}{\partial\alpha}\Big)$$

$$+\tau_{\beta\gamma}Bk_2\frac{\partial k_2}{\partial\alpha}V + \tau_{\alpha\gamma}(k_2-k_1)k_1\frac{\partial B}{\partial\alpha}V + \tau_{\alpha\gamma}Bk_1\frac{\partial k_2}{\partial\alpha}V$$

$$+\tau_{\beta\gamma}k_2\frac{\partial B}{\partial\alpha}\Big(k_2V-\frac{1}{B}\frac{\partial W}{\partial\beta}\Big) + \tau_{\alpha\gamma}k_1\frac{\partial B}{\partial\alpha}\Big(k_2V-\frac{1}{B}\frac{\partial W}{\partial\beta}\Big)$$

$$-\tau_{\beta\gamma}A(k_1-k_2)k_2\frac{\partial U}{\partial\beta} - \tau_{\alpha\gamma}Ak_1\frac{\partial}{\partial\beta}\Big(k_1U-\frac{1}{A}\frac{\partial W}{\partial\alpha}\Big)$$

$$-\tau_{\beta\gamma}Ak_2\frac{\partial}{\partial\beta}\Big(k_1U-\frac{1}{A}\frac{\partial W}{\partial\alpha}\Big) - \tau_{\alpha\gamma}B(k_2-k_1)\frac{\partial V}{\partial\alpha}$$

$$
\begin{aligned}
& - \tau_{\beta\gamma} B k_2 \frac{\partial}{\partial\alpha}\left(k_2 V - \frac{1}{B}\frac{\partial W}{\partial\beta}\right) - \tau_{\alpha\gamma} B k_2 \frac{\partial}{\partial\alpha}\left(k_2 V - \frac{1}{B}\frac{\partial W}{\partial\beta}\right)\Bigg\}\gamma \\
& + \Bigg\{ - \left[(\tau_\alpha + 2\mu_\alpha) + (\tau_\beta + 2\mu_\beta)\right] KAB\Delta_1 + \tau_{\alpha\gamma} A k_1{}^2 \frac{\partial k_1}{\partial\beta} U \\
& + \tau_{\beta\gamma} A(2k_1 - k_2) k_2 \frac{\partial k_1}{\partial\beta} U + \tau_{\alpha\gamma} A k_1 \frac{\partial k_1}{\partial\beta}\left(k_1 U - \frac{1}{A}\frac{\partial W}{\partial\alpha}\right) \\
& + \tau_{\beta\gamma}(k_1 - k_2) k_2 \frac{\partial A}{\partial\beta}\left(k_1 U - \frac{1}{A}\frac{\partial W}{\partial\alpha}\right) + \tau_{\beta\gamma} A k_2 \frac{\partial k_1}{\partial\beta}\left(k_1 U - \frac{1}{A}\frac{\partial W}{\partial\alpha}\right) \\
& + \tau_{\beta\gamma} B k_2{}^2 \frac{\partial k_2}{\partial\alpha} V + \tau_{\alpha\gamma} B(2k_2 - k_1) k_1 \frac{\partial k_2}{\partial\alpha} V \\
& + \tau_{\beta\gamma} B k_2 \frac{\partial k_2}{\partial\alpha}\left(k_2 V - \frac{1}{B}\frac{\partial W}{\partial\beta}\right) + \tau_{\alpha\gamma}(k_2 - k_1) k_1 \frac{\partial B}{\partial\alpha}\left(k_2 V - \frac{1}{B}\frac{\partial W}{\partial\beta}\right) \\
& + \tau_{\alpha\gamma} B k_1 \frac{\partial k_2}{\partial\alpha}\left(k_2 V - \frac{1}{B}\frac{\partial W}{\partial\beta}\right) \\
& - \tau_{\beta\gamma} A(k_1 - k_2) k_2 \frac{\partial}{\partial\beta}\left(k_1 U - \frac{1}{A}\frac{\partial W}{\partial\alpha}\right) \\
& - \tau_{\alpha\gamma} B(k_2 - k_1) k_1 \frac{\partial}{\partial\alpha}\left(k_2 V - \frac{1}{B}\frac{\partial W}{\partial\beta}\right)\Bigg\}\gamma^2 \\
& + \Bigg\{\tau_{\alpha\gamma} A k_1{}^2 \frac{\partial k_1}{\partial\beta}\left(k_1 U - \frac{1}{A}\frac{\partial W}{\partial\alpha}\right) + \tau_{\beta\gamma} A(2k_1 - k_2) k_2 \frac{\partial k_1}{\partial\beta}\left(k_1 U - \frac{1}{A}\frac{\partial W}{\partial\alpha}\right) \\
& + \tau_{\beta\gamma} B k_2{}^2 \frac{\partial k_2}{\partial\alpha}\left(k_2 V - \frac{1}{B}\frac{\partial W}{\partial\beta}\right) + \tau_{\alpha\gamma} B(2k_2 - k_1) k_1 \frac{\partial k_1}{\partial\alpha}\left(k_2 V - \frac{1}{B}\frac{\partial W}{\partial\beta}\right)\Bigg\}\gamma^3 \\
& + 2(\mu_\alpha + \mu_\beta) KABU_\gamma + 2(\mu_\alpha + \mu_\beta) HAB \frac{\partial U_\gamma}{\partial\gamma} \\
& + 2(\mu_\alpha + \mu_\beta) KAB \frac{\partial U_\gamma}{\partial\gamma}\gamma + 2(\mu_\alpha - \mu_\beta) LAB \frac{\partial U_\gamma}{\partial\gamma} \\
& + \frac{\partial}{\partial\alpha}\left(\frac{\sigma_{\alpha\gamma}}{h_2}\right) + \frac{\partial}{\partial\beta}\left(\frac{\sigma_{\beta\gamma}}{h_1}\right) + \frac{\partial}{\partial\gamma}\left(\frac{\sigma_\gamma}{h_1 h_2}\right) + \frac{P_\gamma}{h_1 h_2} = 0 \qquad (25)
\end{aligned}
$$

where

$$H = \frac{k_1+k_2}{2}$$

$$K = k_1 k_2$$

$$L = \frac{k_1-k_2}{2}$$

$$2\chi = h_1 h_2 \left[\frac{\partial}{\partial\alpha}\left(\frac{U\beta}{h_2}\right) - \frac{\partial}{\partial\beta}\left(\frac{U\alpha}{h_1}\right)\right] \tag{26}$$

In the development of Equations (23), (24), and (25), certain simplifications have been made which are in agreement with those generally used in thin shell theory.

In thin shell theory, the assumption is made that the quantity $k\,\delta$, representing the ratio of the shell thickness to some middle surface curvature, is quite small with respect to unity. In reality, this is a limiting statement regarding the range of relative thicknesses for which the theory could be expected to yield results within some acceptable margin of accuracy. Fortunately, the great majority of structural shells that are of interest to engineers fit well within this range. The quantities h_1 and h_2 appearing in the numerators of the double-scripted τ terms were therefore expanded in the following manner and truncated after the term of order $k\,\gamma$:

$$h_1 = \frac{1}{A(1+k_1\gamma)} = \frac{1}{A}\left(1-k_1\gamma + k_1^{\,2}\gamma^{\,2} - k_1^{\,3}\gamma^{\,3} + \ldots\right)$$

$$\approx \frac{1}{A}\left(1-k_1\gamma\right)$$

$$h_2 = \frac{1}{B(1+k_2\gamma)} = \frac{1}{B}(1-k_2\gamma + k_2^{\,2}\gamma^2 - k_2^{\,3}\gamma^3 + \ldots)$$

$$\approx \frac{1}{B}(1-k_2\gamma)$$

Consider next the quantities Δ and χ. The volume dilitation is equal to the sum of the normal strains e_α, e_β, and e_γ. Within the limitations of first order theory, the strains e_α and e_β are found to be linear functions of γ. Furthermore, it will be shown later that the strain e_γ is also a linear function of γ. It follows that the volume dilitation can be expressed as a linear function of γ without introducing greater errors than are already present. A similar argument will hold for the normal rotation. Kozik [3] established that the normal rotation is of the same or smaller order of magnitude as the shearing strain $e_{\alpha\beta}$. As a matter of fact, the normal rotation is expressible as the difference of two quantities whose sum is the shearing strain. As in the case of normal strains, the shearing strain is given as a linear function of γ. It follows that the normal rotation can also be expressed as a linear function of γ. The quantities Δ and χ were therefore written as follows:

$$\begin{aligned} \Lambda &= \Lambda_o + \Delta_1 \gamma \\ \chi &= \chi_o + \chi_1 \gamma \end{aligned} \tag{27}$$

where the coefficients Δ_o, Δ_1, χ_o, and χ_1 are constants whose values will be determined later.

The above arguments do not apply to the quantities U_γ, $\sigma_{\gamma\alpha}$, or $\sigma_{\gamma\beta}$ so they are carried as they are for the present.

Equations (23), (24), and (25) represent the equilibrium conditions for an element within the shell. If each of these equations is multiplied by $d\alpha d\beta d\gamma$, then the equations will represent the resultant forces on an infinitesimal element in the α, β, and γ directions, respectively. The corresponding dimensions of the element will be $A(1 + k_1\gamma)\,d\alpha$, $B(1 + k_2\gamma)d\beta$, and $d\gamma$. Subsequent integration of the three equations with respect to γ between the limits of $-\delta/2$ and $\delta/2$ will therefore yield the resultant forces in the α, β, and γ directions acting on an element of thickness δ and having dimensions of $Ad\alpha$ and $Bd\beta$ at the middle surface.

If Equations (23) and (24) are multiplied by $\gamma\,d\alpha\;d\beta\;d\gamma$, they will represent the moments about tangents to the β and α coordinates, respectively, due to forces acting on the shell element. Subsequent integration with respect to γ from $-\delta/2$ to $\delta/2$ will then yield the resultant moments about tangents to β and α, coordinates acting on an element of thickness δ and having dimensions of $Ad\alpha$ and $Bd\beta$ at the middle surface.

Moments will not be taken about the γ coordinate since this would yield no new information about the shell.

Integration of Equations (23), (24), and (25) according to the scheme presented above results in the following set of equilibrium equations:

$$\Big\{ (\tau_\alpha + 2\mu_\alpha) B \frac{\partial \Delta_0}{\partial\alpha} - 2\mu_{\alpha\beta} A \frac{\partial \chi_0}{\partial\beta} + 2\mu_\alpha ABK\, U$$

$$+ \Big[(\tau_\alpha+2\mu_\alpha) - (\tau_\beta+2\mu_\beta)\Big] \frac{\partial B}{\partial\alpha}\Delta_0 + 2(\mu_\alpha - \mu_{\alpha\beta}) \frac{\partial}{\partial\beta}\left(\frac{1}{B}\frac{\partial A}{\partial\beta}\right) U$$

$$-2(\mu_\alpha-\mu_\beta)\frac{1}{A} \frac{\partial B}{\partial\alpha}\frac{\partial U}{\partial\alpha} - 2(\mu_\alpha-\mu_{\alpha\beta})\frac{\partial^2 V}{\partial\alpha\partial\beta}$$

$$+2(\mu_\beta - \mu_{\alpha\beta})\frac{1}{AB}\frac{\partial A}{\partial\beta}\frac{\partial B}{\partial\alpha} V - \tau_{\alpha\gamma}\frac{\partial}{\partial\alpha}\left(\frac{1}{A}\frac{\partial A}{\partial\beta}\right)U + \tau_{\beta\gamma}\frac{1}{AB}\frac{\partial B}{\partial\alpha}\frac{\partial A}{\partial\beta} U$$

$$+ \tau'_{\beta\gamma}\frac{1}{A}\frac{\partial}{\partial\beta}\left(\frac{A}{B}\frac{\partial B}{\partial\alpha}\right)U - (\tau_{\alpha\gamma}+\tau'_{\alpha\gamma})\frac{1}{A}\frac{\partial A}{\partial\beta}\frac{\partial U}{\partial\alpha} + (\tau'_{\beta\gamma}-\tau_{\beta\gamma})\frac{1}{B}\frac{\partial B}{\partial\alpha}\frac{\partial U}{\partial\beta}$$

$$+ (\tau_{\alpha\gamma}+\tau'_{\alpha\gamma})\frac{\partial^2 U}{\partial\alpha\partial\beta} - \tau_{\alpha\gamma}\frac{\partial}{\partial\alpha}\left(\frac{1}{A}\frac{\partial B}{\partial\alpha}\right)V + \tau_{\beta\gamma}\frac{1}{AB}\left(\frac{\partial B}{\partial\alpha}\right)^2 V$$

$$+ \tau'_{\alpha\gamma}\frac{1}{A}\frac{\partial}{\partial\beta}\left(\frac{A}{B}\frac{\partial A}{\partial\beta}\right)V - \tau_{\alpha\gamma}\frac{B}{A^2}\frac{\partial A}{\partial\beta}\frac{\partial V}{\partial\alpha} - \tau_{\beta\gamma}\frac{1}{A}\frac{\partial B}{\partial\alpha}\frac{\partial V}{\partial\alpha}$$

$$+ \tau'_{\alpha\gamma}\frac{1}{B}\frac{\partial A}{\partial\beta}\frac{\partial V}{\partial\beta} + \tau'_{\beta\gamma}\frac{1}{A}\frac{\partial}{\partial\beta}\left(\frac{A^2}{B}\right)\frac{\partial V}{\partial\beta} + \tau_{\alpha\gamma}\frac{B}{A}\frac{\partial^2 V}{\partial\alpha^2}$$

$$+ \tau'_{\beta\gamma}\frac{A}{B}\frac{\partial^2 V}{\partial\beta^2}\Big\} + \Big\{(\tau_\alpha+2\mu_\alpha) Bk_2\frac{\partial\Delta_1}{\partial\alpha} - 2\mu_{\alpha\beta}Ak_1\frac{\partial\chi_1}{\partial\beta}$$

$$+ \Big[(\tau_\alpha+2\mu_\alpha)-(\tau_\beta+2\mu_\beta)\Big] k_1\frac{\partial B}{\partial\alpha}\Delta_1 - \tau_{\alpha\gamma}\frac{\partial k_1}{\partial\beta}\frac{\partial k_1}{\partial\alpha} U$$

$$+ \tau'_{\beta\gamma}\frac{1}{B}\frac{\partial B}{\partial\alpha}\frac{\partial}{\partial\beta}(2k_1-k_2)U - \tau_{\alpha\gamma}\frac{B}{A}\frac{\partial k_2}{\partial\alpha}\frac{\partial}{\partial\alpha}(2k_2-k_1)V$$

$$+ \tau_{\alpha\gamma}\frac{\partial^2 k_1}{\partial\alpha\partial\beta}\frac{1}{A}\frac{\partial W}{\partial\alpha} - \tau_{\beta\gamma}\frac{1}{AB}\frac{\partial B}{\partial\alpha}\frac{\partial k_1}{\partial\beta}\frac{\partial W}{\partial\alpha} - \tau_{\alpha\gamma}\frac{1}{A^2}\frac{\partial k_1}{\partial\beta}\frac{\partial A}{\partial\alpha}\frac{\partial W}{\partial\alpha}$$

$$- \tau_{\alpha\gamma}\frac{1}{B}(k_1-k_2)\frac{\partial}{\partial\alpha}\left(\frac{1}{A}\frac{\partial B}{\partial\alpha}\right)\frac{\partial W}{\partial\beta} + \tau_{\alpha\gamma}\frac{\partial}{\partial\alpha}\left(\frac{B}{A}\frac{\partial k_2}{\partial\alpha}\right)\frac{1}{B}\frac{\partial W}{\partial\beta}$$

$$- \tau_{\beta\gamma}\frac{1}{AB}\frac{\partial B}{\partial\alpha}\frac{\partial k_2}{\partial\alpha}\frac{\partial W}{\partial\beta} + \tau'_{\alpha\gamma}\frac{1}{B^2}\frac{\partial A}{\partial\beta}\frac{\partial k_1}{\partial\beta}\frac{\partial W}{\partial\beta} - \tau_{\alpha\gamma}\frac{1}{AB}\frac{\partial k_1}{\partial\alpha}\frac{\partial B}{\partial\alpha}\frac{\partial W}{\partial\beta}$$

$$+ \tau'_{\beta\gamma}\frac{A}{B^3}\frac{\partial}{\partial\beta}(2k_1-k_2)\frac{\partial B}{\partial\beta}\frac{\partial W}{\partial\beta} + \tau_{\alpha\gamma}\frac{1}{B}\frac{\partial B}{\partial\alpha}\frac{\partial}{\partial\alpha}\left(\frac{k_1-k_2}{A}\right)\frac{\partial W}{\partial\beta}$$

$$+ \tau_{\alpha\gamma}\frac{1}{A}\frac{\partial k_1}{\partial\beta}\frac{\partial^2 W}{\partial\alpha^2} - \tau'_{\beta\gamma}\frac{A}{B^2}\frac{\partial}{\partial\beta}(2k_1-k_2)\frac{\partial^2 W}{\partial\beta^2}$$

$$-\tau_{\alpha\gamma}\frac{1}{A^2}(k_1-k_2)\frac{\partial A}{\partial\alpha}\frac{\partial^2 W}{\partial\alpha\partial\beta}+\tau_{\alpha\gamma}\frac{1}{A}\frac{\partial k_1}{\partial\alpha}\frac{\partial^2 W}{\partial\alpha\partial\beta}\Bigg\}\frac{\delta^2}{12}$$

$$-\frac{2\mu_\alpha}{\delta}\int_{-\delta/2}^{\delta/2}\frac{\partial}{\partial\gamma}\left(\frac{1}{h_2}\frac{\partial U_\gamma}{\partial\alpha}\right)d\gamma-2\frac{(\mu_\alpha-\mu_\beta)}{\delta}\int_{-\delta/2}^{\delta/2}\frac{\partial}{\partial\gamma}\left(U_\gamma\frac{\partial H_2^{-1}}{\partial\alpha}\right)d\gamma$$

$$+\frac{1}{\delta}\left\{\tau_{\alpha\gamma}'(k_1+k_2)\frac{\partial A}{\partial\beta}+\tau_{\beta\gamma}'\frac{\partial}{\partial\beta}(Ak_2)+\tau_{\beta\gamma}'\frac{1}{B}\frac{\partial A}{\partial\beta}\right\}\int_{-\delta/2}^{\delta/2}U_\gamma\,d\gamma$$

$$+\frac{1}{\delta}\left\{\tau_{\alpha\gamma}'Ak_1+\tau_{\beta\gamma}'Ak_2\right\}\int_{-\delta/2}^{\delta/2}\frac{\partial U_\gamma}{\partial\beta}d\gamma$$

$$+\frac{1}{\delta}\tau_{\beta\gamma}'\;Ak_2\frac{\partial}{\partial\beta}(2k_1-k_2)\int_{-\delta/2}^{\delta/2}\gamma U_\gamma\,d\gamma+\frac{ABk_1}{\delta}Q_\alpha$$

$$+\frac{AB}{\delta}P_\alpha\quad=0\tag{28}$$

$$\Bigg\{(\tau_\beta+2\mu_\beta)A\frac{\partial\Delta_0}{\partial\beta}+2\mu_{\alpha\beta}B\frac{\partial\chi_0}{\partial\alpha}+2\mu_\beta ABKV$$

$$+\left[(\tau_\beta+2\mu_\beta)-(\tau_\alpha+2\mu_\alpha)\right]\frac{\partial A}{\partial\beta}\Delta_0+2(\mu_\beta-\mu_{\alpha\beta})\frac{\partial}{\partial\alpha}\left(\frac{1}{A}\frac{\partial B}{\partial\alpha}\right)V$$

$$-2(\mu_\beta-\mu_\alpha)\frac{1}{B}\frac{\partial A}{\partial\beta}\frac{\partial V}{\partial\beta}-2(\mu_\beta-\mu_{\alpha\beta})\frac{\partial^2 U}{\partial\alpha\partial\beta}$$

$$+2(\mu_\alpha-\mu_{\alpha\beta})\frac{1}{AB}\frac{\partial B}{\partial\alpha}\frac{\partial A}{\partial\beta}U-\tau_{\beta\gamma}\frac{\partial}{\partial\beta}\left(\frac{1}{B}\frac{\partial B}{\partial\alpha}\right)V+\tau_{\alpha\gamma}\frac{1}{AB}\frac{\partial A}{\partial\beta}\frac{\partial B}{\partial\alpha}V$$

$$+\tau'_{\alpha\gamma}\frac{1}{B}\frac{\partial}{\partial\alpha}\left(\frac{B}{A}\frac{\partial A}{\partial\beta}\right)V-(\tau_{\beta\gamma}+\tau'_{\beta\gamma})\frac{1}{B}\frac{\partial B}{\partial\alpha}\frac{\partial V}{\partial\beta}+(\tau'_{\alpha\gamma}-\tau_{\alpha\gamma})\frac{1}{A}\frac{\partial A}{\partial\beta}\frac{\partial V}{\partial\alpha}$$

$$+(\tau_{\beta\gamma}+\tau'_{\beta\gamma})\frac{\partial^2 V}{\partial\alpha\partial\beta}-\tau_{\beta\gamma}\frac{\partial}{\partial\beta}\left(\frac{1}{B}\frac{\partial A}{\partial\beta}\right)U+\tau_{\alpha\gamma}\frac{1}{AB}\left(\frac{\partial A}{\partial\beta}\right)^2 U$$

$$+\tau'_{\beta\gamma}\frac{1}{B}\frac{\partial}{\partial\alpha}\left(\frac{B}{A}\frac{\partial B}{\partial\alpha}\right)U-\tau_{\beta\gamma}\frac{A}{B^2}\frac{\partial B}{\partial\alpha}\frac{\partial U}{\partial\beta}-\tau_{\alpha\gamma}\frac{1}{B}\frac{\partial A}{\partial\beta}\frac{\partial U}{\partial\beta}$$

$$+\tau'_{\beta\gamma}\frac{1}{A}\frac{\partial B}{\partial\alpha}\frac{\partial U}{\partial\alpha}+\tau'_{\alpha\gamma}\frac{1}{B}\frac{\partial}{\partial\alpha}\left(\frac{B^2}{A}\right)\frac{\partial U}{\partial\alpha}+\tau_{\beta\gamma}\frac{A}{B}\frac{\partial^2 U}{\partial\beta^2}$$

$$+\tau'_{\alpha\gamma}\frac{B}{A}\frac{\partial^2 U}{\partial\alpha^2}\Bigg\}+\Bigg\{(\tau_\beta+2\mu_\beta)Ak_1\frac{\partial\Delta_1}{\partial\beta}+2\mu_{\alpha\beta}Bk_2\frac{\partial\chi_1}{\partial\alpha}$$

$$+\left[(\tau_\beta+2\mu_\beta)-(\tau_\alpha+2\mu_\alpha)\right]k_2\frac{\partial A}{\partial\beta}\Delta_1-\tau_{\beta\gamma}\frac{\partial k_2}{\partial\alpha}\frac{\partial k_2}{\partial\beta}V$$

$$+\tau'_{\alpha\gamma}\frac{1}{A}\frac{\partial A}{\partial\beta}\frac{\partial}{\partial\alpha}(2k_2-k_1)V-\tau_{\beta\gamma}\frac{A}{B}\frac{\partial k_1}{\partial\beta}\frac{\partial}{\partial\beta}(2k_1-k_2)U$$

$$+\tau_{\beta\gamma}\frac{\partial^2 k_2}{\partial\alpha\partial\beta}\frac{1}{B}\frac{\partial W}{\partial\beta}-\tau_{\alpha\gamma}\frac{1}{AB}\frac{\partial A}{\partial\beta}\frac{\partial k_2}{\partial\alpha}\frac{\partial W}{\partial\beta}-\tau_{\beta\gamma}\frac{1}{B^2}\frac{\partial k_2}{\partial\alpha}\frac{\partial B}{\partial\beta}\frac{\partial W}{\partial\beta}$$

$$-\tau_{\beta\gamma}\frac{1}{A}(k_2-k_1)\frac{\partial}{\partial\beta}\left(\frac{1}{B}\frac{\partial A}{\partial\beta}\right)\frac{\partial W}{\partial\alpha}+\tau_{\beta\gamma}\frac{\partial}{\partial\beta}\left(\frac{A}{B}\frac{\partial k_1}{\partial\beta}\right)\frac{1}{A}\frac{\partial W}{\partial\alpha}$$

$$-\tau_{\alpha\gamma}\frac{1}{AB}\frac{\partial A}{\partial\beta}\frac{\partial k_1}{\partial\beta}\frac{\partial W}{\partial\alpha}+\tau'_{\beta\gamma}\frac{1}{A^2}\frac{\partial B}{\partial\alpha}\frac{\partial k_2}{\partial\alpha}\frac{\partial W}{\partial\alpha}-\tau_{\beta\gamma}\frac{1}{AB}\frac{\partial k_2}{\partial\beta}\frac{\partial A}{\partial\beta}\frac{\partial W}{\partial\alpha}$$

$$+\tau'_{\alpha\gamma}\frac{B}{A^3}\frac{\partial}{\partial\alpha}(2k_2-k_1)\frac{\partial A}{\partial\alpha}\frac{\partial W}{\partial\alpha}+\tau_{\beta\gamma}\frac{1}{A}\frac{\partial A}{\partial\beta}\frac{\partial}{\partial\beta}\left(\frac{k_2-k_1}{B}\right)\frac{\partial W}{\partial\alpha}$$

$$+\tau_{\beta\gamma}\frac{1}{B}\frac{\partial k_2}{\partial\alpha}\frac{\partial^2 W}{\partial\beta^2}-\tau'_{\alpha\gamma}\frac{B}{A^2}\frac{\partial}{\partial\alpha}(2k_2-k_1)\frac{\partial^2 W}{\partial\alpha^2}$$

$$-\tau_{\beta\gamma}\frac{1}{B^2}(k_2-k_1)\frac{\partial B}{\partial\beta}\frac{\partial^2 W}{\partial\alpha\partial\beta}+\tau_{\beta\gamma}\frac{1}{B}\frac{\partial k_2}{\partial\beta}\frac{\partial^2 W}{\partial\alpha\partial\beta}\Bigg\}\frac{\delta^2}{12}$$

$$-\frac{2\mu_\beta}{\delta}\int_{-\delta/2}^{\delta/2}\frac{\partial}{\partial\gamma}\left(\frac{1}{h_2}\frac{\partial U_\gamma}{\partial\beta}\right)d\gamma-2\frac{(\mu_\beta-\mu_\alpha)}{\delta}\int_{-\delta/2}^{\delta/2}\frac{\partial}{\partial\gamma}\left(U_\gamma\frac{\partial h_1^{-1}}{\partial\beta}\right)d\gamma$$

$$+\frac{1}{\delta}\left\{\tau_{\beta\gamma}'(k_1+k_2)\frac{\partial B}{\partial\alpha}+\tau_{\alpha\gamma}'\frac{\partial}{\partial\alpha}(Bk_1)+\tau_{\alpha\gamma}'\frac{1}{A}\frac{\partial B}{\partial\alpha}\right\}\int_{-\delta/2}^{\delta/2}U_\gamma\,d\gamma$$

$$+\frac{1}{\delta}\left\{\tau_{\beta\gamma}'Bk_2+\tau_{\alpha\gamma}'Bk_1\right\}\int_{-\delta/2}^{\delta/2}\frac{\partial U_\gamma}{\partial\alpha}\,d\gamma$$

$$+\frac{1}{\delta}\tau_{\alpha\gamma}'Bk_1\frac{\partial}{\partial\alpha}(2k_2-k_1)\int_{-\delta/2}^{\delta/2}\gamma U_\gamma\,d\gamma+\frac{ABk_2}{\delta}Q_\beta$$

$$+\frac{AB}{\delta}P_\beta=0 \qquad (29)$$

$$\Big\{-\left[(\tau_\alpha+2\mu_\alpha)+(\tau_\beta+2\mu_\beta)\right]HAB\Delta_o+2\mu_\alpha\frac{\partial}{\partial\alpha}(k_2BU)$$

$$+2\mu_\beta\frac{\partial}{\partial\beta}(k_1AV)-\left[(\tau_\alpha+2\mu_\alpha)-(\tau_\beta+2\mu_\beta)\right]LAB\Delta_o$$

$$-2(\mu_\alpha-\mu_\beta)k_2B\frac{\partial U}{\partial\alpha}-2(\mu_\beta-\mu_\alpha)k_1A\frac{\partial V}{\partial\beta}$$

$$+\tau_{\alpha\gamma}k_1\frac{\partial A}{\partial\beta}U+\tau_{\beta\gamma}k_2\frac{\partial A}{\partial\beta}U+\tau_{\beta\gamma}k_2\frac{\partial B}{\partial\alpha}V+\tau_{\alpha\gamma}k_1\frac{\partial B}{\partial\alpha}V$$

$$-\tau_{\alpha\gamma}Ak_1\frac{\partial U}{\partial\beta}-\tau_{\beta\gamma}Ak_2\frac{\partial U}{\partial\beta}-\tau_{\beta\gamma}Bk_2\frac{\partial V}{\partial\alpha}-\tau_{\alpha\gamma}Bk_1\frac{\partial V}{\partial\alpha}\Big\}$$

$$+\Big\{\left[(\tau_\alpha+2\mu_\alpha)+(\tau_\beta+2\mu_\beta)\right]KAB\Delta_1-\tau_{\alpha\gamma}k_1\frac{\partial k_1}{\partial\beta}\frac{\partial W}{\partial\alpha}-\tau_{\beta\gamma}k_2\frac{\partial k_1}{\partial\beta}\frac{\partial W}{\partial\alpha}$$

$$-\tau_{\beta\gamma}k_2\frac{\partial k_2}{\partial\alpha}\frac{\partial W}{\partial\beta}-\tau_{\alpha\gamma}k_1\frac{\partial k_2}{\partial\alpha}\frac{\partial W}{\partial\beta}\Big\}\frac{\delta^2}{12}$$

$$+2(\mu_\alpha+\mu_\beta)\frac{KAB}{\delta}\int_{-\delta/2}^{\delta/2} U_\gamma d\gamma + 2(\mu_\alpha+\mu_\beta)\frac{HAB}{\delta}\int_{-\delta/2}^{\delta/2}\frac{\partial U_\gamma}{\partial\gamma}d\gamma$$

$$+2(\mu_\alpha+\mu_\beta)\frac{KAB}{\delta}\int_{-\delta/2}^{\delta/2}\gamma\frac{\partial U_\gamma}{\partial\gamma}d\gamma + 2(\mu_\alpha-\mu_\beta)\frac{LAB}{\delta}\int_{-\delta/2}^{\delta/2}\frac{\partial U_\gamma}{\partial\gamma}d\gamma$$

$$+\frac{\partial}{\partial\alpha}\left(\frac{BQ_\alpha}{\delta}\right)+\frac{\partial}{\partial\beta}\left(\frac{AQ_\beta}{\delta}\right)+\frac{ABP_\gamma}{\delta}=0 \qquad (30)$$

$$\Big\{(\tau_\alpha+2\mu_\alpha)Bk_2\frac{\partial\Delta_0}{\partial\alpha}+(\tau_\alpha+2\mu_\alpha)B\frac{\partial\Delta_1}{\partial\alpha}-2\mu_{\alpha\beta}Ak_1\frac{\partial\chi_0}{\partial\beta}$$

$$-2\mu_{\alpha\beta}A\frac{\partial\chi_1}{\partial\beta}+2\mu_\alpha ABKk_1U-2\mu_\alpha BK\frac{\partial W}{\partial\alpha}$$

$$+\Big[(\tau_\alpha+2\mu_\alpha)-(\tau_\beta+2\mu_\beta)\Big]k_1\frac{\partial B}{\partial\alpha}\Delta_0+\Big[(\tau_\alpha+2\mu_\alpha)-(\tau_\beta+2\mu_\beta)\Big]\frac{\partial B}{\partial\alpha}\Delta_1$$

$$+2(\mu_\alpha-\mu_{\alpha\beta})k_1\frac{\partial}{\partial\beta}\left(\frac{1}{B}\frac{\partial A}{\partial\beta}\right)U-2(\mu_\alpha-\mu_{\alpha\beta})\frac{1}{A}\frac{\partial}{\partial\beta}\left(\frac{1}{B}\frac{\partial A}{\partial\beta}\right)\frac{\partial W}{\partial\alpha}$$

$$-2(\mu_\alpha-\mu_\beta)\frac{1}{A}\frac{\partial B}{\partial\alpha}\frac{\partial}{\partial\alpha}(k_1U)+2(\mu_\alpha-\mu_\beta)\frac{1}{A}\frac{\partial B}{\partial\alpha}\frac{\partial}{\partial\alpha}\left(\frac{1}{A}\frac{\partial W}{\partial\alpha}\right)$$

$$-2(\mu_\alpha-\mu_{\alpha\beta})\frac{\partial^2}{\partial\alpha\partial\beta}(k_2V)+2(\mu_\alpha-\mu_{\alpha\beta})\frac{\partial^2}{\partial\alpha\partial\beta}\left(\frac{1}{B}\frac{\partial W}{\partial\beta}\right)$$

$$+2(\mu_\beta-\mu_{\alpha\beta})\frac{k_2}{AB}\frac{\partial A}{\partial\beta}\frac{\partial B}{\partial\alpha}V-2(\mu_\beta-\mu_{\alpha\beta})\frac{1}{AB^2}\frac{\partial A}{\partial\beta}\frac{\partial B}{\partial\alpha}\frac{\partial W}{\partial\beta}$$

$$-\tau_{\alpha\gamma}\frac{\partial^2k_1}{\partial\alpha\partial\beta}U+\tau_{\beta\gamma}\frac{1}{B}\frac{\partial B}{\partial\alpha}\frac{\partial k_1}{\partial\beta}U+\tau_{\alpha\gamma}\frac{1}{A}\frac{\partial B}{\partial\alpha}\frac{\partial}{\partial\alpha}(k_1-k_2)V$$

$$
- \tau_{\alpha\gamma} \frac{\partial}{\partial \alpha}\left(\frac{B}{A} \frac{\partial k_2}{\partial \alpha}\right) V + \tau_{\beta\gamma} \frac{1}{A} \frac{\partial B}{\partial \alpha} \frac{\partial k_2}{\partial \alpha} V + \tau'_{\alpha\gamma} \frac{1}{B} \frac{\partial A}{\partial \beta} \frac{\partial k_1}{\partial \beta} V
$$

$$
- \tau_{\alpha\gamma} \frac{\partial k_1}{\partial \beta} \frac{\partial U}{\partial \alpha} - \tau_{\alpha\gamma} \frac{B}{A} \frac{\partial k_1}{\partial \alpha} \frac{\partial V}{\partial \alpha} + \tau'_{\beta\gamma} \frac{A}{B} \frac{\partial}{\partial \beta} (2k_1 - k_2) \frac{\partial V}{\partial \beta}
$$

$$
+ \tau_{\alpha\gamma} \frac{\partial}{\partial \alpha}\left(\frac{1}{A} \frac{\partial A}{\partial \beta}\right) \frac{1}{A} \frac{\partial W}{\partial \alpha} - \tau_{\beta\gamma} \frac{1}{A^2 B} \frac{\partial B}{\partial \alpha} \frac{\partial A}{\partial \beta} \frac{\partial W}{\partial \alpha}
$$

$$
- \tau'_{\beta\gamma} \frac{1}{A^2} \frac{\partial}{\partial \beta}\left(\frac{A}{B} \frac{\partial B}{\partial \alpha}\right) \frac{\partial W}{\partial \alpha} + \tau_{\alpha\gamma} \frac{\partial}{\partial \alpha}\left(\frac{1}{A} \frac{\partial B}{\partial \alpha}\right) \frac{1}{B} \frac{\partial W}{\partial \beta}
$$

$$
- \tau_{\beta\gamma} \frac{1}{AB^2} \left(\frac{\partial B}{\partial \alpha}\right)^2 \frac{\partial W}{\partial \beta} - \tau'_{\alpha\gamma} \frac{1}{AB} \frac{\partial}{\partial \beta}\left(\frac{A}{B} \frac{\partial A}{\partial \beta}\right) \frac{\partial W}{\partial \beta}
$$

$$
+ \tau_{\alpha\gamma} \frac{1}{A} \frac{\partial A}{\partial \beta} \frac{\partial}{\partial \alpha}\left(\frac{1}{A} \frac{\partial W}{\partial \alpha}\right) - \tau'_{\alpha\gamma} \frac{1}{A} \frac{\partial A}{\partial \beta} \frac{\partial}{\partial \alpha}\left(\frac{1}{A} \frac{\partial W}{\partial \alpha}\right)
$$

$$
- (\tau'_{\beta\gamma} - \tau_{\beta\gamma}) \frac{1}{B} \frac{\partial B}{\partial \alpha} \frac{\partial}{\partial \beta}\left(\frac{1}{A} \frac{\partial W}{\partial \alpha}\right) - (\tau_{\alpha\gamma} + \tau'_{\alpha\gamma}) \frac{\partial^2}{\partial \alpha \partial \beta}\left(\frac{1}{A} \frac{\partial W}{\partial \alpha}\right)
$$

$$
+ \tau_{\alpha\gamma} \frac{B}{A^2} \frac{\partial A}{\partial \alpha} \frac{\partial}{\partial \alpha}\left(\frac{1}{B} \frac{\partial W}{\partial \beta}\right) + \tau_{\beta\gamma} \frac{1}{A} \frac{\partial B}{\partial \alpha} \frac{\partial}{\partial \alpha}\left(\frac{1}{B} \frac{\partial W}{\partial \beta}\right)
$$

$$
- \tau'_{\alpha\gamma} \frac{1}{B} \frac{\partial A}{\partial \beta} \frac{\partial}{\partial \beta}\left(\frac{1}{B} \frac{\partial W}{\partial \beta}\right) - \tau'_{\beta\gamma} \frac{1}{A} \frac{\partial}{\partial \beta}\left(\frac{A^2}{B}\right) \frac{\partial}{\partial \beta}\left(\frac{1}{B} \frac{\partial W}{\partial \beta}\right)
$$

$$
- \tau_{\alpha\gamma} \frac{B}{A} \frac{\partial^2}{\partial \alpha^2}\left(\frac{1}{B} \frac{\partial W}{\partial \beta}\right) - \tau'_{\beta\gamma} \frac{A}{B} \frac{\partial^2}{\partial \beta^2}\left(\frac{1}{B} \frac{\partial W}{\partial \beta}\right) \Bigg\} \frac{\delta^2}{12}
$$

$$
- \frac{2\mu_\alpha}{\delta} \int_{-\delta/2}^{\delta/2} \gamma \frac{\partial}{\partial \gamma}\left(\frac{1}{h_2} \frac{\partial U_\gamma}{\partial \gamma}\right) d\gamma - \frac{2(\mu_\alpha - \mu_\beta)}{\delta} \int_{-\delta/2}^{\delta/2} \gamma \frac{\partial}{\partial \gamma}\left(U_\gamma \frac{\partial h_2^{-1}}{\partial \alpha}\right) d\gamma
$$

$$
+ \frac{1}{\delta} \left\{ \tau'_{\alpha\gamma}(k_1 + k_2) \frac{\partial A}{\partial \beta} + \tau'_{\beta\gamma} \frac{\partial}{\partial \beta}(A k_2) + \tau'_{\beta\gamma} \frac{1}{B} \frac{\partial A}{\partial \beta} \right\} \int_{-\delta/2}^{\delta/2} \gamma \, U_\gamma \, d\gamma
$$

$$+\frac{1}{\delta}\left\{\tau_{\alpha\gamma}'Ak_1+\tau_{\beta\gamma}'Ak_2\right\}\int_{-\delta/2}^{\delta/2}\gamma\,\frac{\partial U_\gamma}{\partial\beta}\,d\gamma$$

$$+\frac{1}{\delta}\tau_{\beta\gamma}'Ak_2\frac{\partial}{\partial\beta}(2k_1-k_2)\int_{-\delta/2}^{\delta/2}\gamma^2\,U_\gamma\,d\gamma-\frac{AB}{\delta}Q_\alpha=0 \qquad (31)$$

$$\Big\{(\tau_\beta+2\mu_\beta)Ak_1\frac{\partial\Delta_0}{\partial\beta}+(\tau_\beta+2\mu_\beta)A\frac{\partial\Delta_1}{\partial\beta}+2\mu_{\alpha\beta}Bk_2\frac{\partial\chi_0}{\partial\alpha}$$

$$+2\mu_{\alpha\beta}B\frac{\partial\chi_1}{\partial\alpha}+2\mu_\beta ABKk_2V-2\mu_\beta AK\frac{\partial W}{\partial\beta}$$

$$+\Big[(\tau_\beta+2\mu_\beta)-(\tau_\alpha+2\mu_\alpha)\Big]k_2\frac{\partial A}{\partial\beta}\Delta_0+\Big[(\tau_\beta+2\mu_\beta)-(\tau_\alpha+2\mu_\alpha)\Big]\frac{\partial A}{\partial\beta}\Delta_1$$

$$+2(\mu_\beta-\mu_{\alpha\beta})k_2\frac{\partial}{\partial\alpha}\left(\frac{1}{A}\frac{\partial B}{\partial\alpha}\right)V-2(\mu_\beta-\mu_{\alpha\beta})\frac{1}{B}\frac{\partial}{\partial\alpha}\left(\frac{1}{A}\frac{\partial B}{\partial\alpha}\right)\frac{\partial W}{\partial\beta}$$

$$-2(\mu_\beta-\mu_\alpha)\frac{1}{B}\frac{\partial A}{\partial\beta}\frac{\partial}{\partial\beta}(k_2V)+2(\mu_\beta-\mu_\alpha)\frac{1}{B}\frac{\partial A}{\partial\beta}\frac{\partial}{\partial\beta}\left(\frac{1}{B}\frac{\partial W}{\partial\beta}\right)$$

$$-2(\mu_\beta-\mu_{\alpha\beta})\frac{\partial^2}{\partial\alpha\partial\beta}(k_1U)+2(\mu_\beta-\mu_{\alpha\beta})\frac{\partial^2}{\partial\alpha\partial\beta}\left(\frac{1}{A}\frac{\partial W}{\partial\alpha}\right)$$

$$+2(\mu_\alpha-\mu_{\alpha\beta})\frac{k_1}{AB}\frac{\partial B}{\partial\alpha}\frac{\partial A}{\partial\beta}U-2(\mu_\alpha-\mu_{\alpha\beta})\frac{1}{A^2B}\frac{\partial B}{\partial\alpha}\frac{\partial A}{\partial\beta}\frac{\partial W}{\partial\alpha}$$

$$-\tau_{\beta\gamma}\frac{\partial^2k_2}{\partial\alpha\partial\beta}V+\tau_{\alpha\gamma}\frac{1}{A}\frac{\partial A}{\partial\beta}\frac{\partial k_2}{\partial\alpha}V+\tau_{\beta\gamma}\frac{1}{B}\frac{\partial A}{\partial\beta}\frac{\partial}{\partial\beta}(k_2-k_1)U$$

$$-\tau_{\beta\gamma}\frac{\partial}{\partial\beta}\left(\frac{A}{B}\frac{\partial k_1}{\partial\beta}\right)U+\tau_{\alpha\gamma}\frac{1}{B}\frac{\partial A}{\partial\beta}\frac{\partial k_1}{\partial\beta}U+\tau_{\beta\gamma}'\frac{1}{A}\frac{\partial B}{\partial\alpha}\frac{\partial k_2}{\partial\alpha}U$$

$$-\tau_{\beta\gamma}\frac{\partial k_2}{\partial\alpha}\frac{\partial V}{\partial\beta}-\tau_{\beta\gamma}\frac{A}{B}\frac{\partial k_2}{\partial\beta}\frac{\partial U}{\partial\beta}+\tau_{\alpha\gamma}'\frac{B}{A}\frac{\partial}{\partial\alpha}(2k_2-k_1)\frac{\partial U}{\partial\alpha}$$

$$+\tau_{\beta\gamma}\frac{\partial}{\partial\beta}\left(\frac{1}{B}\frac{\partial B}{\partial\alpha}\right)\frac{1}{B}\frac{\partial W}{\partial\beta}-\tau_{\alpha\gamma}\frac{1}{AB^2}\frac{\partial A}{\partial\beta}\frac{\partial B}{\partial\alpha}\frac{\partial W}{\partial\beta}$$

$$- \tau_{\alpha\gamma}' \frac{1}{B^2} \frac{\partial}{\partial \alpha} \left(\frac{B}{A} \frac{\partial A}{\partial \beta} \right) \frac{\partial W}{\partial \beta} + \tau_{\beta\gamma} \frac{\partial}{\partial \beta} \left(\frac{1}{B} \frac{\partial A}{\partial \beta} \right) \frac{1}{A} \frac{\partial W}{\partial \alpha}$$

$$- \tau_{\alpha\gamma} \frac{1}{A^2 B} \left(\frac{\partial A}{\partial \beta} \right)^2 \frac{\partial W}{\partial \alpha} - \tau_{\beta\gamma}' \frac{1}{AB} \frac{\partial}{\partial \alpha} \left(\frac{B}{A} \frac{\partial B}{\partial \alpha} \right) \frac{\partial W}{\partial \alpha}$$

$$+ \tau_{\beta\gamma} \frac{1}{B} \frac{\partial B}{\partial \alpha} \frac{\partial}{\partial \beta} \left(\frac{1}{B} \frac{\partial W}{\partial \beta} \right) - \tau_{\beta\gamma}' \frac{1}{B} \frac{\partial B}{\partial \alpha} \frac{\partial}{\partial \beta} \left(\frac{1}{B} \frac{\partial W}{\partial \beta} \right)$$

$$- (\tau_{\alpha\gamma}' - \tau_{\alpha\gamma}) \frac{1}{A} \frac{\partial A}{\partial \beta} \frac{\partial}{\partial \alpha} \left(\frac{1}{B} \frac{\partial W}{\partial \beta} \right) - (\tau_{\beta\gamma} + \tau_{\beta\gamma}') \frac{\partial^2}{\partial \alpha \partial \beta} \left(\frac{1}{B} \frac{\partial W}{\partial \beta} \right)$$

$$+ \tau_{\beta\gamma} \frac{A}{B^2} \frac{\partial B}{\partial \beta} \frac{\partial}{\partial \beta} \left(\frac{1}{A} \frac{\partial W}{\partial \alpha} \right) + \tau_{\alpha\gamma} \frac{1}{B} \frac{\partial A}{\partial \beta} \frac{\partial}{\partial \beta} \left(\frac{1}{A} \frac{\partial W}{\partial \alpha} \right)$$

$$- \tau_{\beta\gamma}' \frac{1}{A} \frac{\partial B}{\partial \alpha} \frac{\partial}{\partial \alpha} \left(\frac{1}{A} \frac{\partial W}{\partial \alpha} \right) - \tau_{\alpha\gamma}' \frac{1}{B} \frac{\partial}{\partial \alpha} \left(\frac{B^2}{A} \right) \frac{\partial}{\partial \alpha} \left(\frac{1}{A} \frac{\partial W}{\partial \alpha} \right)$$

$$- \tau_{\beta\gamma} \frac{A}{B} \frac{\partial^2}{\partial \beta^2} \left(\frac{1}{A} \frac{\partial W}{\partial \alpha} \right) - \tau_{\alpha\gamma}' \frac{B}{A} \frac{\partial^2}{\partial \alpha^2} \left(\frac{1}{A} \frac{\partial W}{\partial \alpha} \right) \Bigg\} \frac{\delta^2}{12}$$

$$- \frac{2\mu_\beta}{\delta} \int_{-\delta/2}^{\delta/2} \gamma \frac{\partial}{\partial \gamma} \left(\frac{1}{h_1} \frac{\partial U_\gamma}{\partial \gamma} \right) d\gamma - \frac{2(\mu_\beta - \mu_\alpha)}{\delta} \int_{-\delta/2}^{\delta/2} \gamma \frac{\partial}{\partial \gamma} \left(U_\gamma \frac{\partial h_1^{-1}}{\partial \beta} \right) d\gamma$$

$$+ \frac{1}{\delta} \left\{ \tau_{\beta\gamma}' (k_1 + k_2) \frac{\partial B}{\partial \alpha} + \tau_{\alpha\gamma}' \frac{\partial}{\partial \alpha} (B k_1) + \tau_{\alpha\gamma}' \frac{1}{A} \frac{\partial B}{\partial \alpha} \int_{-\delta/2}^{\delta/2} \gamma \, U_\gamma \, d\gamma \right.$$

$$+ \frac{1}{\delta} \left\{ \tau_{\beta\gamma}' B k_2 + \tau_{\alpha\gamma}' B k_1 \right\} \int_{-\delta/2}^{\delta/2} \gamma \frac{\partial U_\gamma}{\partial \alpha} \, d\gamma$$

$$+ \frac{1}{\delta} \tau_{\alpha\gamma}' B k_1 \frac{\partial}{\partial \alpha} (2k_2 - k_1) \int_{-\delta/2}^{\delta/2} \gamma^2 U_\gamma \, d\gamma - \frac{AB}{\delta} Q_\beta = 0 \qquad (32)$$

In the preceding equations, Q_α, Q_β, P_α, and P_β are defined as

$$Q_\alpha = \frac{1}{B} \int_{-\delta/2}^{\delta/2} \frac{\sigma_{\alpha\gamma}}{h_2} d\gamma$$

$$Q_\beta = \frac{1}{A} \int_{-\delta/2}^{\delta/2} \frac{\sigma_{\beta\gamma}}{h_1} d\gamma \tag{33}$$

$$P_\alpha = \frac{1}{AB} \left\{ \frac{\sigma_{\alpha\gamma}}{h_1 h_2} \Bigg|_{-\delta/2}^{\delta/2} + \int_{-\delta/2}^{\delta/2} \frac{p_\alpha}{h_1 h_2} d\gamma \right\}$$

$$P_\beta = \frac{1}{AB} \left\{ \frac{\sigma_{\beta\gamma}}{h_1 h_2} \Bigg|_{-\delta/2}^{\delta/2} + \int_{-\delta/2}^{\delta/2} \frac{p_\beta}{h_1 h_2} d\gamma \right\}$$

$$P_\gamma = \frac{1}{AB} \left\{ \frac{\sigma_{\gamma}}{h_1 h_2} \Bigg|_{-\delta/2}^{\delta/2} + \int_{-\delta/2}^{\delta/2} \frac{p_\gamma}{h_1 h_2} d\gamma \right\} \tag{34}$$

The quantities Q_α and Q_β are the transverse shearing forces per unit length of shell middle surface while P_α, P_β, and P_γ represent the summations of the external and body force components per unit area of the shell middle surface.

The five equilibrium equations contain, at this point in the development, 10 unknown quantities, the middle surface displacement components

U, V, and W, the transverse shearing forces per unit length of middle surface Q_α and Q_β, and the quantitities Δ_0, Δ_1, χ_0, χ_1, and U_γ. The equations for the latter terms will now be developed, reducing the number of unknown quantities to five.

B. Rotation Components

The normal rotation χ was defined in Equations (26) as

$$\chi = \frac{h_1 h_2}{2} \left[\frac{\partial}{\partial\alpha}\left(\frac{U_\beta}{h_2}\right) - \frac{\partial}{\partial\beta}\left(\frac{U_\alpha}{h_1}\right)\right]$$

Substituting the expressions for h_1, h_2, U_α, and U_β into the above, expanding the quantity $h_1 h_2$ in series form, and discarding terms of the second power of γ and higher yields

$$\chi = \frac{1}{2AB}\left\{\frac{\partial}{\partial\alpha}(BV) - \frac{\partial}{\partial\beta}(AU)\right\} - \frac{(k_1-k_2)}{2}\left\{\frac{A}{B}\frac{\partial}{\partial\beta}\left(\frac{U}{A}\right) + \frac{B}{A}\frac{\partial}{\partial\alpha}\left(\frac{V}{B}\right)\right\}\gamma$$

The normal rotation was given in Equation (27) as

$$\chi = \chi_0 + \chi_1\gamma$$

Equating coefficients of like powers of γ in the above equations,

$$\chi_0 = \frac{1}{2AB}\left\{\frac{\partial}{\partial\alpha}(BV) - \frac{\partial}{\partial\beta}(AU)\right\}$$

$$\chi_1 = \frac{-(k_1-k_2)}{2}\left\{\frac{A}{B}\frac{\partial}{\partial\beta}\left(\frac{U}{A}\right) + \frac{B}{A}\frac{\partial}{\partial\alpha}\left(\frac{V}{B}\right)\right\} \qquad (35)$$

C. Normal Displacement

For the case of plane stress, the normal strain e_γ is given by the third of Equations (20) as

$$e_\gamma = a_{13}\,\sigma_\alpha + a_{23}\,\sigma_\beta + a_{36}\,\sigma_{\alpha\beta} \tag{36}$$

Simulanteous solution of the remaining equations for σ_α, σ_β, and $\sigma_{\alpha\beta}$ yields

$$\sigma_\alpha = \frac{e_\alpha(a_{22}a_{66}-a_{26}^2) - e_\beta(a_{12}a_{66}-a_{26}a_{16}) + e_{\alpha\beta}(a_{12}a_{26}-a_{22}a_{16})}{a_{11}(a_{22}a_{66}-a_{26}^2) - a_{12}(a_{12}a_{66}-a_{26}a_{16}) + a_{16}(a_{12}a_{26}-a_{22}a_{16})}$$

$$\sigma_\beta = \frac{-e_\alpha(a_{12}a_{66}-a_{16}a_{26}) + e_\beta(a_{11}a_{66}-a_{16}^2) - e_{\alpha\beta}(a_{11}a_{26}-a_{12}a_{16})}{a_{11}(a_{22}a_{66}-a_{26}^2) - a_{12}(a_{12}a_{66}-a_{26}a_{16}) + a_{16}(a_{12}a_{26}-a_{22}a_{16})}$$

$$\sigma_{\alpha\beta} = \frac{e_\alpha(a_{12}a_{26}-a_{16}a_{22}) - e_\beta(a_{11}a_{26}-a_{16}a_{12}) + e_{\alpha\beta}(a_{11}a_{22}-a_{12}^2)}{a_{11}(a_{22}a_{66}-a_{26}^2) - a_{12}(a_{12}a_{66}-a_{26}a_{16}) + a_{16}(a_{12}a_{26}-a_{22}a_{16})} \tag{37}$$

Substitution of Equations (37) into Equation (36) then yields the following expression for the normal strain e_γ in terms of the normal strains e_α and e_β and the shearing strain $e_{\alpha\beta}$:

$$e_\gamma = C_\alpha e_\alpha + C_\beta e_\beta + C_{\alpha\beta} e_{\alpha\beta} \tag{38}$$

where

$$C_\alpha = \frac{a_{13}(a_{22}a_{66}-a_{26}^2) - a_{23}(a_{12}a_{66}-a_{16}a_{26}) + a_{36}(a_{12}a_{26}-a_{16}a_{22})}{a_{11}(a_{22}a_{66}-a_{26}^2) - a_{12}(a_{12}a_{66}-a_{26}a_{16}) + a_{16}(a_{12}a_{16}-a_{22}a_{16})}$$

$$C_{\beta} = \frac{-a_{13}(a_{12}a_{66}-a_{26}a_{16})+a_{23}(a_{11}a_{66}-a_{16}^{2})-a_{36}(a_{11}a_{26}-a_{16}a_{12})}{a_{11}(a_{22}a_{66}-a_{26}^{2})-a_{12}(a_{12}a_{66}-a_{26}a_{16})+a_{16}(a_{12}a_{16}-a_{22}a_{16})}$$

$$C_{\alpha\beta} = \frac{a_{13}(a_{12}a_{26}-a_{22}a_{16})-a_{23}(a_{11}a_{26}-a_{12}a_{16})+a_{36}(a_{11}a_{22}-a_{12}^{2})}{a_{11}(a_{22}a_{66}-a_{26}^{2})-a_{12}(a_{12}a_{66}-a_{26}a_{16})+a_{16}(a_{12}a_{16}-a_{22}a_{16})}$$

The strain at any point in a shell can be stated in terms of middle surface strains, curvature changes and twist by the following:[1]

$$e_{\alpha} = \frac{1}{(1+k_1\gamma)}(e_1 + k_{\alpha}\gamma)$$

$$e_{\beta} = \frac{1}{(1+k_2\gamma)}(e_2 + k_{\beta}\gamma)$$

$$e_{\alpha\beta} = \frac{1}{(1+k_1\gamma)(1+k_2\gamma)}\left\{(1-k\gamma^2)e_{12}+2(1+H\gamma)\gamma k_{\alpha\beta}\right\}$$

where e_1, e_2, e_{12}, k_{α}, k_{β}, and $k_{\alpha\beta}$ are the middle surface normal strains, shear strain, changes in curvature and twist given by

$$e_1 = \frac{1}{A}\frac{\partial U}{\partial \alpha} + \frac{1}{AB}\frac{\partial A}{\partial \beta}V + k_1 W$$

$$e_2 = \frac{1}{B}\frac{\partial V}{\partial \beta} + \frac{1}{AB}\frac{\partial B}{\partial \alpha}U + k_2 W$$

$$e_{12} = \frac{A}{B}\frac{\partial}{\partial \beta}\left(\frac{U}{A}\right) + \frac{B}{A}\frac{\partial}{\partial \alpha}\left(\frac{V}{B}\right)$$

$$k_{\alpha} = -\frac{1}{A}\frac{\partial}{\partial \alpha}\left(\frac{1}{A}\frac{\partial W}{\partial \alpha} - k_1 U\right) - \frac{1}{AB}\frac{\partial A}{\partial \beta}\left(\frac{1}{B}\frac{\partial W}{\partial \beta} - k_2 V\right)$$

$$k_{\beta} = -\frac{1}{B}\frac{\partial}{\partial \beta}\left(\frac{1}{B}\frac{\partial W}{\partial \beta} - k_2 V\right) - \frac{1}{AB}\frac{\partial B}{\partial \alpha}\left(\frac{1}{A}\frac{\partial W}{\partial \alpha} - k_1 U\right)$$

$$k_{\alpha\beta} = -\frac{1}{AB}\left(\frac{\partial^2 W}{\partial\alpha\partial\beta} - \frac{1}{A}\frac{\partial A}{\partial\beta}\frac{\partial W}{\partial\alpha} - \frac{1}{B}\frac{\partial B}{\partial\alpha}\frac{\partial W}{\partial\beta}\right)$$

$$+ k_1\left(\frac{1}{B}\frac{\partial U}{\partial\beta} - \frac{1}{AB}\frac{\partial A}{\partial\beta}U\right) + k_2\left(\frac{1}{A}\frac{\partial V}{\partial\alpha} - \frac{1}{AB}\frac{\partial B}{\partial\alpha}V\right)$$

Discarding terms of order k or smaller with respect to unity in the above equations results in the following simplified form:

$$e_\alpha = e_1 + k_\alpha \gamma$$

$$e_\beta = e_2 + k_\beta \gamma$$

$$e_{\alpha\beta} = e_{12} + 2k_{\alpha\beta}\gamma \tag{39}$$

Substitution of Equations (39) into Equation (38), results in the following expression for e_γ :

$$e_\gamma = \left\{C_\alpha e_1 + C_\beta e_2 + C_{\alpha\beta} e_{12}\right\} + \left\{C_\alpha k_\alpha + C_\beta k_\beta + 2C_{\alpha\beta} k_{\alpha\beta}\right\}\gamma \tag{40}$$

From the third of Equations (11),

$$e_\gamma = \frac{\partial U_\gamma}{\partial \gamma}$$

Equation (40) can therefore be integrated directly to yield the following expression for the normal displacement component U_γ :

$$U_\gamma = W + \left\{C_\alpha e_1 + C_\beta e_2 + C_{\alpha\beta} e_{12}\right\}\gamma + \left\{C_\alpha k_\alpha + C_\beta k_\beta + 2C_{\alpha\beta} k_{\alpha\beta}\right\}\frac{\gamma^2}{2} \tag{41}$$

The constant of integrating was set equal to W to satisfy the boundary condition that $U_\gamma = W$ for $\gamma = 0$.

D. Volume Dilitation Components

The volume dilitation is given by the equation

$$\Delta = e_\alpha + e_\beta + e_\gamma , \tag{42}$$

It has been established that it can be approximated by the equation

$$\Delta = \Delta_o + \Delta_1 \tag{43}$$

without introducing errors of appreciable magnitude in applications to thin shell theory. The purpose here is to evaluate the coefficients Δ_o and Δ_1. Substitution of the first two of Equation (39) and Equation (40) into Equation (42) results in the following expression for Δ:

$$\Delta = \left\{(1 + C_\alpha)\, e_1 + (1 + C_\beta)\, e_2 + (1 + C_{\alpha\beta})\, e_{12}\right\} + \left\{(1 + C_\alpha)\, k_\alpha + (1 + C_\beta)\, k_\beta + 2C_{\alpha\beta}\, k_{\alpha\beta}\right\} \gamma \tag{44}$$

The coefficients Δ_o and Δ_1 are therefore given by

$$\Delta_o = (1 + C_\alpha)\, e_1 + (1 + C_\beta)\, e_2 + (1 + C_{\alpha\beta})\, e_{12}$$

$$\Delta_1 = (1 + C_\alpha)\, k_\alpha + (1 + C_\beta)\, k_\beta + 2C_{\alpha\beta}\, k_{\alpha\beta} \tag{45}$$

E. Transverse Shear Stress Resultants

Having determined an expression for U_γ as a finite polynomial in γ and the equations for the coefficients χ_o, χ_1, Δ_o, and Δ_1, one may now state the equilibrium equations (28)-(32) in terms of the middle surface displacement components U, V, and W and the transverse shear forces per unit length of middle surface Q_α and Q_β, reducing the number of unknown quantities to five. Following a rather conventional procedure, Equations (31) and (32) will first be solved for Q_α and Q_β. These quantities will then be substituted in Equations (28), (29), and (30), yielding three simultaneous differential equations in the three middle surface displacement components U, V, and W.

The solution of Equations (31) and (32) for Q_α and Q_β merely involves the placing of the terms containing these quantities on the opposite sides of the equal signs with appropriate changes of sign so there will be no advantage in doing this until some simplifications have been made.

The changes in curvatures and twist of the middle surface have been given by the following equations:

$$k_\alpha = -\frac{1}{A}\frac{\partial}{\partial\alpha}\left(\frac{1}{A}\frac{\partial W}{\partial\alpha} - k_1 U\right) - \frac{1}{AB}\frac{\partial A}{\partial\beta}\left(\frac{1}{B}\frac{\partial W}{\partial\beta} - k_2 V\right)$$

$$k_\beta = -\frac{1}{B}\frac{\partial}{\partial\beta}\left(\frac{1}{B}\frac{\partial W}{\partial\beta} - k_2 V\right) - \frac{1}{AB}\frac{\partial B}{\partial\alpha}\left(\frac{1}{A}\frac{\partial W}{\partial\alpha} - k_1 U\right)$$

$$k_{\alpha\beta} = -\frac{1}{AB}\left(\frac{\partial^2 W}{\partial\alpha\partial\beta} - \frac{1}{A}\frac{\partial A}{\partial\beta}\frac{\partial W}{\partial\alpha} - \frac{1}{B}\frac{\partial B}{\partial\alpha}\frac{\partial W}{\partial\beta}\right)$$
$$+ k_1\left(\frac{1}{B}\frac{\partial U}{\partial\beta} - \frac{1}{AB}\frac{\partial A}{\partial\beta}U\right) + k_2\left(\frac{1}{A}\frac{\partial V}{\partial\alpha} - \frac{1}{AB}\frac{\partial B}{\partial\alpha}V\right)$$

where k_α and k_β are the changes in curvature in the α and β directions respectively and $k_{\alpha\beta}$ is the twist of the middle surface. The analysis to be carried out here is based on the assumption that the contributions of the tangential displacement components will have a negligible effect on these terms.

They can therefore be reduced to the following form:

$$k_\alpha = -\frac{1}{A}\frac{\partial}{\partial\alpha}\left(\frac{1}{A}\frac{\partial W}{\partial\alpha}\right) - \frac{1}{AB^2}\frac{\partial A}{\partial\beta}\frac{\partial W}{\partial\beta}$$

$$k_\beta = -\frac{1}{B}\frac{\partial}{\partial\beta}\left(\frac{1}{B}\frac{\partial W}{\partial\beta}\right) - \frac{1}{A^2B}\frac{\partial B}{\partial\alpha}\frac{\partial W}{\partial\alpha}$$

$$k_{\alpha\beta} = -\frac{1}{AB}\frac{\partial^2 W}{\partial\alpha\partial\beta} + \frac{1}{AB^2}\frac{\partial B}{\partial\alpha}\frac{\partial W}{\partial\beta} + \frac{1}{A^2B}\frac{\partial A}{\partial\beta}\frac{\partial W}{\partial\alpha} \qquad (46)$$

To be consistent with the above assumption, certain simplifications must be made in Equations (31) and (32). An inspection of Equations (31) and (32) reveals that the tangential displacement components contained therein are of the same order of magnitude with respect to the normal components as in the change of curvature and twist equations. These terms can therefore be eliminated.

After making the above substitutions and simplifications in Equations (31) and (32) and writing the resultant equations in terms of middle surface curvatures and twist, the transverse shearing forces per unit length of middle surface are found to be given by the equations on the following page.

$$
\begin{aligned}
\frac{12\,AB\,Q_\alpha}{\delta^3} = {} & \left\{ \left(\frac{T_\alpha + 2\mu_\alpha}{1-\eta_\alpha}\right) - \left(\frac{2\mu_\alpha \eta_\alpha}{1-\eta_\alpha}\right) \right\} B \frac{\partial k_\alpha}{\partial \alpha} \\
& + \left\{ \left(\frac{T_\alpha + 2\mu_\alpha}{1-\eta_\beta}\right) - \left(\frac{2\mu_\alpha \eta_\beta}{1-\eta_\beta}\right) - 2\left(\mu_\alpha - \mu_{\alpha\beta}\right) \right\} B \frac{\partial k_\beta}{\partial \alpha} \\
& + \left\{ \left(\frac{T_\alpha + 2\mu_\alpha}{1-\eta_\alpha}\right) - \left(\frac{T_\beta + 2\mu_\beta}{1-\eta_\alpha}\right) - 2\eta_\alpha \left(\frac{\mu_\alpha - \mu_\beta}{1-\eta_\alpha}\right) \right. \\
& \left. - 2\left(\mu_\alpha - \mu_\beta\right) + 2\left(\mu_\alpha - \mu_{\alpha\beta}\right) \right\} \frac{\partial B}{\partial \alpha} k_\alpha \\
& + \left\{ \left(\frac{T_\alpha + 2\mu_\alpha}{1-\eta_\beta}\right) - \left(\frac{T_\beta + 2\mu_\beta}{1-\eta_\beta}\right) - 2\eta_\beta \left(\frac{\mu_\alpha - \mu_\beta}{1-\eta_\beta}\right) \right. \\
& \left. - 2\left(\mu_\alpha - \mu_{\alpha\beta}\right) \right\} \frac{\partial B}{\partial \alpha} k_\beta + \left\{ \left(\frac{2\,T_\alpha \eta_{\alpha\beta}}{2-\eta_\alpha - \eta_\beta}\right) \right. \\
& \left. + 2\,T_{\alpha\gamma} \right\} B \frac{\partial k_{\alpha\beta}}{\partial \alpha} + \left\{ \left(\frac{2\,T_\alpha \eta_{\alpha\beta}}{2-\eta_\alpha - \eta_\beta}\right) \right. \\
& \left. - \left(\frac{2\,T_\beta \eta_{\alpha\beta}}{2-\eta_\alpha - \eta_\beta}\right) + 2\left(T_{\alpha\gamma} - T_{\beta\gamma}\right) \right\} \frac{\partial B}{\partial \alpha} k_{\alpha\beta} \\
& + 2\,T'_{\alpha\gamma} \frac{\partial A}{\partial \beta} k_\alpha + 2\,T'_{\alpha\gamma} A \frac{\partial k_\alpha}{\partial \beta} \\
& + T'_{\beta\gamma} A \frac{\partial k_\beta}{\partial \beta} + 2\,T'_{\beta\gamma} \frac{\partial A}{\partial \beta} k_\beta \qquad (47)
\end{aligned}
$$

$$
\begin{aligned}
\frac{12ABQ_\beta}{\delta^3} = {} & \left\{ \left(\frac{\tau_\beta + 2\mu_\beta}{1-\eta_\beta}\right) - \left(\frac{2\mu_\beta \eta_\beta}{1-\eta_\beta}\right) \right\} A \frac{\partial k_\beta}{\partial \beta} \\
& + \left\{ \left(\frac{\tau_\beta + 2\mu_\beta}{1-\eta_\alpha}\right) - \left(\frac{2\mu_\beta \eta_\alpha}{1-\eta_\alpha}\right) - 2(\mu_\beta - \mu_{\alpha\beta}) \right. A \frac{\partial k_\alpha}{\partial \beta} \\
& + \left\{ \left(\frac{\tau_\beta + 2\mu_\beta}{1-\eta_\beta}\right) - \left(\frac{\tau_\alpha + 2\mu_\alpha}{1-\eta_\beta}\right) - 2\eta_\beta \left(\frac{\mu_\beta - \mu_\alpha}{1-\eta_\beta}\right) \right. \\
& \left. - 2(\mu_\beta - \mu_\alpha) + 2(\mu_\beta - \mu_{\alpha\beta}) \right\} \frac{\partial A}{\partial \beta} k_\beta \\
& + \left\{ \left(\frac{\tau_\beta + 2\mu_\beta}{1-\eta_\alpha}\right) - \left(\frac{\tau_\alpha + 2\mu_\alpha}{1-\eta_\alpha}\right) - 2\eta_\alpha \left(\frac{\mu_\beta - \mu_\alpha}{1-\eta_\alpha}\right) \right. \\
& \left. - 2(\mu_\beta - \mu_{\alpha\beta}) \right\} \frac{\partial A}{\partial \beta} k_\alpha + \left\{ \left(\frac{2\tau_\beta \eta_{\alpha\beta}}{2-\eta_\alpha-\eta_\beta}\right) \right. \\
& \left. + 2\tau_{\beta\gamma} \right\} A \frac{\partial k_{\alpha\beta}}{\partial \beta} + \left\{ \left(\frac{2\tau_\beta \eta_{\alpha\beta}}{2-\eta_\alpha-\eta_\beta}\right) \right. \\
& \left. - \left(\frac{2\tau_\alpha \eta_{\alpha\beta}}{2-\eta_\alpha-\eta_\beta}\right) + 2(\tau_{\beta\gamma} - \tau_{\alpha\gamma}) \right\} \frac{\partial A}{\partial \beta} k_{\alpha\beta} \\
& + 2\tau_{\beta\gamma}' \frac{\partial B}{\partial \alpha} k_\beta + 2\tau_{\beta\gamma}' B \frac{\partial k_\beta}{\partial \alpha} \\
& + \tau_{\alpha\gamma}' B \frac{\partial k_\alpha}{\partial \alpha} + 2\tau_{\alpha\gamma}' \frac{\partial B}{\partial \alpha} k_\alpha
\end{aligned}
\qquad (48)
$$

F. Resultant Shell Equations

Equations (47) and (48) can now be substituted into the remaining equilibrium equations (28), (29), and (30) to obtain the three desired differential equations in terms of the middle surface displacement components U, V, and W.

An inspection of the bracketed terms preceding the quantity $\delta^2/12$ in Equations (28), (29), and (30) reveals that all these terms contain curvatures or derivatives of curvatures. In part III, section 1 of his book, Vlasov[5] discusses terms of this type and points out that, consistent with the assumptions of thin shell theory, terms of this type can be discarded. This simplification can also be used in the evaluation of the various integrals contained in Equations (28), (29), and (30).

Substitution of the expressions for Q_α, Q_β and their derivatives in Equations (28), (29), and (30) and simplification of these equations in accordance with the above remarks results in the following set of differential equations:

$$
\begin{aligned}
&\Big\{(\tau_\alpha + 2\mu_\alpha) B \frac{\partial}{\partial\alpha}\left(\frac{1}{1-\eta_\alpha}e_1 + \frac{1}{1-\eta_\beta}e_2 + \frac{\eta_{\alpha\beta}}{2-\eta_\alpha-\eta_\beta}e_{12}\right) \\
&-2\mu_{\alpha\beta} A \frac{\partial}{\partial\beta}\left(\frac{1}{2AB}\left[\frac{\partial}{\partial\alpha}(BV) - \frac{\partial}{\partial\beta}(AU)\right]\right) + 2\mu_\alpha ABKU \\
&+\left[(\tau_\alpha+2\mu_\alpha) - (\tau_\beta+2\mu_\beta)\right] \frac{\partial B}{\partial\alpha}\left(\frac{1}{1-\eta_\alpha}e_1 + \frac{1}{1-\eta_\beta}e_2 + \frac{\eta_{\alpha\beta}}{2-\eta_\alpha-\eta_\beta}e_{12}\right) \\
&+2(\mu_\alpha-\mu_{\alpha\beta})\frac{\partial}{\partial\beta}\left(\frac{1}{B}\frac{\partial A}{\partial\beta}\right)U - 2(\mu_\alpha-\mu_\beta)\frac{1}{A}\frac{\partial B}{\partial\alpha}\frac{\partial U}{\partial\alpha} - 2(\mu_\alpha-\mu_{\alpha\beta})\frac{\partial^2 V}{\partial\alpha\partial\beta} \\
&+2(\mu_\alpha-\mu_{\alpha\beta})\frac{1}{AB}\frac{\partial A}{\partial\beta}\frac{\partial B}{\partial\alpha}V\Big\} - 2\mu_\alpha B\Big\{\frac{\eta_\alpha}{1-\eta_\alpha}\frac{\partial e_1}{\partial\alpha} + \frac{\eta_\beta}{1-\eta_\beta}\frac{\partial e_2}{\partial\alpha} \\
&+\frac{\eta_{\alpha\beta}}{2-\eta_\alpha-\eta_\beta}\frac{\partial e_{12}}{\partial\alpha}\Big\} - 2(\mu_\alpha-\mu_\beta)\frac{\partial B}{\partial\alpha}\Big\{\frac{\eta_\alpha}{1-\eta_\alpha}e_1 + \frac{\eta_\beta}{1-\eta_\beta}e_2 \\
&+\frac{\eta_{\alpha\beta}}{2-\eta_\alpha-\eta_\beta}e_{12}\Big\} - \tau_{\alpha\gamma}\frac{\partial}{\partial\alpha}\left(\frac{1}{A}\frac{\partial A}{\partial\beta}\right)U + \tau_{\beta\gamma}\frac{1}{AB}\frac{\partial B}{\partial\alpha}\frac{\partial A}{\partial\beta}U \\
&+\tau'_{\beta\gamma}\frac{1}{A}\frac{\partial}{\partial\beta}\left(\frac{A}{B}\frac{\partial B}{\partial\alpha}\right)U - (\tau_{\alpha\gamma}+\tau'_{\alpha\gamma})\frac{1}{A}\frac{\partial A}{\partial\beta}\frac{\partial U}{\partial\alpha} \\
&+(\tau'_{\beta\gamma}-\tau_{\beta\gamma})\frac{1}{B}\frac{\partial B}{\partial\alpha}\frac{\partial U}{\partial\beta} + (\tau_{\alpha\gamma}+\tau'_{\alpha\gamma})\frac{\partial^2 U}{\partial\alpha\partial\beta} - \tau_{\alpha\gamma}\frac{\partial}{\partial\alpha}\left(\frac{1}{A}\frac{\partial B}{\partial\alpha}\right)V \\
&+\tau'_{\beta\gamma}\frac{1}{AB}\left(\frac{\partial B}{\partial\alpha}\right)^2 V + \tau'_{\alpha\gamma}\frac{1}{A}\frac{\partial}{\partial\beta}\left(\frac{A}{B}\frac{\partial A}{\partial\beta}\right)V - \tau_{\alpha\gamma}\frac{B}{A^2}\frac{\partial A}{\partial\beta}\frac{\partial V}{\partial\alpha} \\
&-\tau_{\beta\gamma}\frac{1}{A}\frac{\partial B}{\partial\alpha}\frac{\partial V}{\partial\alpha} + \tau'_{\alpha\gamma}\frac{1}{B}\frac{\partial A}{\partial\beta}\frac{\partial V}{\partial\beta} + \tau'_{\beta\gamma}\frac{1}{A}\frac{\partial}{\partial\beta}\left(\frac{A^2}{B}\right)\frac{\partial V}{\partial\beta} \\
&+\tau_{\alpha\gamma}\frac{B}{A}\frac{\partial^2 V}{\partial\alpha^2} + \tau'_{\beta\gamma}\frac{A}{B}\frac{\partial^2 V}{\partial\beta^2} + \tau'_{\alpha\gamma}(k_1+k_2)\frac{\partial A}{\partial\beta}W + \tau'_{\beta\gamma}\frac{\partial}{\partial\beta}(Ak_2)W \\
&+\tau'_{\beta\gamma}\frac{1}{B}\frac{\partial A}{\partial\beta}W + \tau'_{\alpha\gamma}Ak_1\frac{\partial W}{\partial\beta} + \tau'_{\beta\gamma}Ak_2\frac{\partial W}{\partial\beta} + \frac{AB}{\delta}P_\alpha = 0 \qquad (49)
\end{aligned}
$$

$$\Big\{(\tau_\beta+2\mu_\beta)\,A\frac{\partial}{\partial\beta}\Big(\frac{1}{1-\eta_\beta}\Big)\,e_2+\frac{1}{1-\eta_\alpha}e_1+\frac{\eta_{\alpha\beta}}{2-\eta_\alpha-\eta_\beta}\;e_{12}\Big)$$

$$-2\mu_{\alpha\beta}B\frac{\partial}{\partial\alpha}\Big(\frac{1}{2AB}\Big[\frac{\partial}{\partial\beta}(AU)-\frac{\partial}{\partial\alpha}(BV)\Big]\Big)+2\mu_\beta ABKV$$

$$+\Big[(\tau_\beta+2\mu_\beta)-(\tau_\alpha+2\mu_\alpha)\Big]\;\frac{\partial A}{\partial\beta}\Big(\frac{1}{1-\eta_\beta}e_2+\frac{1}{1-\eta_\alpha}e_1+\frac{\eta_{\alpha\beta}}{2-\eta_\alpha-\eta_\beta}e_{12}\Big)$$

$$+2(\mu_\beta-\mu_{\alpha\beta})\frac{\partial}{\partial\alpha}\Big(\frac{1}{A}\frac{\partial B}{\partial\alpha}\Big)V-2(\mu_\beta-\mu_\alpha)\frac{1}{B}\frac{\partial A}{\partial\beta}\frac{\partial V}{\partial\beta}$$

$$-2(\mu_\beta-\mu_{\alpha\beta})\frac{\partial^2 U}{\partial\alpha\partial\beta}-2(\mu_\alpha-\mu_{\alpha\beta})\frac{1}{AB}\;\frac{\partial B}{\partial\alpha}\;\frac{\partial A}{\partial\beta}U\Big\}$$

$$-2\mu_\beta A\Big\{\frac{\eta_\beta}{1-\eta_\beta}\frac{\partial e_2}{\partial\beta}+\frac{\eta_\alpha}{1-\eta_\alpha}\frac{\partial e_1}{\partial\beta}+\frac{\eta_{\alpha\beta}}{2-\eta_\alpha-\eta_\beta}\frac{\partial e_{12}}{\partial\beta}\Big\}$$

$$-2(\mu_\beta-\mu_\alpha)\frac{\partial A}{\partial\beta}\Big\{\frac{\eta_\beta}{1-\eta_\beta}e_2+\frac{\eta_\alpha}{1-\eta_\alpha}e_1+\frac{\eta_{\alpha\beta}}{2-\eta_\alpha-\eta_\beta}\;e_{12}\Big\}$$

$$-\tau_{\beta\gamma}\frac{\partial}{\partial\beta}\Big(\frac{1}{B}\frac{\partial B}{\partial\alpha}\Big)V+\tau_{\alpha\gamma}\frac{1}{AB}\frac{\partial A}{\partial\beta}\frac{\partial B}{\partial\alpha}V+\tau'_{\alpha\gamma}\frac{1}{B}\frac{\partial}{\partial\alpha}\Big(\frac{B}{A}\frac{\partial A}{\partial\beta}\Big)V$$

$$-(\tau_{\beta\gamma}+\tau'_{\beta\gamma})\frac{1}{B}\frac{\partial B}{\partial\alpha}\frac{\partial V}{\partial\beta}+(\tau'_{\alpha\gamma}-\tau_{\alpha\gamma})\frac{1}{A}\frac{\partial A}{\partial\beta}\frac{\partial V}{\partial\alpha}$$

$$+(\tau_{\beta\gamma}+\tau'_{\beta\gamma})\frac{\partial^2 V}{\partial\alpha\,\partial\beta}-\tau_{\beta\gamma}\frac{\partial}{\partial\beta}\Big(\frac{1}{B}\frac{\partial A}{\partial\beta}\Big)U+\tau'_{\alpha\gamma}\frac{1}{AB}\Big(\frac{\partial A}{\partial\beta}\Big)^2U$$

$$+\tau'_{\beta\gamma}\frac{1}{B}\frac{\partial}{\partial\alpha}\Big(\frac{B}{A}\frac{\partial B}{\partial\alpha}\Big)U-\tau_{\beta\gamma}\frac{A}{B^2}\;\frac{\partial B}{\partial\alpha}\frac{\partial U}{\partial\beta}-\tau_{\alpha\gamma}\frac{1}{B}\frac{\partial A}{\partial\beta}\frac{\partial U}{\partial\beta}$$

$$+\tau'_{\beta\gamma}\frac{1}{A}\frac{\partial B}{\partial\alpha}\frac{\partial U}{\partial\alpha}+\tau'_{\alpha\gamma}\frac{1}{B}\frac{\partial}{\partial\alpha}\Big(\frac{B^2}{A}\Big)\frac{\partial U}{\partial\alpha}+\tau_{\beta\gamma}\frac{A}{B}\frac{\partial^2 U}{\partial\beta^2}$$

$$+ \tau_{\alpha\gamma}' \frac{B}{A} \frac{\partial^2 U}{\partial \alpha^2} + \tau_{\beta\gamma}'(k_1 + k_2) \frac{\partial B}{\partial \alpha} W + \tau_{\alpha\gamma}' \frac{\partial}{\partial \alpha}(Bk_1) W$$

$$+ \tau_{\alpha\gamma}' \frac{1}{A} \frac{\partial B}{\partial \alpha} W + \tau_{\beta\gamma}' Bk_2 \frac{\partial W}{\partial \alpha} + \tau_{\alpha\gamma}' Bk_1 \frac{\partial W}{\partial \alpha}$$

$$+ \frac{AB}{\delta} P_\beta = 0 \qquad (50)$$

$$\Big\{ -2 \frac{(\tau_\alpha + 2\mu_\alpha) + (\tau_\beta + 2\mu_\beta)}{2} HAB \left(\frac{1}{1-\eta_\alpha} e_1 + \frac{1}{1-\eta_\beta} e_2 + \frac{\eta_{\alpha\beta}}{2-\eta_\alpha-\eta_\beta} e_{12} \right)$$

$$+ 2\mu_\alpha \frac{\partial}{\partial \alpha}(k_2 BU) + 2\mu_\beta \frac{\partial}{\partial \beta}(k_1 AV)$$

$$- \left[(\tau_\alpha + 2\mu_\alpha) - (\tau_\beta + 2\mu_\beta) \right] LAB \left(\frac{1}{1-\eta_\alpha} e_1 + \frac{1}{1-\eta_\beta} e_2 + \frac{\eta_{\alpha\beta}}{2-\eta_\alpha-\eta_\beta} e_{12} \right)$$

$$-2(\mu_\alpha - \mu_\beta) k_2 B \frac{\partial U}{\partial \alpha} - 2(\mu_\beta - \mu_\alpha) k_1 A \frac{\partial V}{\partial \beta}$$

$$+ \left\{ - \left[\frac{(\tau_\alpha + 2\mu_\alpha) + (\tau_\beta + 2\mu_\beta)}{2} \right] KAB \left(\frac{1}{1-\eta_\alpha} k_\alpha + \frac{1}{1-\eta_\beta} k_\beta + \frac{2\eta_{\alpha\beta}}{2-\eta_\alpha-\eta_\beta} k_{\alpha\beta} \right) \right\} \frac{\delta^2}{6}$$

$$+ 2(\mu_\alpha + \mu_\beta) KAB \left\{ W + \left(\frac{\eta_\alpha}{1-\eta_\alpha} k_\alpha + \frac{\eta_\beta}{1-\eta_\beta} k_\beta + \frac{2\eta_{\alpha\beta}}{2-\eta_\alpha-\eta_\beta} k_{\alpha\beta} \right) \frac{\delta^2}{24} \right\}$$

$$+ 2(\mu_\alpha + \mu_\beta) HAB \left\{ \frac{\eta_\alpha}{1-\eta_\alpha} e_1 + \frac{\eta_\beta}{1-\eta_\beta} e_2 + \frac{\eta_{\alpha\beta}}{2-\eta_\alpha-\eta_\beta} e_{12} \right\}$$

$$+ 2(\mu_\alpha + \mu_\beta) KAB \left\{ \frac{\eta_\alpha}{1-\eta_\alpha} k_\alpha + \frac{\eta_\beta}{1-\eta_\beta} k_\beta + \frac{2\eta_{\alpha\beta}}{2-\eta_\alpha-\eta_\beta} k_{\alpha\beta} \right\} \frac{\delta^2}{12}$$

$$+2(\mu_\alpha-\mu_\beta)LAB\left(\frac{\eta_\alpha}{1-\eta_\alpha}e_1+\frac{\eta_\beta}{1-\eta_\beta}e_2+\frac{\eta_{\alpha\beta}}{2-\eta_\alpha-\eta_\beta}e_{12}\right)$$

$$+\Big\{\left(\frac{T_\alpha+2\mu_\alpha}{1-\eta_\alpha}-\frac{2\mu_\alpha\eta_\alpha}{1-\eta_\alpha}\right)\frac{\partial}{\partial\alpha}\left(\frac{B}{A}\frac{\partial k_\alpha}{\partial\alpha}\right)+\left(\frac{T_\beta+2\mu_\beta}{1-\eta_\beta}-\frac{2\mu_\beta\eta_\beta}{1-\eta_\beta}\right)\frac{\partial}{\partial\beta}\left(\frac{A}{B}\frac{\partial k_\beta}{\partial\beta}\right)$$

$$+\left(\frac{T_\alpha+2\mu_\alpha}{1-\eta_\beta}-\frac{2\mu_\alpha\eta_\beta}{1-\eta_\beta}-2(\mu_\alpha-\mu_{\alpha\beta})\right)\frac{\partial}{\partial\alpha}\left(\frac{B}{A}\frac{\partial k_\beta}{\partial\alpha}\right)$$

$$+\left(\frac{T_\beta+2\mu_\beta}{1-\eta_\alpha}-\frac{2\mu_\beta\eta_\alpha}{1-\eta_\alpha}-2(\mu_\beta-\mu_{\alpha\beta})\right)\frac{\partial}{\partial\beta}\left(\frac{A}{B}\frac{\partial k_\alpha}{\partial\beta}\right)$$

$$+\left(\frac{T_\alpha+2\mu_\alpha}{1-\eta_\alpha}-\frac{T_\beta+2\mu_\beta}{1-\eta_\alpha}-2\eta_\alpha\frac{\mu_\alpha-\mu_\beta}{1-\eta_\alpha}+2(\mu_\beta-\mu_{\alpha\beta})\right)\frac{\partial}{\partial\alpha}\left(\frac{1}{A}\frac{\partial B}{\partial\alpha}k_\alpha\right)$$

$$+\left(\frac{T_\beta+2\mu_\beta}{1-\eta_\beta}-\frac{T_\alpha+2\mu_\alpha}{1-\eta_\beta}-2\eta_\beta\frac{\mu_\beta-\mu_\alpha}{1-\eta_\beta}+2(\mu_\alpha-\mu_{\alpha\beta})\right)\frac{\partial}{\partial\beta}\left(\frac{1}{B}\frac{\partial A}{\partial\beta}k_\beta\right)$$

$$+\left(\frac{T_\alpha+2\mu_\alpha}{1-\eta_\beta}-\frac{T_\beta+2\mu_\beta}{1-\eta_\beta}-2\eta_\beta\frac{\mu_\alpha-\mu_\beta}{1-\eta_\beta}-2(\mu_\alpha-\mu_{\alpha\beta})\right)\frac{\partial}{\partial\alpha}\left(\frac{1}{A}\frac{\partial B}{\partial\alpha}k_\beta\right)$$

$$+\left(\frac{T_\beta+2\mu_\beta}{1-\eta_\alpha}-\frac{T_\alpha+2\mu_\alpha}{1-\eta_\alpha}-2\eta_\alpha\frac{\mu_\beta-\mu_\alpha}{1-\eta_\alpha}-2(\mu_\beta-\mu_{\alpha\beta})\right)\frac{\partial}{\partial\beta}\left(\frac{1}{B}\frac{\partial A}{\partial\beta}k_\alpha\right)$$

$$+\left(\frac{2T_\alpha\eta_{\alpha\beta}}{2-\eta_\alpha-\eta_\beta}+2T_{\alpha\gamma}\right)\frac{\partial}{\partial\alpha}\left(\frac{B}{A}\frac{\partial k_{\alpha\beta}}{\partial\alpha}\right)$$

$$+\left(\frac{2T_\beta\eta_{\alpha\beta}}{2-\eta_\alpha-\eta_\beta}+2T_{\beta\gamma}\right)\frac{\partial}{\partial\beta}\left(\frac{A}{B}\frac{\partial k_{\alpha\beta}}{\partial\beta}\right)$$

$$+\left(\frac{2T_\alpha\eta_{\alpha\beta}}{2-\eta_\alpha-\eta_\beta}-\frac{2T_\beta\eta_{\alpha\beta}}{2-\eta_\alpha-\eta_\beta}+2(T_{\alpha\gamma}-T_{\beta\gamma})\right)\frac{\partial}{\partial\alpha}\left(\frac{1}{A}\frac{\partial B}{\partial\alpha}k_{\alpha\beta}\right)$$

$$+\left(\frac{2T_\beta\eta_{\alpha\beta}}{2-\eta_\alpha-\eta_\beta}-\frac{2T_\alpha\eta_{\alpha\beta}}{2-\eta_\alpha-\eta_\beta}+2(T_{\beta\gamma}-T_{\alpha\gamma})\right)\frac{\partial}{\partial\beta}\left(\frac{1}{B}\frac{\partial A}{\partial\beta}k_{\alpha\beta}\right)$$

$$+ 2\tau'_{\alpha\gamma}\frac{\partial}{\partial\alpha}\left(\frac{1}{A}\frac{\partial Ak_\alpha}{\partial\beta}\right) + 2\tau'_{\beta\gamma}\frac{\partial}{\partial\beta}\left(\frac{1}{B}\frac{\partial Bk_\beta}{\partial\alpha}\right)$$

$$+ \tau'_{\beta\gamma}\frac{\partial^2 k_\beta}{\partial\alpha\partial\beta} + \tau'_{\alpha\gamma}\frac{\partial^2 k_\alpha}{\partial\alpha\partial\beta} + 2\tau'_{\beta\gamma}\frac{\partial}{\partial\alpha}\left(\frac{1}{A}\frac{\partial A}{\partial\beta}k_\beta\right)$$

$$+ 2\tau'_{\alpha\gamma}\frac{\partial}{\partial\beta}\left(\frac{1}{B}\frac{\partial B}{\partial\alpha}k_\alpha\right)\Bigg\}\frac{\delta^2}{12}$$

$$+\Bigg\{\tau_{\alpha\gamma}k_1\frac{\partial A}{\partial\beta}U + \tau_{\beta\gamma}k_2\frac{\partial A}{\partial\beta}U + \tau_{\beta\gamma}k_2\frac{\partial B}{\partial\alpha}V$$

$$+\tau_{\alpha\gamma}\ k_1\frac{\partial B}{\partial\alpha}V - \tau_{\alpha\gamma}Ak_1\frac{\partial U}{\partial\beta} - \tau_{\beta\gamma}Ak_2\frac{\partial U}{\partial\beta}$$

$$- \tau_{\beta\gamma}Bk_2\frac{\partial V}{\partial\alpha} - \tau_{\alpha\gamma}Bk_1\frac{\partial V}{\partial\alpha}\Bigg\}$$

$$+\Bigg\{-\tau_{\alpha\gamma}k_1\frac{\partial k_1}{\partial\beta}\ \frac{\partial W}{\partial\alpha} - \tau_{\beta\gamma}k_2\frac{\partial k_1}{\partial\beta}\ \frac{\partial W}{\partial\alpha}$$

$$- \tau_{\beta\gamma}k_2\frac{\partial k_2}{\partial\alpha}\frac{\partial W}{\partial\beta} - \tau_{\alpha\gamma}k_1\frac{\partial k_2}{\partial\alpha}\ \frac{\partial W}{\partial\beta}\Bigg\}\ \frac{\delta^2}{12}$$

$$+ \frac{AB}{\delta}P_\gamma = 0 \qquad (51)$$

G. Boundary Conditions

The solution to Equations (49), (50), and (51) which satisfies the appropriate boundary conditions for a particular problem will constitute the solution to the problem. The boundary conditions can usually be best stated in terms of middle surface displacements or in terms of stress resultants at the middle surface. In general, they will be of the mixed type where some of the boundary conditions are stated in terms of displacements while others are stated in terms of stress resultants. For the case of elastic restraint, one or more boundary conditions will contain both displacement and stress resultant terms.

Boundary conditions stated in terms of displacements specify some degree of restraint; for example, an edge deflection or rotation may be required to be equal to zero due to the nature of the support at the edge. Since these boundary conditions are, in their stated form, already in terms of the same quantities as the differential equations, their applications should be straightforward. The stress resultant type boundary conditions, on the other hand, are not stated directly in terms of displacements so that some manipulations are necessary to put them in the required form.

The stress resultants at the middle surface of the shell are given by the following:

$$T_{\alpha} = \int_{-\delta/2}^{\delta/2} \sigma_{\alpha}(1+k_2\gamma)d\gamma$$

$$T_{\beta} = \int_{-\delta/2}^{\delta/2} \sigma_{\beta}(1+k_1\gamma)d\gamma$$

$$T_{\alpha\beta} = \int_{-\delta/2}^{\delta/2} \sigma_{\alpha\beta}(1+k_2\gamma)\, d\gamma$$

$$T_{\beta\alpha} = \int_{-\delta/2}^{\delta/2} \sigma_{\beta\alpha}(1+k_1\gamma)d\gamma$$

$$Q_\alpha = \int_{-\delta/2}^{\delta/2} \sigma_{\alpha\gamma} (1+k_2\gamma) d\gamma$$

$$Q_\beta = \int_{-\delta/2}^{\delta/2} \sigma_{\beta\gamma} (1+k_1\gamma) d\gamma$$

$$M_\alpha = \int_{-\delta/2}^{\delta/2} \sigma_\alpha (1+k_2\gamma)\gamma\, d\gamma$$

$$M_\beta = \int_{-\delta/2}^{\delta/2} \sigma_\beta (1+k_1\gamma)\gamma\, d\gamma$$

$$M_{\alpha\beta} = \int_{-\delta/2}^{\delta/2} \sigma_{\alpha\beta} (1+k_2\gamma)\gamma\, d\gamma$$

$$M_{\beta\alpha} = \int_{-\delta/2}^{\delta/2} \sigma_{\beta\alpha} (1+k_1\gamma)\gamma\, d\gamma \qquad (52)$$

The quantities T_α, T_β, $T_{\alpha\beta}$, $T_{\beta\alpha}$, Q_α, and Q_β represent normal, tangential shear, and transverse shear forces per unit length of middle surface as indicated in Figure 4, while the quantities M_α, M_β, $M_{\alpha\beta}$, and $M_{\beta\alpha}$ represent the bending and twisting moments per unit length of middle surface as indicated in Figure 5.

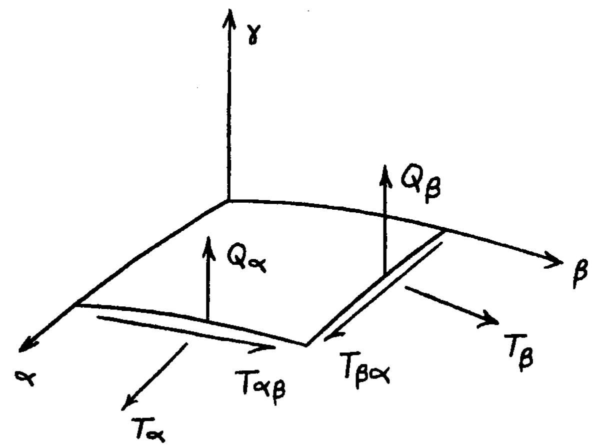

Figure 4. Stress Resultant Forces per Unit Length of Middle Surface.

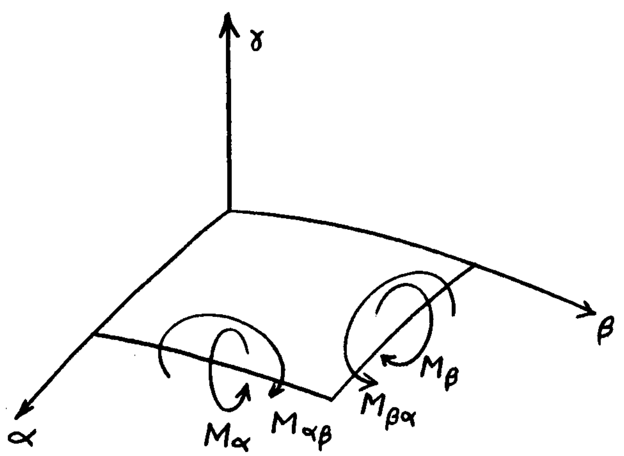

Figure 5. Stress Resultant Moments per Unit Length of Middle Surface.

Let one of the coordinate lines, for example, the line $\beta = \beta_0 =$ constant be a boundary of a shell. It can be shown [1] that the state of stress at this edge will be completely defined by the specification of the four quantities

$$T_\beta, \; T_{\beta\alpha} + k_1 M_{\beta\alpha}, Q_\beta + \frac{1}{A}\frac{\partial M_{\beta\alpha}}{\partial \alpha}, \; M_\beta$$

The twisting moment per unit length enters into these boundary conditions in the form of statically equivalent tangential and transverse shear forces per unit length, resulting in a set of four boundary conditions instead of five. This reduction in boundary conditions was introduced, for the special case of the flat plate, by Kirchoff, who showed that this is necessary to provide a set of boundary conditions that can be enforced in conjunction with solutions of the governing differential equations.

In terms of the above quantities and the middle surface displacement components, some commonly encountered boundary conditions for an edge as just specified are given by the following:

a) Free edge

$$T_\beta = 0$$

$$T_{\beta\gamma} + k_1 M_{\beta\alpha} = 0$$

$$Q_\beta + \frac{\partial M_{\beta\alpha}}{A\,\partial \alpha} = 0$$

$$M_\beta = 0$$

b) Hinged edge with fixed support

$$M_\beta = U = V = W = 0$$

c) Hinged edge with support free to move in the normal direction

$$M_{\beta} = 0$$

$$Q_{\beta} + \frac{1}{A}\frac{\partial M_{\beta\alpha}}{\partial \alpha} = 0$$

$$U = V = 0$$

d) Clamped edge

$$U = V = W = \frac{\partial W}{\partial \beta} = 0$$

It should be emphasized that these are but a few of a large number of possible sets of boundary conditions and are listed only as representative examples.

Within the order of accuracy of thin shell theory, the set of Equations (52) can be simplified by discarding the $k\gamma$ terms in the integrands.

REFERENCES

1. Novozhilov, V., The Theory of Thin Shells, Groningen, The Netherlands, P. Noordhoff, Ltd. (1959).

2. Pogorelov, A. V., Differential Geometry, Groningen, The Netherlands, P. Noordhoff, Ltd.

3. Kozik, T. J., "A General Theory of Thin Shells for Isotropic and Orthotropic Materials," unpublished Ph.D. dissertation, Graduate School, The Ohio State University (1962).

4. Love, A. E. H., A Treatise on the Mathematical Theory of Elasticity, 4th edition, Cambridge at the University Press (1934).

5. Vlasov, V. Z., "General Theory of Shells and its Applications in Engineering," English translation, National Aeronautics and Space Administration, Technical Translation F-99 (1964).

N65-33660

PROGRESS REPORT ON

DYNAMIC ENERGY ABSORPTION CHARACTERISTICS

OF AN ALUMINUM FRANGIBLE TUBE

by

W. B. Ledbetter and C. H. Samson, Jr.

Enclosure 2

INTRODUCTION

Background

The critical weight, size, and environmental requirements demanded of spacecraft landing systems have resulted in an extensive research program to formulate, analyze, and experimentally investigate promising energy-absorption systems. Of the many systems investigated, one general method of energy absorption indicated wide application because of its efficiency, simplicity, and reliability. The method is that of mechanically loading a metal structure to produce an impact energy-absorption stroke. (1)*

One system employing the above method which appears to satisfy all the stringent requirements demanded of an effective landing impact dissipation system is the frangible-tube energy-absorption system. The frangible-tube energy-absorption system dissipates impact energy by a fragmentation process. A tube is pressed over a die shaped such that the end of the tube is caused to enlarge thereby breaking and fragmenting. This fragmentation is generally referred to as "franging."

Analytical and experimental research investigations have been underway for more than two years at Texas A&M University on the frangible-tube system. Two reports have been prepared from the

---

* Numbers in parentheses refer to references contained at the close of this report.

results obtained (2, 3). These reports cover the preliminary analytical investigation and static experimental investigation on frangible 2024-T3 aluminum tubing of various geometries.

Scope

This phase of the investigation is essentially an extension of the previous work into an experimental investigation of the dynamic energy-absorption capabilities of the 2024-T3 aluminum frangible tubing. Dynamic and static characteristics, including energy absorption and peak franging force under selected conditions, are being analyzed and correlated.

The following variables are included in this phase of the study:

a. Tube Geometry. Four tube geometries are being used. They are:

   1 in. O. D. x .065 in. wall.

   1 in. O. D. x .049 in. wall.

   3/4 in. O. D. x .049 in. wall.

   1/2 in. O. D. x .049 in. wall.

b. Die Tolerance. Two dies for each tube size have been machined to yield the effects of typical variations in manufacturing tolerances on tube performance.

c. Type of Test. One dynamic and one static loading rate are being used.

In order to fully investigate the effects of each of the preceeding variables on the franging behavior of the tubes, the following parameters were held, in so far as possible, constant for this phase of research.

a. Length to outside diameter ratio of each tube (L/D ratio of 6 was selected).

b. Static loading rate (approximately 1000 lb. per sec. on all tests).

c. Dynamic energy input per square inch of tube area.

d. Material - 2024-T3 aluminum tubing was used.

e. Geometry of franged end of the tube. The ends of all tubes were full thickness, cut perpendicular to the length of the tube, and polished.

EXPERIMENTAL PROGRAM

Instrumentation

All static tests were carried out on a Baldwin 60,000 lb. universal test machine. The load was measured by a calibrated strain gage, 10,000 lb., load cell; and amplified and read by a Minneapolis-Honeywell recording oscillograph (Fig. 1). Tube deformations were measured by a linear variable differential transformer (LVDT) with a 6-in. stroke and read by the oscillograph. All dynamic tests were conducted on a drop-test facility which has the capability of impacting the test specimen with any mass up to 300 lb. from any height up to 25 ft. For these tests, an impacting mass of 107 lb. was selected. Dynamic load-versus-time traces and deformation-versus-time traces were taken by the same equipment as used on the static tests. In the dynamic test facility, an impacting plunger was provided to impart, as nearly as possible, a vertical impact stroke to the specimen (Fig. 2).

Typical load-versus-time and tube deformation-versus-time oscillograph traces are given in Figs. 3 and 4. From these traces load-deformation curves for each test can be developed and analyzed.

Dies

As stated in the Introduction, dies were manufactured in two lots. A sketch of the cross section of a die is given in Fig. 5. Each die's reference number and dimensions are given in Table 1.

Preliminary Data

As of the writing of this report, data are still being taken and analyzed. Therefore, no conclusions nor recommendations can yet be made. The data presented herein are presented to exhibit the progress of the research.

The data reported herein include selected dynamic franging-load versus tube-franging-deformation plots. These are given in Figs. 6, 7, and 8.

Several points should be noted on these figures. First, the average franging load is plotted for each deformation, with the exception that the initial peak franging load is shown. The load-deformation phenomenon is highly irregular. At the initial peak load, the tube fractures by franging at the die end, causing the load to drop momentarily. As the franging continues, the load vacillates

Fig. 1 Static Test Instrumentation

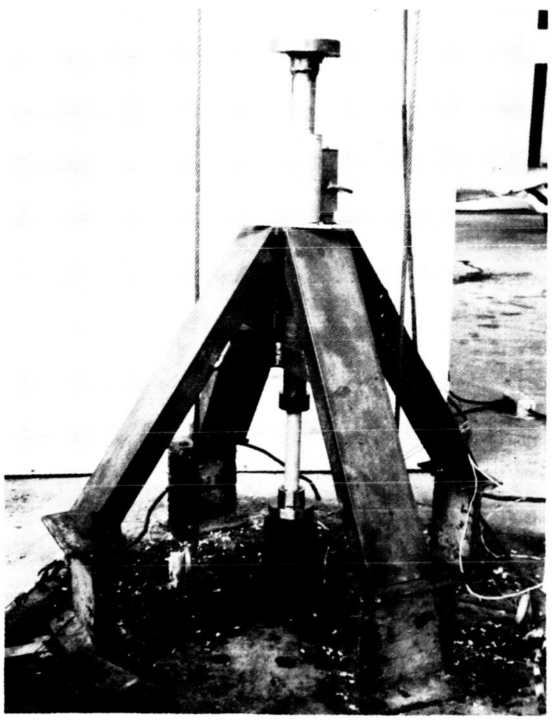

Fig. 2 Vertical Impact Stroke Device For Drop Test Impact Facility

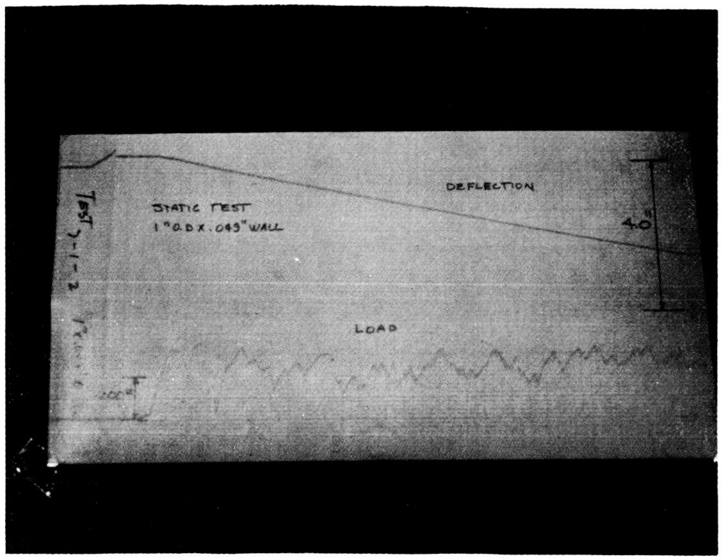

Fig. 3 Typical Oscillograph Trace From Static Test Showing Deflection vs. Time And Load vs. Time

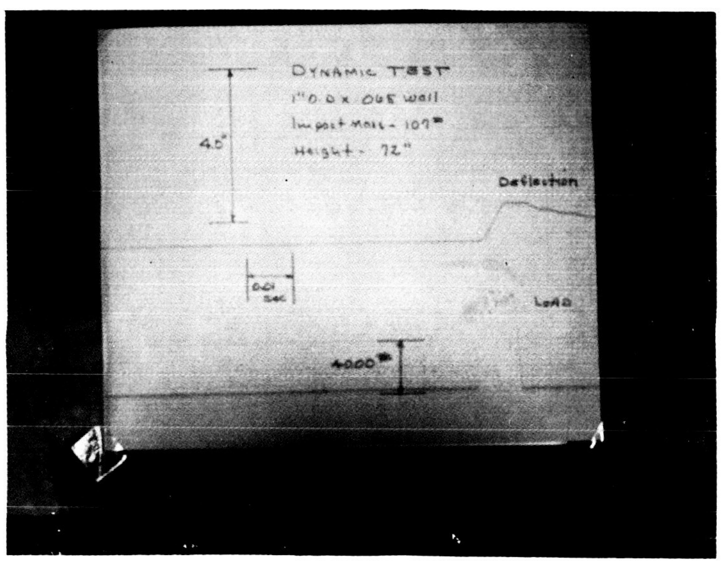

Fig. 4 Typical Oscillograph Trace From Dynamic Test Showing Deflection vs. Time and Load vs. Time

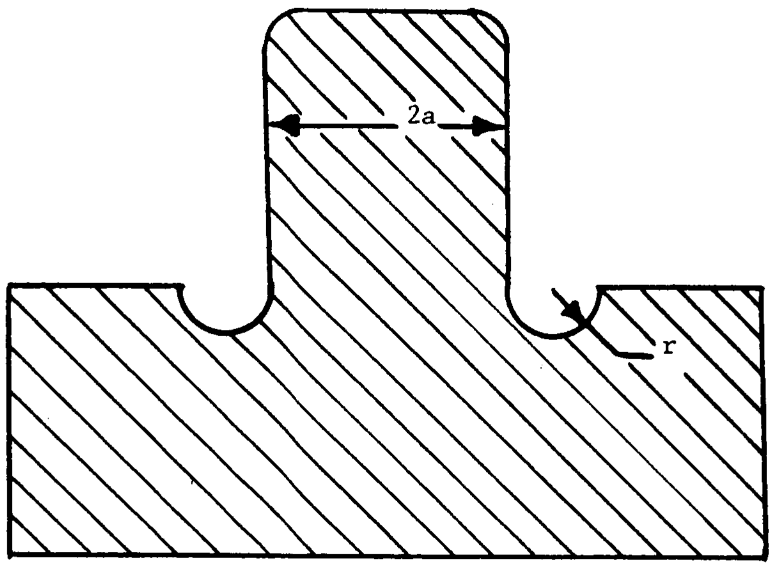

Fig. 5 Cross-Sectional View of Die

Table 1 Die Reference Numbers & Dimensions

Die Reference Number	2a (in.)	2r (in.)
1A	0.863	0.206
1B	0.875	0.201
3/4A	0.660	0.171
3/4B	0.665	0.183
1/2A	0.431	0.174
1/2B	0.404	0.169

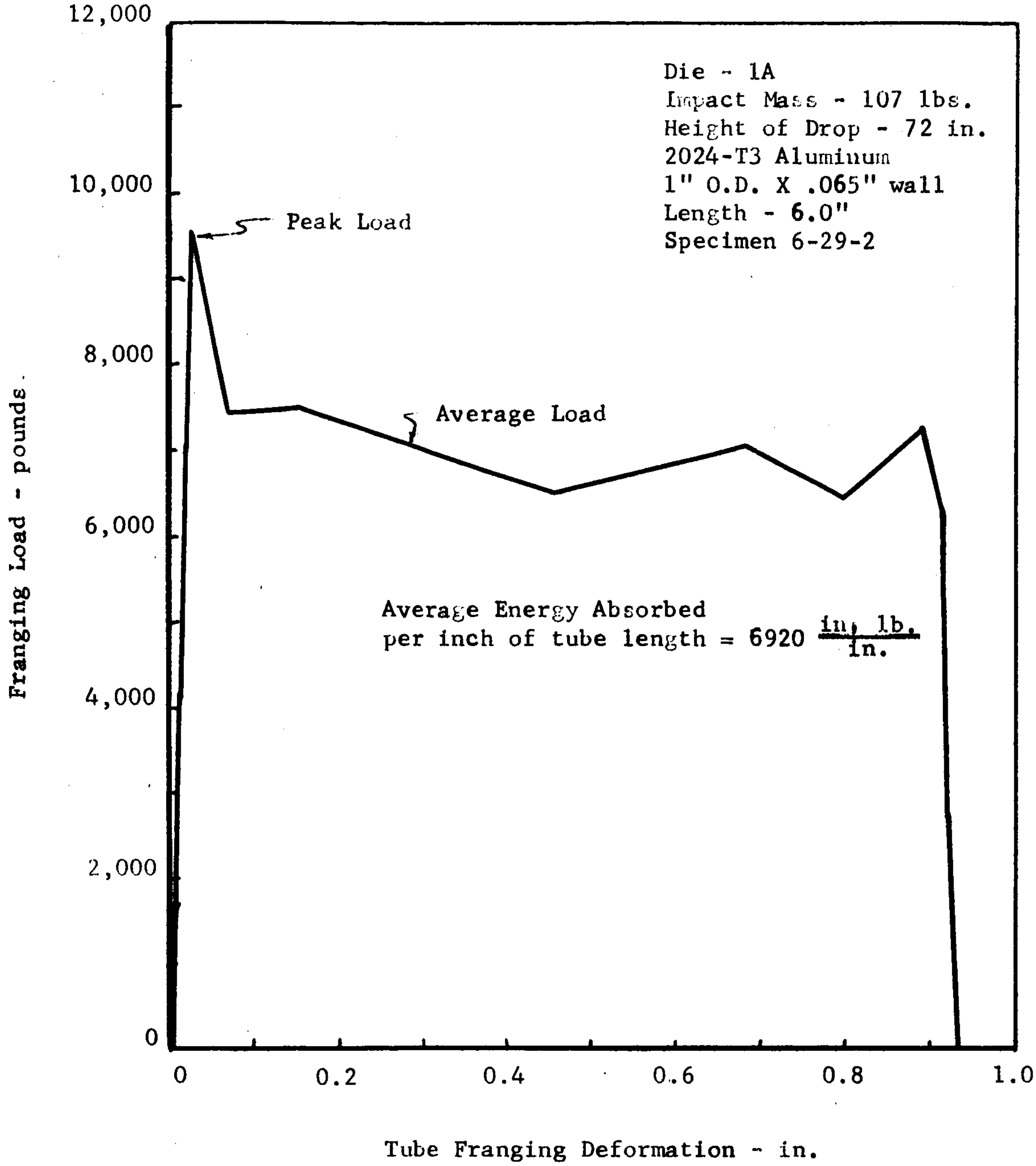

Fig. 6 Dynamic Franging Load versus Franging Deformation of Aluminum Frangible Tube - 1" O.D. X .065" Wall on Die 1A.

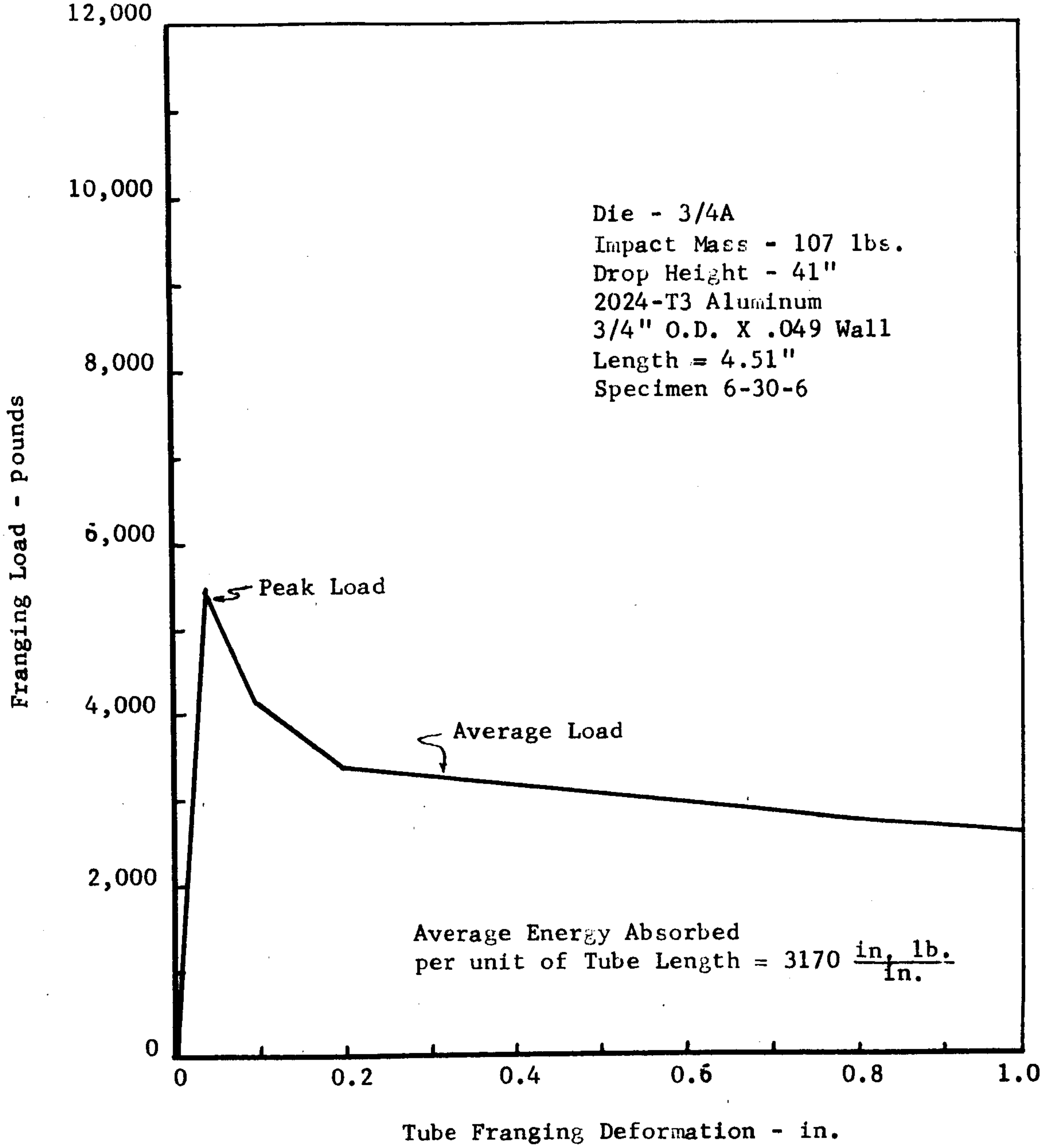

Fig. 7 Dynamic Franging Load versus Franging Deformation of Aluminum Frangible Tube - 3/4" O.D. X .049 Wall Die 3/4A.

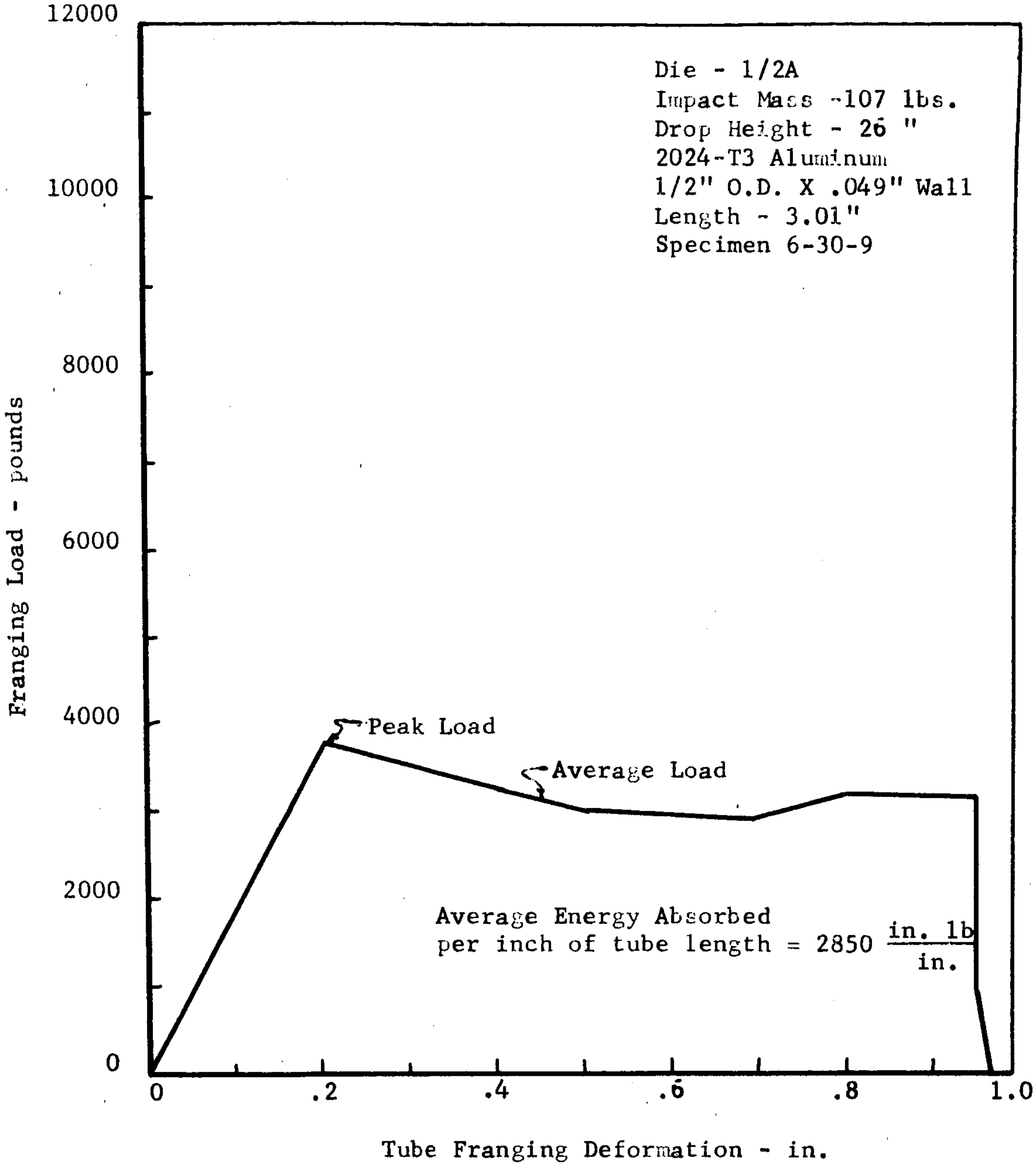

Fig. 8 Dynamic Franging Load versus Franging Deformation of Aluminum Frangible Tube 1/2" O.D. X .049" Wall on Die 1/2A.

up and down, varying in magnitudes of 2000 or more pounds. Consequently, for the purposes of data analysis, the average franging forces are plotted. Another important point to note is the peak franging force for each tube size. These forces are being analyzed and will be discussed in detail in the next report. The last point which should be noted from the figures is the average energy absorbed per inch of tube length. In terms of energy dissipation, this parameter is highly significant. It, too, will be further analyzed.

CLOSURE

In this progress report the scope and extent of the experimental research program now underway at Texas A&M University have been presented. Also, selected dynamic franging-load versus tube-franging-deformation plots were given and briefly discussed to show the type of information being gathered and analyzed.

References

1. McGehee, J. R., "A Preliminary Experimental Investigation of an Energy-Absorption Process Employing Frangible Metal Tubing", NASA TN D 1477, October, 1962.

2. Chaput, A. J., "An Analytical Investigation of the Frangible Tube Energy Absorption System," Thesis, Texas A&M University, July, 1964.

3. Chaput, A. J., "An Analytical Investigation of the Frangible Tube Energy Absorption System to Determine the Average Static Fragmentation Force," Progress Report to NASA on Research Grant No. NsG 239-62, Texas A&M University, January, 1965.

SPACE TECHNOLOGY PROJECT NO. 9

SOLUTIONS OF ELASTICITY PROBLEMS USING BOUNDARY CONDITIONS OBTAINED EXPERIMENTALLY

SOLUTIONS OF ELASTICITY PROBLEMS USING BOUNDARY CONDITIONS OBTAINED EXPERIMENTALLY

Project Investigator:

Dr. J. G. H. Thompson, Professor of Mechanical Engineering.

I. Introduction

The object of this research is to develop a rapid method of calculating stresses in irregular-shaped bodies. It is intended to provide a practical means for solution of difficult stress-analysis problems which are not investigated today because of the great time and cost involved.

II. Present Status

Mr. Darl Droste, under Dr. Thompson's supervision, is studying a conductive sheet method of producing stress trajectories. Dr. Thompson is developing digital computer solutions of plane elastic problems. After a brief summary of the digital computer program, the remainder of this report will discuss Mr. Droste's study of a conductive sheet method of producing stress trajectories.

The digital computer program is designed to solve a set of partial differential equations. It is well known that if all surface stresses are known along the periphery of a plane stress problem and a solution can be found for the equilibrium equations and compatibility conditions at every point in the field, the values of the state of stress at every interior point of the field can be established. Since in practice it is not always convenient to get number values for these internal stresses, the capabilities of a large digital computer may be utilized to supply them rapidly but approximately. Care must be taken, however, to obtain results sufficiently accurate for a given need.

Three basic steps are employed in each solution:

1. Make a reasonable assumption of the surface stresses. This can be done with little real difficulty. Estimation of the surface tangential stresses is not so easy, and often the first estimate of these will not be satisfactory.

2. By satisfying the two conditions of static equilibrium, namely, $\Sigma F = 0$ and $\Sigma M = 0$, at each of many interior cuts of the body and by suitably relating the stress values produced at each interval point by consideration of different cuts going through that point, obtain a starting estimate of each interval stress in the body.

3. Modify these interval stress values so as to preserve $\Sigma F = 0$ and $\Sigma M = 0$ at each cut of the body but also satisfy the equilibrium equations and compatibility conditions at each point in the body.

When the above steps have been carried out, a second set of estimates of surface radial and tangential stresses can be made. Work done so far indicates that the second approximation of surface stresses is more realistic than the first. The steps are repeated with succeeding estimates until results are refined to the desired degree of convergence.

Though results suggest that the program will converge, no proof of convergence has yet been developed. Instead of rigorous proof of convergence a practical test will be undertaken by running this program for a number of different problems. It is felt that a sufficient variety of problems will reveal whether or not the program will in fact converge. Though the theoretical treatment of convergence will not be ignored, it will not be the objective of this investigation.

A separate phase of this research project is Mr. Droste's efforts to provide a better way to obtain stress trajectories. Electrically conductive paper is used to produce a set of stress trajectories quickly and accurately. Although the method has been used for some time, it has been difficult to apply. A set of practical rules has now been developed which simplify its application and extend its use to more complicated problems. An analogy between stress trajectories and a potential field has been used to do this.

The basis for an analogy between stress trajectories in a two-dimensional elastic field and the equipotential and flow lines in an electric field is indicated in a paper by P. S. Theocaris.* He sets forth a technique to apply this analogy and illustrates his methods by finding the stress trajectories of a plane strip in tension due to a uniform load on one end and a pin in a hole at the other. This problem is complicated by the fact that two isotropic points exist on the boundary of the hole.

Close examination of the stress trajectories Theocaris obtained reveals that his two families are not always orthogonal. This has to be an error for the two families of stress trajectories have to be orthogonal. It is this non-orthogonality that has prompted an investigation leading to the development of a more consistent and exact technique.

The first step in the research investigation was to obtain a correct set of stress trajectories for the pinned-strip-in-tension problem by some other method. The method chosen was photoelasticity and a correct set of stress trajectories was subsequently obtained. As was expected the photoelastically determined set of stress trajectories differed from the set presented by Theocaris.

---

* A later paper by Theocaris gave a more consistent set of stress trajectories that agreed with photoelasticity for the pinned-strip-in-tension problem. However, Theocaris still refers to his first paper for technique and no additional information is given as to construction of the electric analog.

Analysis of the stress trajectories revealed the errors in the Theocaris technique and made possible an extension of his method to handle many more practical plane stress problems.

It is known that a free boundary (unloaded boundary) or a perpendicularly loaded boundary of a two dimensional stress field will have a stress trajectory of one family coincident with it and a stress trajectory of the conjugate family perpendicular to it. In the electrical analogy a boundary maintained at constant potential will correspond to an equipotential, and the current must flow into or out of this boundary in a perpendicular manner. Similarly an insulated boundary requires the equipotentials determined by the potential function to be perpendicular to the boundary and the direction of current flow to be parallel with the boundary.

It is stated by Theocaris that sufficient analogy exists to justify using analogous boundary conditions in an electric field to simulate boundaries of the stress trajectory field. In many cases of loading, shear forces on a boundary can be neglected. Thus one family or the other of the stress trajectories may be taken as perpendicular to the boundaries. Due to the orthogonal relationship between the two families of stress trajectories one of the families must also coincide with the boundaries. The relationship of the stress trajectories to the boundaries in the two dimensional stress field may then be simulated in the electrical analog by the use of either highly conductive electrodes or insulation on the boundaries of the electric field.

Points where a boundary changes from coincidence with one family of stress trajectories to coincidence with the other family, or points where a boundary coincident with a given family is intersected by a single trajectory of the same family, are known as isotropic points (these points will be discussed in detail later in the report). These points must be determined by some method (e.g. Photoelasticity) so that they may be incorporated in the electrical analogy.

Basically Theocaris' technique to set up the electrical analogy requires determination of the portions of the boundary of a plane stressed region belonging to a given family of stress trajectories. In most cases this must be accomplished by the use of photo-elastic methods. A conductive sheet is then cut to the same shape as the plane region and electrodes are applied to the portion of the boundary belonging to a given family. The two extreme trajectories of the family are then determined and a potential is applied to the corresponding electrodes. No potential is externally applied to the electrodes on the boundaries belonging to intermediate stress trajectories of the family. The equipotentials are then traced using a bridge circuit. Symmetry could be used to reduce the problem size by dividing the region considered into smaller regions on a line of symmetry.

The problems in the Theocaris technique arise primarily in his failure to supply the intermediate electrodes with voltage. Each intermediate boundary not supplied with the correct potential will introduce an additional unwanted isotropic point into the potential field.

In elasticity there are two basic types of isotropic points--the interlocking type (positive type) and the asymptotic type (negative type). Figures 1 through 6 are sketches of these types of isotropic points and the surrounding stress trajectories for isotropic points located both in the interior of a stressed region and on a boundary or line of symmetry of a stressed region. Solid and dashed lines have been used to indicate the two different orthogonal families.

These points located on the boundary of a stressed field are simulated on the boundary of a potential field by the use of electrodes and insulators. When an intermediate boundary electrode is not externally supplied with potential in the electrical analog and allowed to seek its own potential level, and isotropic point of the form shown in Figure 6 will arise somewhere on this boundary. In Figure 6 the solid lines represent equipotentials and it should be noted that the

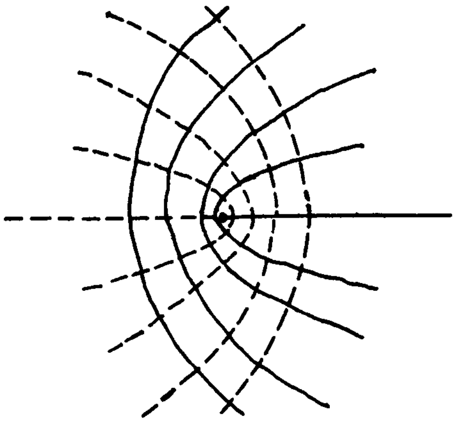

Fig. 1 - Interlocking isotropic point in interior of region.

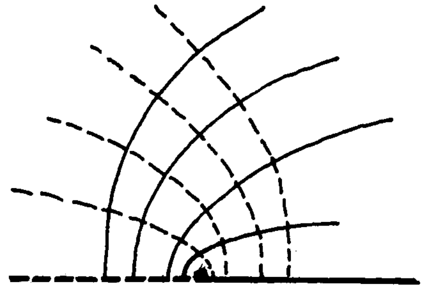

Fig. 2 - Interlocking isotropic point on a boundary or a line of symmetry.

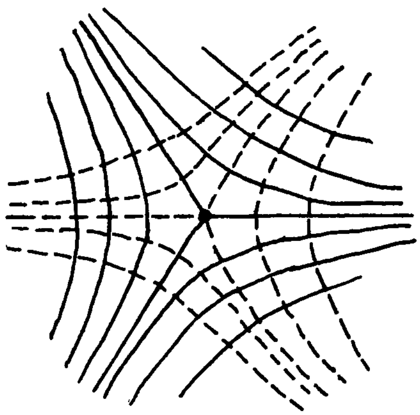

Fig. 3 - Asymptotic isotropic point (3 asymptotes) in interior of region.

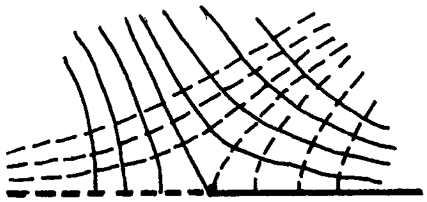

Fig. 4 - Asymptotic isotropic point (3 asymptotes) on a boundary or on a line of symmetry.

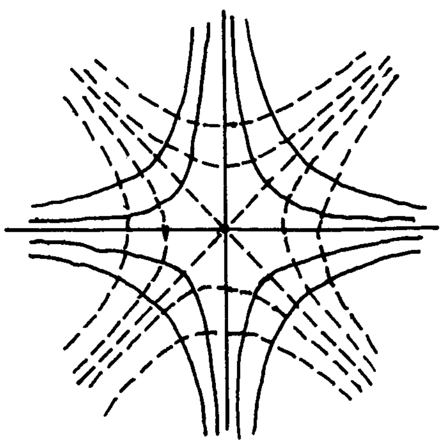

Fig. 5 - Asymptotic isotropic point (4 asymptotes) in interior or region.

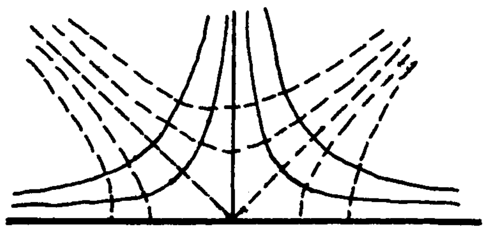

Fig 6 - Asymptotic isotropic point (4 asymptotes) on a boundary or on a line of symmetry.

boundary equipotential is intersected by an equipotential of the same potential level at the isotropic point. All other equipotentials are asymptotic to these equipotentials. In some cases this configuration may be desired; however, in the pinned-strip-in-tension problem it was not.

Applying an external voltage source to the boundary shown in Figure 6 will cause the asymptotic isotropic point to change position on the boundary. If the potential is adjusted to the correct value, the isotropic point can be moved down the boundary electrode until it is located at one edge of the electrode (i.e., where an insulated boundary starts and the boundary electrode ends). When the potential of the intermediate boundary is so adjusted, the equipotential configuration will be that shown in Figure 4. Therefore, when a boundary is known to have an isotropic point of the type shown in Figure 4, the potential on the adjacent electrode must be adjusted to the proper value.

The isotropic point of the form shown in Figure 2 will always result at the junction of an equipotential and an insulated boundary, unless the potential of the equipotential boundary is adjusted as indicated in the previous paragraph to obtain an isotropic point of the form shown in Figure 4.

By careful analysis of the isotropic points a technique has been developed for construction of electric analogs to determine stress trajectories in a plane elastic field. In summary this technique is as follows:

1. The two-dimensional region must have free boundaries or boundaries subjected to normal stresses or point loads in order to apply the analogy. A point load or a normal distributed stress will be the type of loading or a good approximation of the type of loading of the majority of plane stress problems.

2. The plane region must be simply connected. If it is not it can be made so by making a cut through to the internal boundaries. The sides of the cut now become boundaries of the simply connected region and thus the cuts must be made so that one family or the other of the stress trajectories is now coincident with the sides of the cut. Thus the cuts must be made along stress trajectories. A line of symmetry is a good choice on which to make this cut, since a line of symmetry must belong to one family or the other of the stress trajectories. If no symmetry exists, the stress trajectory to cut into an internal boundary must be determined by some other means, such as by photoelasticity.

3. The location and type of isotropic points, if any exist, in the region or on the boundary of the region must now be determined. This can sometimes be done by inspection; however,

the use of photoelastic isochromatic fringe patterns and isoclinic fringe patterns is necessary for complex shapes.

4. When an isotropic point of the form shown in Figure 1 occurs internally in a region, the equipotential in an electrical analogy would have to be discontinuous at that point. Therefore these points must be removed from the region since such an equipotential configuration can not exist. Removal of these points once again makes the region multiply connected and another cut must be made as discussed in part 2. In many cases an isotropic point of the type shown in Figure 1 will occur on a line of symmetry and cutting the region on this line will result in the form of isotropic point shown in Figure 2. In some cases an entire line of isotropic points will occur (e.g., pure bending). In this case the entire line must be cut from the region.

5. Two models are now cut from conductive sheet to the same configuration as the desired two dimensional stress field with the boundary modification indicated in the previous steps. On one model parts of a boundary belonging to a given family of stress trajectories are made into an electrode by the use of silver conductive paint. The unpainted boundaries are thus insulated by the air. On the other model the parts of the boundary belonging to the conjugate set of stress trajectories are made into electrodes in a similar manner.

Points on the boundary subjected to a point load can be approximated by a small circular area.

6. The electrodes corresponding to the two extreme equipotentials of a given family are then connected across a potential source (e.g., a battery). The intermediate electrodes are then each connected to the movable contact on separate precision potentiometers. The end contacts of the potentiometers are then connected across the potential source.

7. The potential of the intermediate electrodes is now adjusted via the potentiometers to obtain the known isotropic point configuration. This will be a step by step process if there is more than one intermediate boundary electrode, since the potential on one electrode will have some effect on the equipotential configuration around the other electrodes.

8. Using a bridge circuit with a D.C. scope as the balance indicator and a precision potentiometer as the reference, the equipotentials in the conductive sheet can quickly be traced very accurately.

Consider, for example, a ring subjected to a diametrical compressive force. Using the technique previously set forth, the symmetry of the problem enables consideration of only one-quarter of the ring to apply the electrical analogy. Figure 8 shows p and q stress trajectories obtained by the electrical

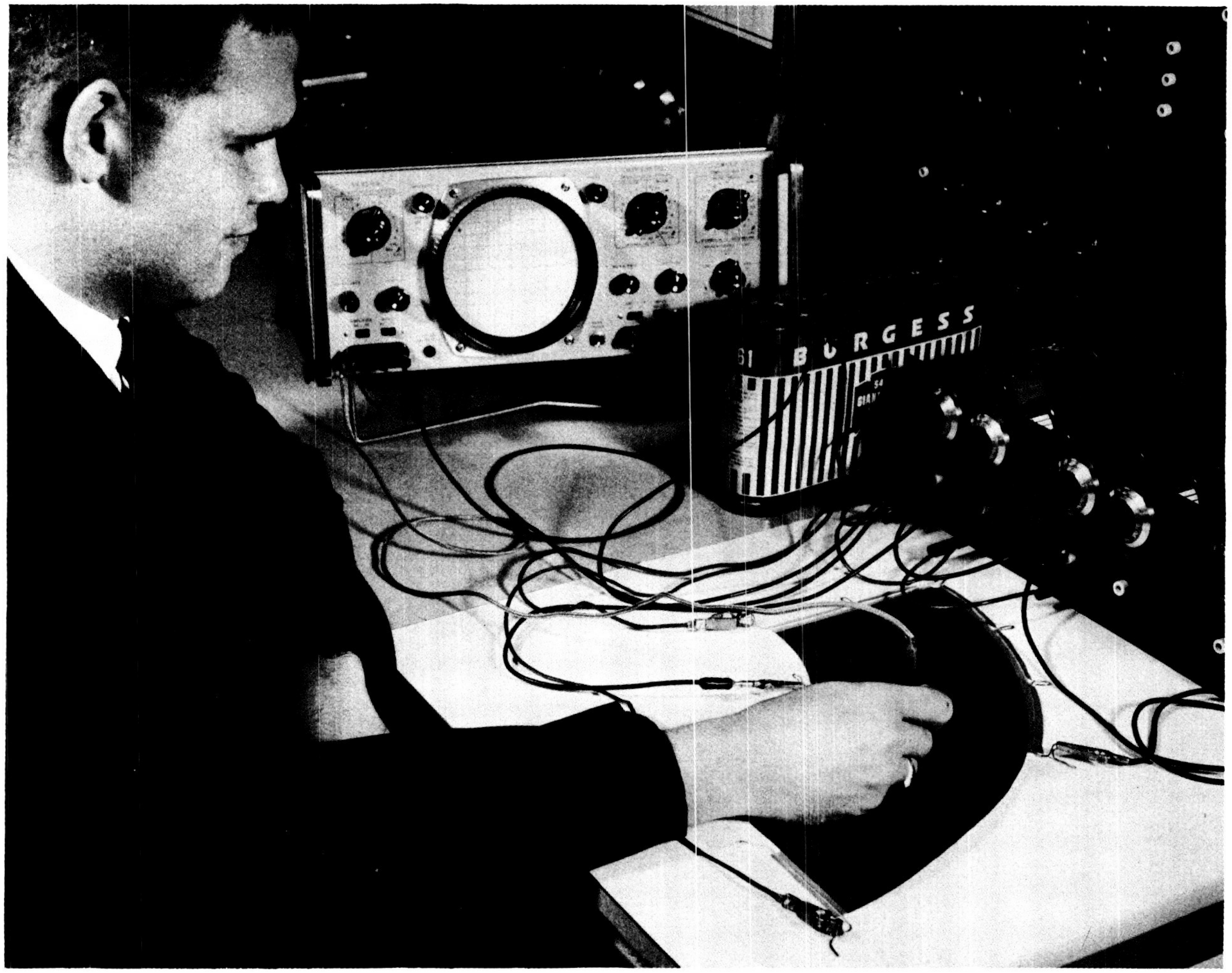

Fig. 7 - Mr. Droste tracing stress trajectories by means of conductive sheet analogy.

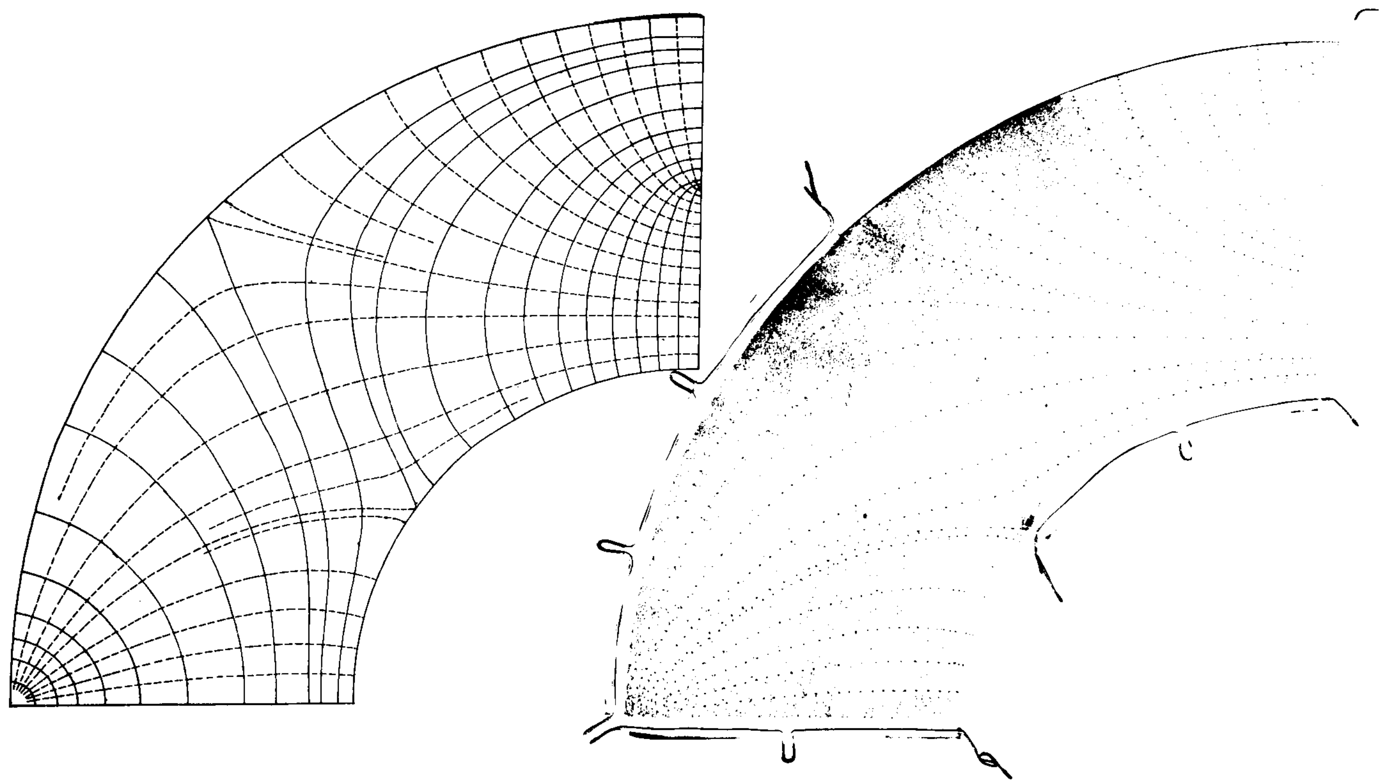

Fig. 8 - One quarter segment of a circular ring subjected to a diametrical force:

Top - Electrically determined stress trajectories; p - solid lines, q - dashed lines.

Bottom - Electrical model used to determine the q family of stress trajectories.

analogy and the electrical model used to obtain the q family of stress trajectories. The segment considered includes three isotropic points on the boundary. Two are of the form shown in Figure 4 and one is of the form shown in Figure 2. Note also the excellent orthogonality obtained at all points in the field.

The presented technique has been applied to the problems of a square plate in compression on a diagonal, a circular ring in compression on a diameter, a beam in pure bending, a split ring in compression across the split end, and a pinned strip in tension. The results have been in very good agreement with theory and published findings experimentally determined by other methods.

Once the configuration of the stress trajectories is known, it can be used to separate the principal stresses and the principal stress difference data obtained, from the isochromatic fringe pattern obtained from photoelasticity. The photoelastic method used to obtain this separation requires the use of the isoclinic fringe patterns. At best the isoclinic fringes are very hard to determine accurately, especially in the vicinity of isotropic points. However, the stress trajectories determined by the electric analog are very clearly defined, thus providing a more accurate separation of the principal stresses.

Theocaris develops an approximate method to determine the differential parameter of the first order for the functions determining the stress trajectories. He then transforms the Lamé-Maxwell equations into a form whereby the differential parameter of the first order is used in a step by step process to separate the principal stresses along a stress trajectory.

The signs involved in the process outlined by Theocaris present a problem and efforts have been made to find a more consistent way to perform the separation process done by Theocaris without the use of the differential parameter of the first order. Using a relation given by Frocht, a method has been developed to use the radius of curvature of the stress trajectories and the incremental distance along the stress trajectories to separate the principal stresses. Numerically the method developed is identical to that of Theocaris, however, the Lamé sign conventions can now be easily applied. At the present time these equations are being analog determined stress trajectories to separate the principal stresses. The equation has been checked on one problem with very good agreement. Other problems are now being considered.

SPACE TECHNOLOGY PROJECT # 10

CHARACTERISTICS OF SOLID PROPELLANT OXIDIZER SUSPENSIONS

N65-33662

CHARACTERISTICS OF SOLID PROPELLANT OXIDIZER SUSPENSIONS

Project Investigators:

Dr. P. T. Eubank
Department of Chemical Engineering

Mr. B. F. Fort
Graduate Assistant

Independent experimental measurement of shear stress versus shear rate with a rotational viscometer and of pressure drop versus volumetric flow rate in a pipe apparatus has been completed for the aqueous solutions of two polymers at 25°C. The polymers, polyvinyl alcohol (PVA) and sodium carboxylmethylcellulose (CMC), were present in solutions of 0-7% by weight.

It is the principal object of this project to find a single numerical method or rheological equation of state that will convert viscometer to pipe data without the occurrence of errors greater than 4% for all pseudoplastic, time-independent liquids. Rotational viscometer results are integrated via the Rabinowitsch equation to produce calculated pipe results. Deviation of the calculated from the experimental pipe data results from (1) experimental viscometer error, (2) experimental pipe apparatus error, and (3) integration procedure error. The latter error depends on the numerical integration technique used or rheological model assumed.

Progress to Date

1. Numerical

This project has used three different integration procedures:

(a) A strictly numerical method based on an overlapping parabola fit of experimental data.[1]

(b) The standard Newton-Coates equations for numerical integration by polynomial fit.

(c) A new equation of state,

$$\tau = A \dot{\gamma}^{B} e^{C \dot{\gamma}} \tag{1}$$

which has fit all experimental data thus far obtained to a high degree of accuracy. This equation may be integrated analytically by the Rabinowitsch equation to yield

$$\frac{Q}{\pi R^3} = \frac{1}{3}\left[\gamma_W - \left(\frac{1}{3C}\right) + \frac{1}{3C} \sum_{i=1}^{\infty} (-1)^{i-1} \dot{\gamma}_W^{-1} \prod_{j=1}^{i} \frac{3B-j+1}{3C} \right] \tag{2}$$

if 3B = integer.

or

$$\frac{Q}{\pi R^3} = \left(\frac{\dot{\gamma} W}{3B+1}\right)\left[B + \frac{C\dot{\gamma}W}{3B+2} - \frac{C}{3B+2} \sum_{i=2}^{\infty} (-1)^{i} \dot{\gamma}_W^{i} \prod_{j=2}^{i} \frac{3C}{3B+1+j} \right] \tag{3}$$

if 3B ≠ integer.

The relative merit of the three methods is presently under study utilizing the experimental PVA and CMC data and also by the assumption of ideal power-law, Ellis, and Reiner-Phillippoff model fluids. Final data and results on this investigation will be available by 1 September 1965.

---

[1] Osinski, C. A., M. S. Thesis, Texas A&M University, 1963, College Station, Texas

2. Experimental

An improvement has been made in the rotational viscometer whereby readings may be obtained at any intermediate angular velocity of the bob. The original unit was limited to eight fixed speeds.

Both the rotational and pipe apparatus have been revised for data procurement over the temperature range, 25-100°C. A constant temperature bath has been constructed around the rotational viscometer, and the pipe apparatus kettle and tubes have been jacketed for hot water.

SPACE TECHNOLOGY PROJECT # 11

MAGNETIC PROPERTIES OF SOLIDS

N65-33663

MAGNETIC PROPERTIES OF SOLIDS

Project Investigators

Dr. Charles F. Squire, Associate Dean for Science, Principal Investigator

Mr. Tom W. Adair, III, NASA Graduate Fellow

Mr. R. Zamecki, Graduate Fellow

Mr. E. Sharp, Graduate Fellow

I. Introduction

The new magnetic property reported by Adair and Squire[1] on a number of single crystals of LiF has been extended in the present work to include 13 crystals of NaCl, 5 of KCl, and 6 of LiF. Considerably more information has resulted from the experiments reported herein and we are ready to attribute the new effect to lattice imperfections such as dislocations or certain types of vacancies in these high purity, optical quality, single crystals of alkali halides. Gammel[2] gave a phenomenological interpretation of the original experiments and the major features of his theory are confirmed by the present more extensive study.

Briefly recapitulating, the experimental arrangement was a 3/4 inch diameter by 1 inch long cylindrical sample of alkali halide which was suspended along its cylindrical axis to form a sensitive

---

1 T. W. Adair, III and C. F. Squire, Phys. Rev. 137, 949 (1965)

2 J. L. Gammel, Phys. Rev. 137, 951, (1965)

torsion pendulum (see Figure 1 of Reference 1). This pendulum system, known as a torque magnetometer, was arranged so that the crystal sample was in the uniform and constant magnetic field of a 12-inch diameter pole-face magnet. A small torque, M x B, was the unexpected result when a steady field, B, was applied. The torque depended on the orientation, θ, of the magnetic field relative to the crystalline axes and torque curves indicated the requirement of uniaxial anisotropy. It was observed that this torque could be increased by X-irradiation and could be decreased by heat annealing. The angular frequency, ω , of the pendulum was observed to be modulated by the direction, θ, which the magnetic field made with the basic cubic crystal lattice such that a maximum and a minimum always corresponded to the field direction along a (100) axis of the crystal. The data taken corresponded to an equation for the angular frequency:

$$\omega = \omega_o + \omega_1(B) + \omega_2(B) \cos 2(\theta - \phi) \qquad (1)$$

The present work was undertaken to answer a number of questions and to investigate the new magnetic effect in other alkali halides. The results will surely convince the severest critic that we are dealing with something quite basic and not an impurity of pure iron or similar ferromagnetic substance.

II. Experimental Results

The torque measurements were made on the very sensitive torsion pendulum system described in our previous publication[1]. Each milli-

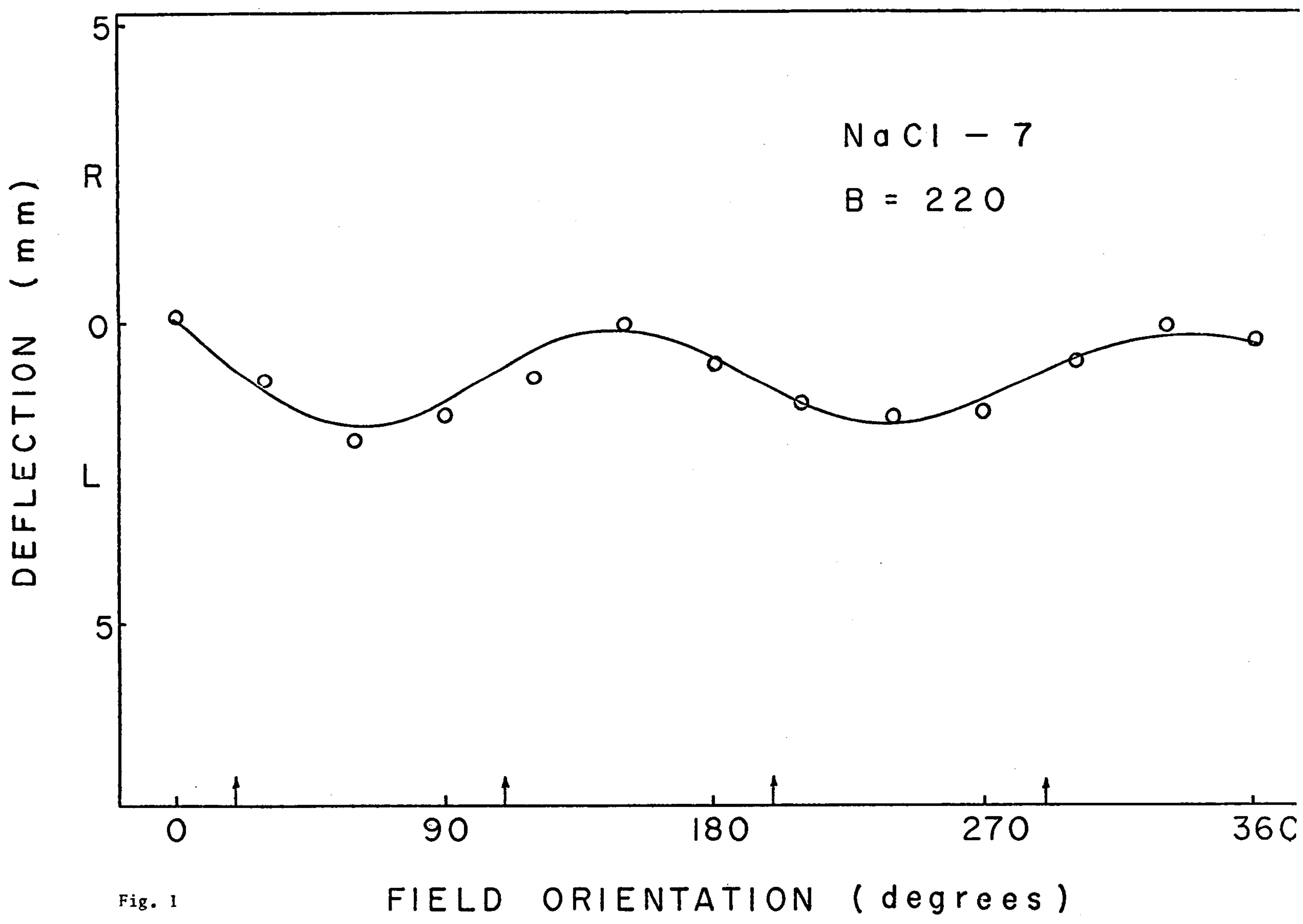
NaCl – 7
B = 220
DEFLECTION (mm)
5
R
0
L
5
0
90
180
270
360
FIELD ORIENTATION (degrees)

Fig. 1

meter of deflection of the light beam on the ground glass scale was the result of a torque of the order 1.4×10^{-4} dyne-centimeters. When a sample in the "as received" condition[3] from Harshaw Chemical Company or from Optovac Company was suspended in the uniform magnetic field, a torque which varied with the orientation of the field relative to the crystalline axes was observed.

Crystalline axes were determined by x-ray diffraction. Fig. 1 shows the deflection on the galvanometer scale and therefore the torque as a function of the field orientation relative to the crystalline axis for the sodium chloride sample NaCl-7 in a magnetic field of 220 G. Arrows at the bottom of the figure indicate positions of the magnet for which the field was along a crystalline 100 direction. Therefore, the extremes of the torque correspond to positions of the magnetic field along crystalline 110 directions. The curve generated by the data points has a periodicity of 180 degrees. These data will be discussed in terms of a torque arising from a magnetic susceptibility that is different along one axis (e.g., the x-axis) than along another (e.g., the y-axis). Note, however, that the curve described by the sin 2θ dependence has a small steady bias to the left in order to fit the data points.

After these measurements were made, the magnetic induction was

---

3 The crystal has never been in a magnetic field greater than the earth's field and has never been exposed to any significant ionizing radiation.

increased to a value of 3500 G. Then the field was reduced to zero, and measurements in 220 G. were obtained. The results, of these measurements are shown in Fig. 2 which now shows a sin θ dependence. The curve in this figure has a periodicity of 360 degrees with the extremes of the torque approximately 90 degrees on either side of the position at which the 3500 G. was applied. The magnitude of the torque has been increased, and it appears as if the crystal has been given a permanent magnetization. The data curves will be discussed in terms of a fixed-to-the-lattice residual magnetization M_o. The permanent moment can be reduced by a standard demagnetizing technique: the magnet is set at a position and the field adjusted to 1000 G, the magnet is turned off and rotated 180 degrees, the field is now adjusted to 900 G, the magnet is again turned off and rotated 180 degrees, the field adjusted to 800 G, etc.

As the field is increased from B = 200 G to large values (B = 400 G, B = 600 G, etc.) the curve gradually regains the sin 2Q dependence. Curves that illustrate this gradual return are shown in Fig. 3 on a sample which had been strongly magnetized. In Fig. 3a the deflection as a function of field orientation is shown for a measuring field of 185 G and the curve produced has a periodicity of 360 degrees with the two extremes 180 degrees apart. Next the measuring field was increased until B was 350 G and the measurements repeated. Fig. 3b shows that the two extremes have moved until they are only 120 degrees apart. It is seen in Fig. 3c that, when the

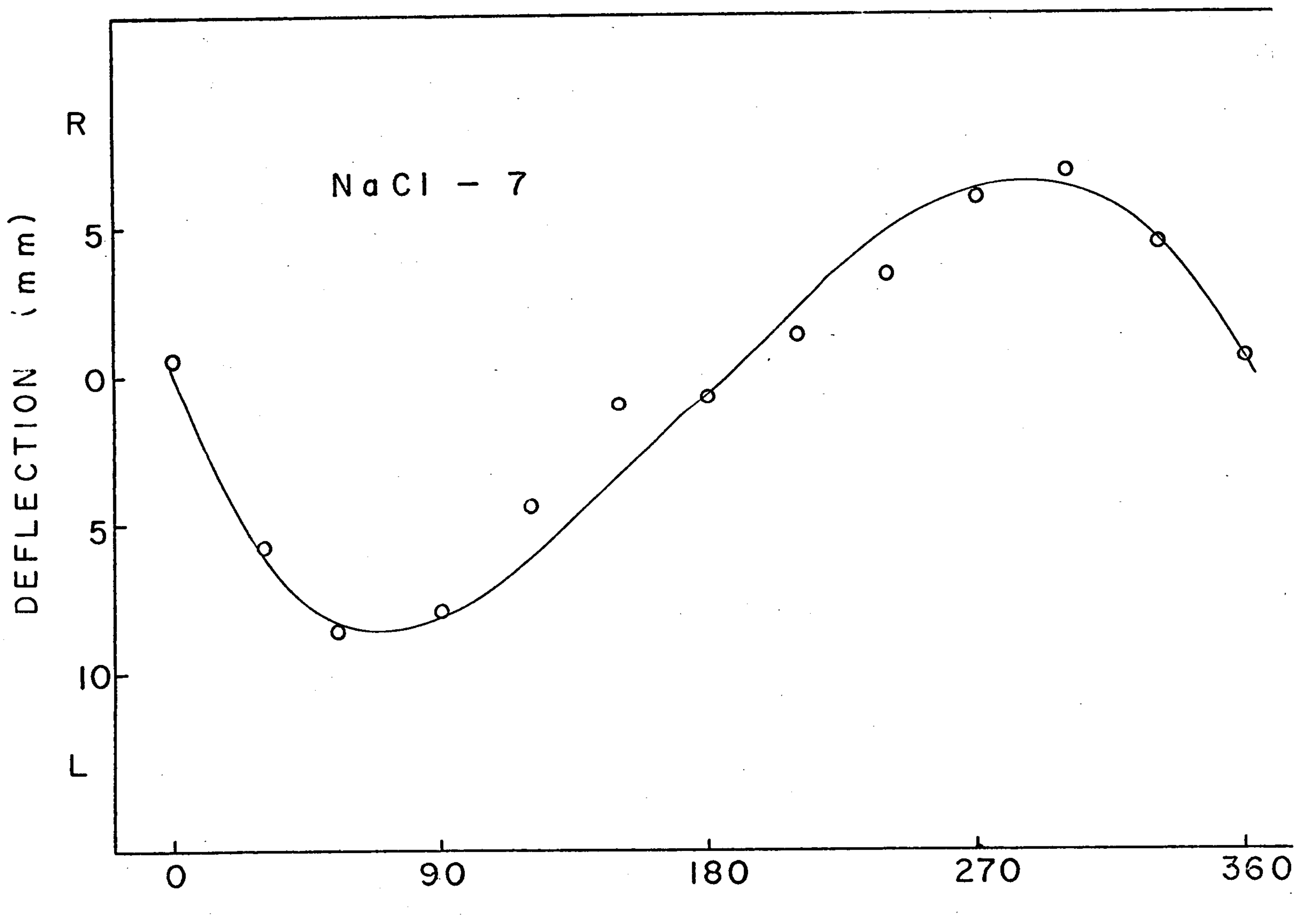
NaCl - 7
R
5
0
5
10
L
DEFLECTION (mm)
0
90
180
270
360
FIELD ORIENTATION (degrees)
Fig. 2

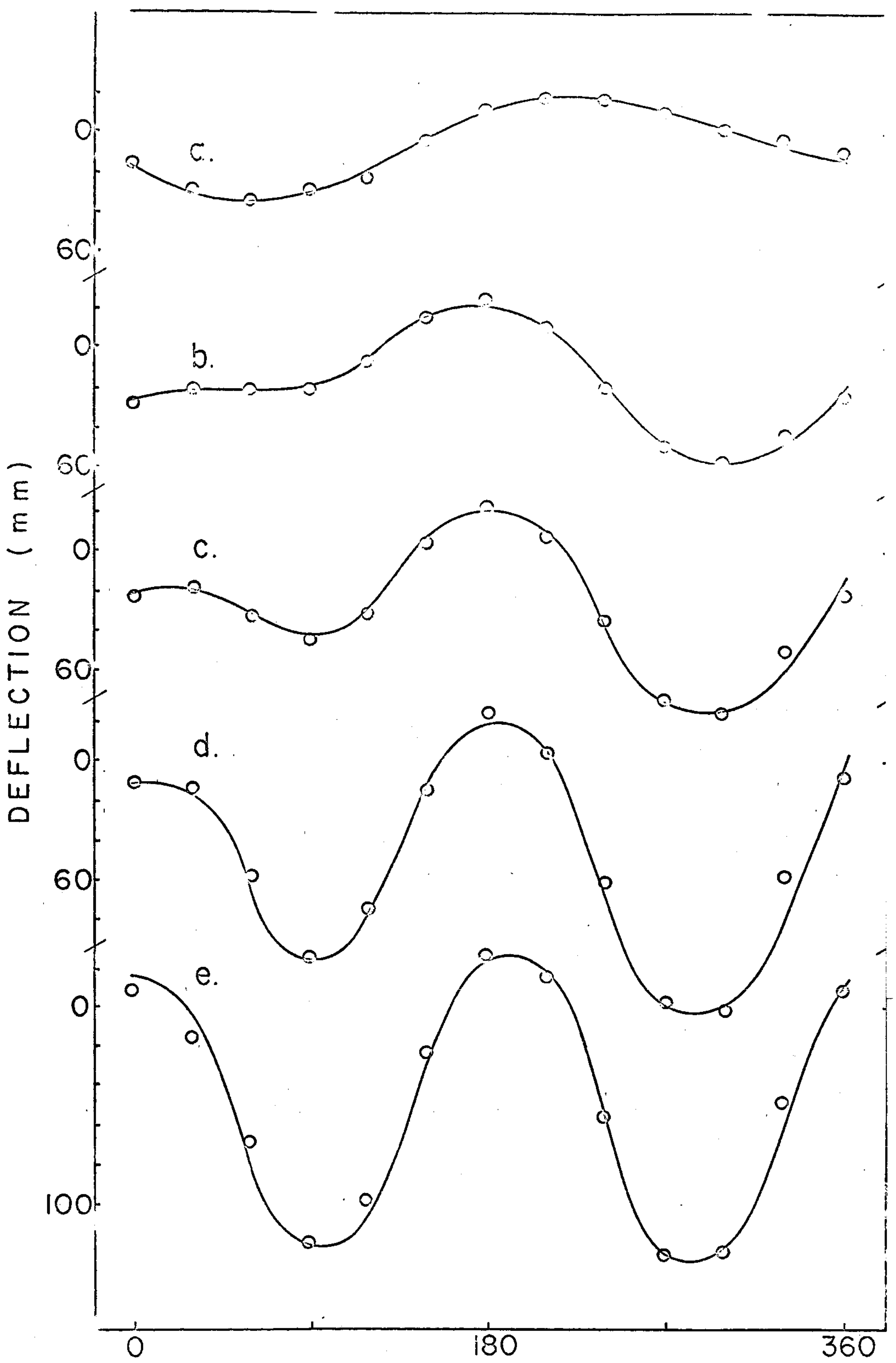

Fig. 3 FIELD ORIENTATION (degrees)

magnetic induction was increased to 240 G, two small additional peaks about 70 degrees apart appeared and the two major peaks were shifted to about 100 degrees apart. In Fig. 3d, where B has been raised to 650 G, the maxima and minima are 90 degrees apart, and the maxima are approaching the same value (125 mm left), and the minima are approaching the same value (20 mm right). Finally, Fig. 3e shows that for B = 760 G the periodicity is again 180 degrees, that each maximum is 90 degrees from the adjacent minimum, and that the maxima are equal and the minima are equal.

Figs. 3a through 3e all illustrate data curves which are not symmetric about the zero deflection axis, but are shifted toward left deflection, as was always the case if the data points were taken after the magnet was shifted to each measuring position by a clockwise movement. If the magnet were shifted to the measuring positions by a counter clockwise movement the curves would be shifted an equal amount to the right. Both effects were illustrated for LiF in Fig. 4 of reference 1 and are illustrated for KCl in Fig. 4 of this paper. The data points of the lower curve were taken after clockwise shifts and those of the upper, after counterclockwise shifts. Such hysteresis-type effects are caused by the lack of complete alignment of the fixed moment with the magnetic field that was used for the torque measurements. Both curves have a periodicity of 180 degrees since B was 1000 G -- i.e. well above the range of transition. Similar data were obtained for all 24 crystals. The amplitudes of

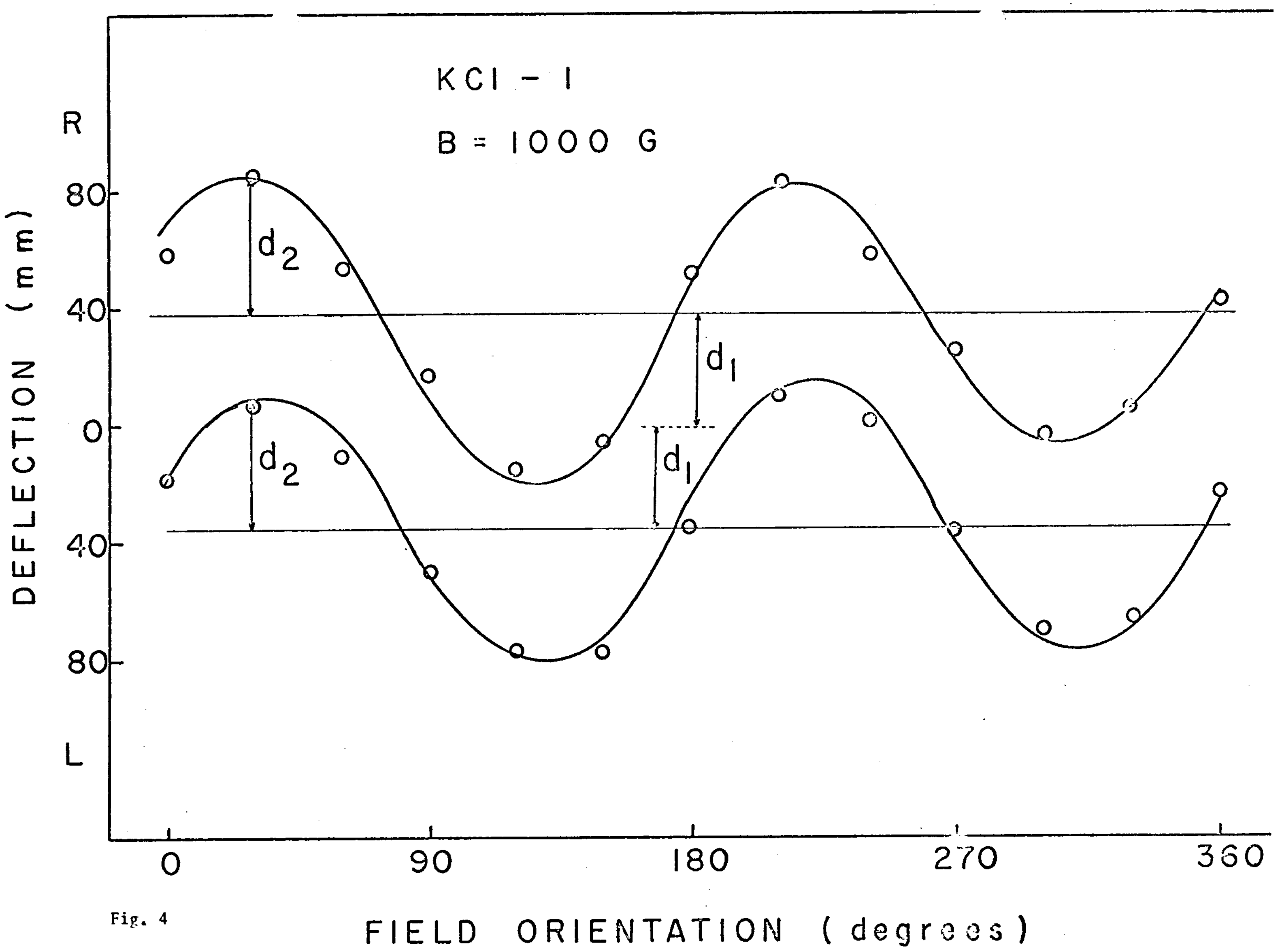
KCl - I
B = 1000 G
R
80
40
0
40
80
L
DEFLECTION (mm)
d2
d1
d1
d2
0
90
180
270
360
FIELD ORIENTATION (degrees)

Fig. 4

modulation of the curves in Fig. 4 are equal and are defined as d_2 and the displacements of the curves from the zero axis are equal and are defined as d_1. All of the crystal samples except one were cut with the cylindrical axis along a 100 crystalline direction. The exception was a lithium fluoride sample (LiF-5) which was cut with its cylindrical axis along a 111 crystalline direction. Even though the crystal is cut differently, its torque-field orientation curve is similar to the curves for the other crystals -- i.e. the curves have a 180° periodicity.

The torque exerted on the crystals in the uniform magnetic field resulted in changes in the angular frequency of the pendulum. In zero field the pendulum system oscillated with a natural frequency ω_o. Application of a magnetic field increased this frequency by an amount that depended on the orientation of the field relative to the crystalline axes. This was shown in Fig. 2 of reference 1 for LiF. Similar results that satisfied equation (1) were obtained for KCl and NaCl.

The quantity d_1 was defined as the amount the modulated torque curve was shifted from the zero axis and the quantity d_2 was defined as the amplitude of the modulated curve. Both are functions of the magnetic field. The quantity d_1 is a linear function of B for B less than about 600 G. Fig. 5 shows this displacement as a function of the magnetic induction for potassium chloride sample KCl-1. In Fig. 6 the amplitude d_2 of the modulated curve is plotted as a

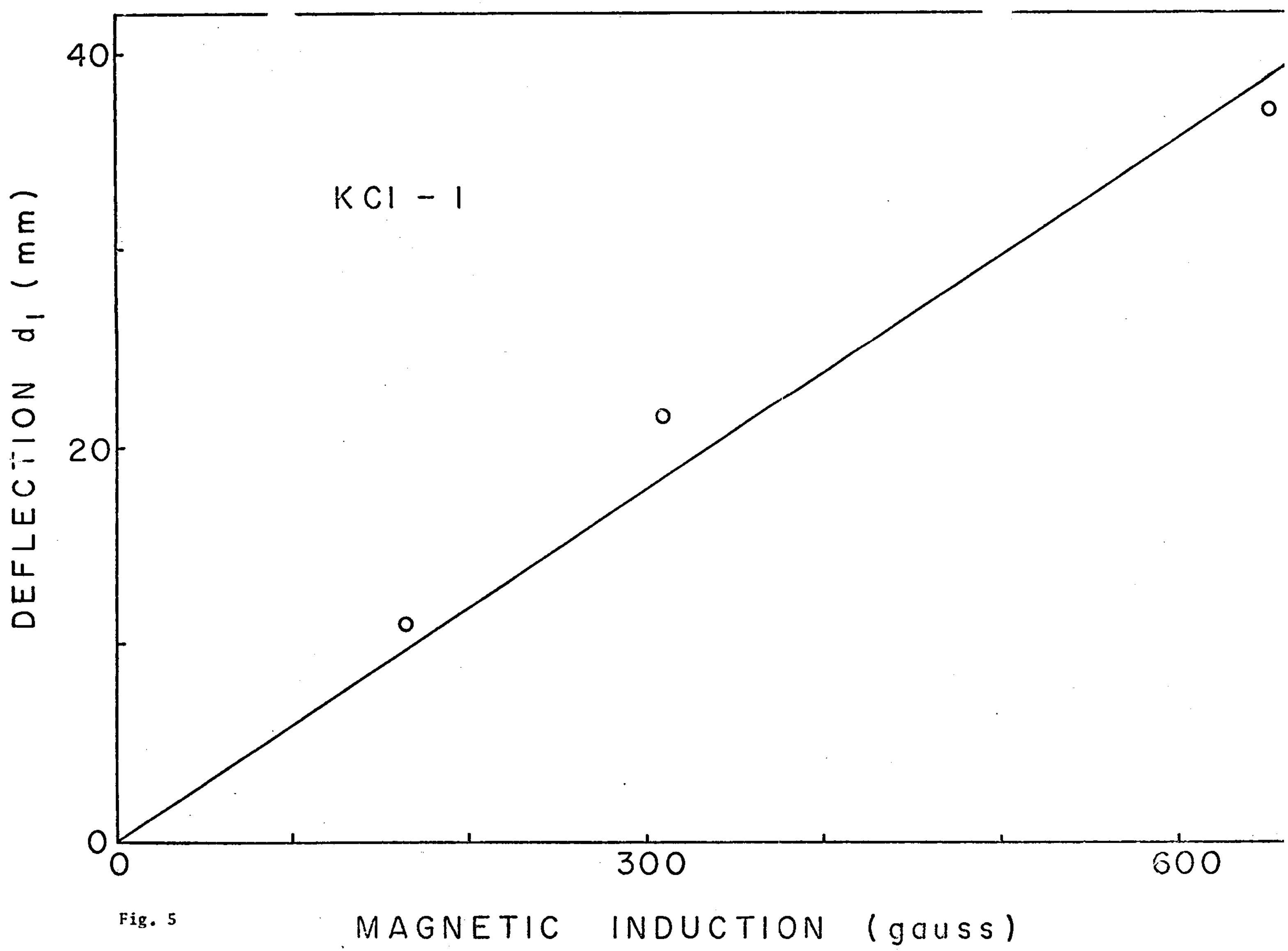
KCl - I
DEFLECTION d1 (mm)
40
20
0
0
300
600
MAGNETIC INDUCTION (gauss)

Fig. 5

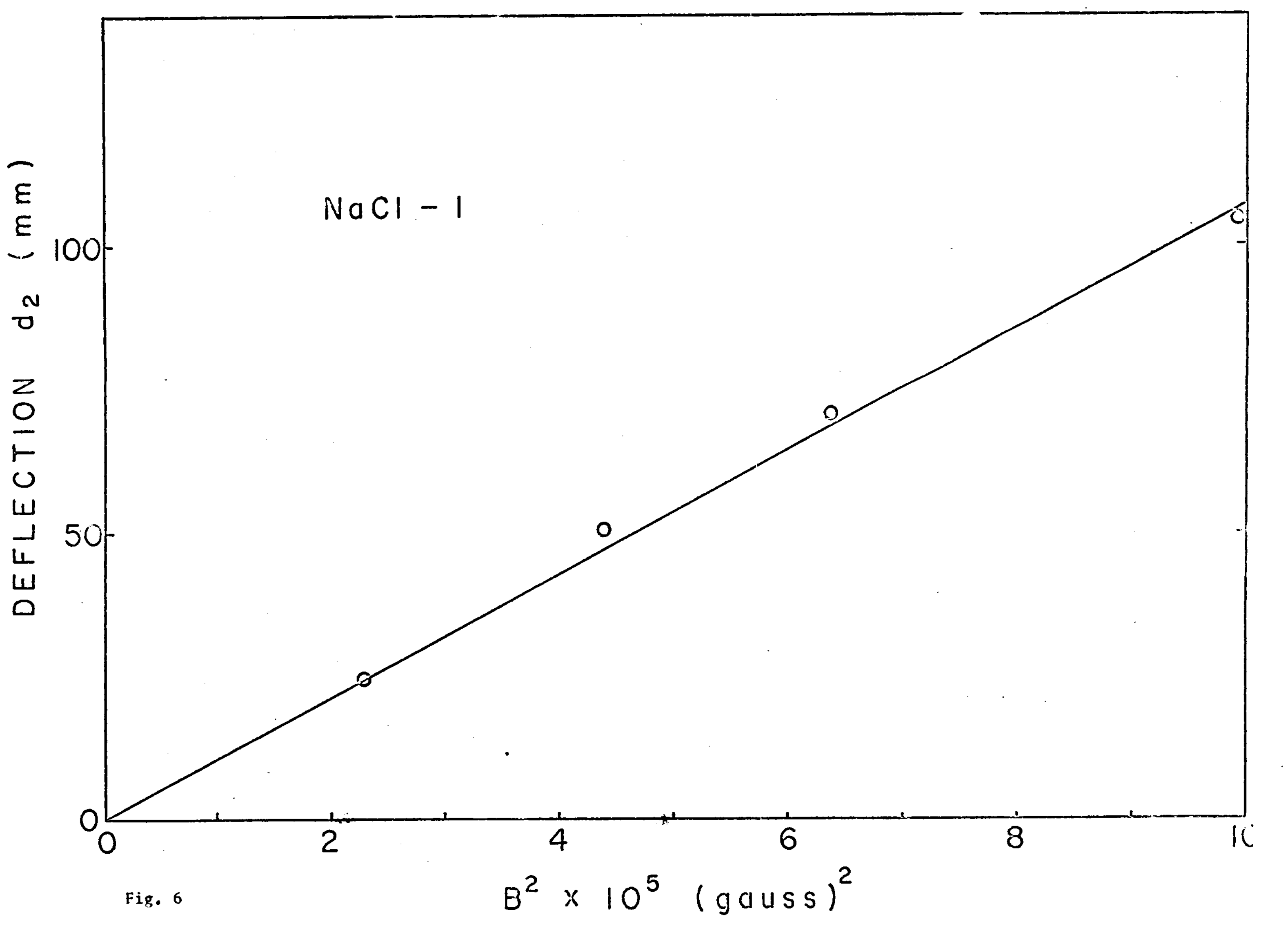

Fig. 6

function of the square of the magnetic induction for the sodium chloride sample NaCl-1. It is seen that d_2 varies as the square of the magnetic field.

Sample NaCl-10 was a sodium chloride crystal 2.54 cm (one inch) long and 3.18 cm (1-½ inches) in diameter. After torque measurements were made on this sample and the value for d_2 obtained, the crystal was carefully removed and placed in a clean microlathe. The radius was reduced from 1.58 cm to 1.38 cm with the lathe, and then several thousandths of an inch were removed with distilled water. The crystal was replaced in the pendulum and the value of d_2 obtained for this new radius. This procedure was repeated to obtain values of d_2 for radii of 1.11, 0.83, and 0.59 cm. The results of these measurements are shown in Fig. 7 where d_2 is plotted as a function of the square of the radius. A fairly good straight line can be drawn through the data points with the exception of one point. Thus the torque is proportional to the square of the radius of the crystal sample, and the magnetization is a bulk property of the crystal and not a surface effect. Specifically these experiments would seem to remove doubts about a speck of pure iron on the surface.

Data were taken at liquid nitrogen temperature ($T = 78^{\circ}K$), liquid methane temperature ($T = 111^{\circ}K$) as well as at room temperature ($T = 295^{\circ}K$). Fig. 8 shows the torque-field orientation curve for these three temperatures. The value of the amplitude of the modulated curve d_2 remained approximately the same when the temperature was

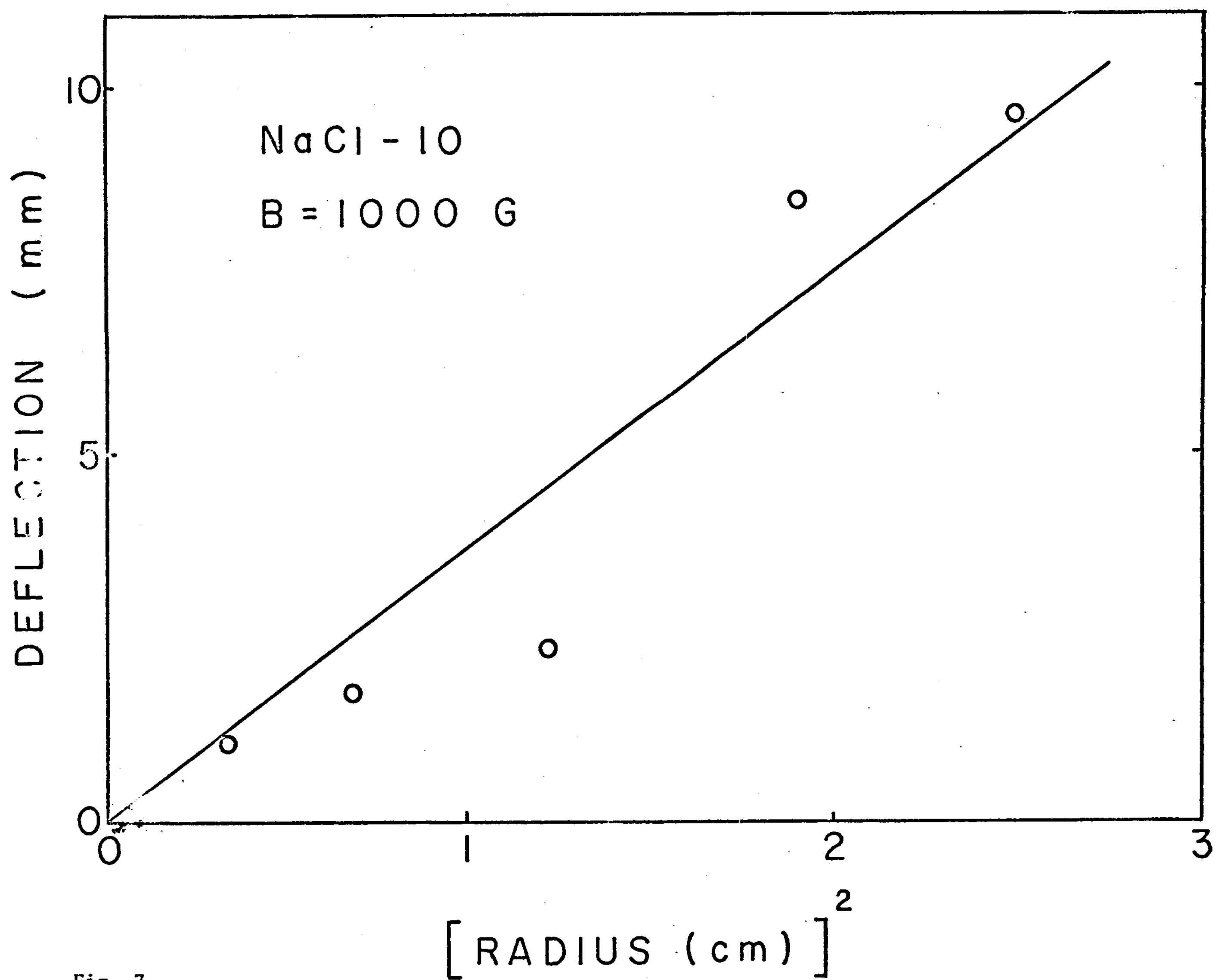

Fig. 7

varied. However, the shift of the curve from the zero axis d_1 increased as the temperature was lowered. The insert in Fig. 8 shows the values of d_1 for the three temperatures.

A number of measurements were taken to insure that the observed effect was a property of the crystal and not of the associated equipment. Data were obtained from a suspended crystal. The crystal was then carefully removed from the support rod and rotated a known amount (e.g., 30 degrees). It was replaced on the support rod and the measurements repeated. The data were found to have shifted by the same amount (i.e., 30 degrees). This procedure was repeated several times with the same positive results.

Next a crystal was suspended in the field without the use of DuPont glue. The support rod was forced into a small hole drilled in the end of the crystal and the results for this method of support were found to be the same as the results when the glue was used.

All crystals were carefully handled. However, for added assurance several were washed in water, alcohol, and acetone between measurements. This special washing had no effect on the observed data.

Finally, an alpha source was placed in the sample chamber to reduce or remove any built up electric charge. This also had no effect on the observed data. Details can be obtained from the Dissertation submitted by the author to the Graduate College of Texas A&M University for the degree of Doctor of Philosophy.

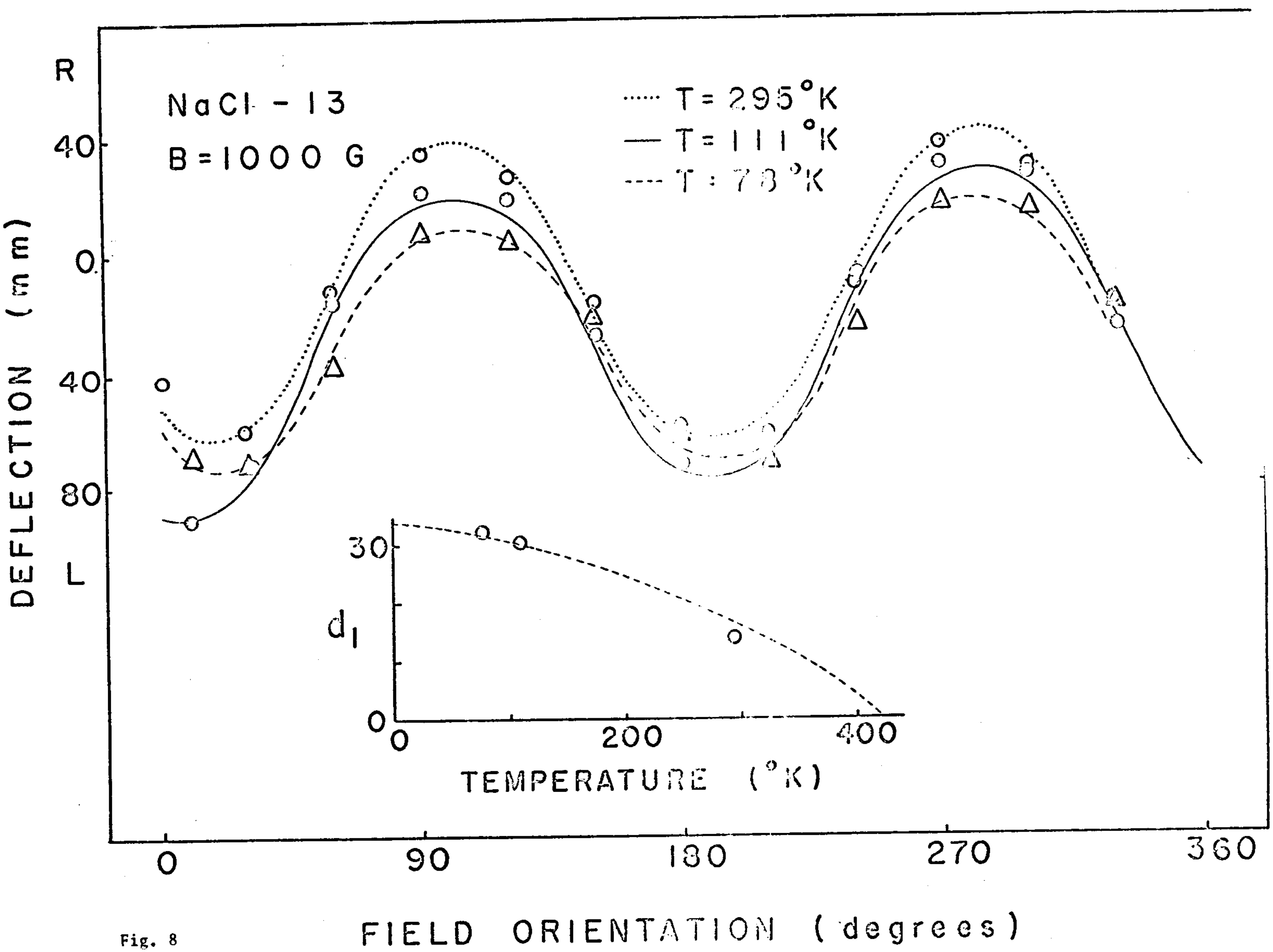
NaCl - 13
B = 1000 G
T = 295 °K
T = 111 °K
T = 78 °K
R
40
0
40
80
L
DEFLECTION (mm)
0
90
180
270
360
FIELD ORIENTATION (degrees)
30
d_1
0
0
200
400
TEMPERATURE (°K)

Fig. 8

III. Discussion of Results

The resultant torque, M x B, that acts on these alkali halide crystals in a uniform magnetic field may be described as a combination of two torques -- one caused by the interaction of the field with an induced moment and the other by the interaction of the field with a permanent moment. If a crystal in the "as received" condition is placed in the field, the induced moment is predominant (see Fig. 1), but if the crystal is placed in a large field (e.g., 3500 G) before the measurements are made, the permanent moment is predominant (see Fig. 2). The application of the large field causes the torque due to the permanent moment to become large enough to overshadow that caused by the induced moment.

The 180 degree periodicity of the curve in Fig. 1 can be understood if it is assumed that the susceptibility is different along the X-axis than it is along the Y-axis. A crystal with such an anisotropic susceptibility would yield a torque curve similar to that of Fig. 1, An equation for this torque is (in MKS units):

$$\text{Torque} = -1/2V \mu_o H^2 (\chi_x - \chi_y) \sin 2\theta \qquad (2)$$

where V is the volume of the sample, μ_o is the permeability of free space, H is the field, and θ is the angle between the field and the x-axis[4]. This torque equation gives a value of about 10^{-9} per unit volume for $\chi_x - \chi_y$ for the observed data. If it is

---

[4] L. F. Bates, Modern Magnetism (Cambridge, 1961), Chapter 4, p. 161.

assumed that this anisotropy is due to the 10^{13} atoms per cm^3 around dislocations[5] then the effective susceptibility per unit volume of these atoms would have to be about unity and we would demand more dislocation lines along the x-axis than along the y-axis. In view of the cooperative behavior leading to permanent moments, this (χ = 1) seems reasonable. If the anisotropy is assumed to be caused by a magnetic center that has a susceptibility of about 10^{-5} per unit volume then it would take about 10^{17} per cm^3 of these centers to have a susceptibility of 10^{-9}. This number (10^{17}) is approximately the number of point defects per cm^3 in the alkali halide crystals. Only certain clusters of vacancies might be expected to have the anisotropy required.

The 360 degree periodicity of the curve in Fig. 2 can be understood if it is assumed that the crystal has a permanent magnetic moment that is coupled to the lattice. The two maxima then correspond to positions where the magnetic field is perpendicular to the permanent moment. When the field is increased above 400 G, this coupling breaks down and the moment shifts to a position parallel to or nearly parallel to the field direction. For measurements in

---

5 According to W. G. Johnson and J. J. Gilman, J. Applied Phys. 30, 129 (1959) there are about 5 x 10^4 dislocations per cm^2 in LiF crystals as received from Harshaw Chemical Company and therefore there are about 10^{13} atoms per cm^3 adjacent to these dislocations.

fields greater than about 600 G the magnetic moment shifts until it is almost aligned with the field and is thus responsible for the shift d_1 of the modulated torque curve in Fig. 4. Since it was observed that for small values, say less than 400 Gauss, of the field the deflection d_1 was a linear function of the induction, the magnetic moment that causes this deflection is field independent.

Since it was observed that the amplitude d_2 varies linearly with B^2 (see Fig. 6), the magnetic moment that causes the modulated torque (see Fig. 4) is field dependent (i.e., the magnetic moment is induced in agreement with Equation (2).

The amplitude d_2 of the modulated torque-field orientation curve is temperature independent -- at least from room temperature (295^oK) down to liquid nitrogen temperature (78^oK). Fig. 8, which shows the torque data for the three temperatures -- 295^oK, 111^oK, and 78^oK -- shows that the displacement d_1 of the modulated curve from the zero axis changes when the temperature is lowered to 78^oK. The value of d_1 at 295^oK is 13.5 mm, the value at 111^oK is 30.5 mm, and the value at 78^oK is 32 mm. This increase in d_1, and therefore the increase in the magnetic moment which is responsible for the torque, is characteristic of the permanent magnetization that is described by the Bloch[6] $T^{3/2}$ law. The Bloch equation for the magnetization M at temperature T is

---

6 F. Bloch, Zeits. f. Physik, 61, 206 (1930)

$$M(T) = M(0) \left[1 - \left(\frac{T}{T_c}\right)^{3/2}\right] \qquad (3)$$

where M_o is the $T = 0^oK$ value of the magnetization and T_c is the Curie temperature. If d_1 is assumed to be proportional to the magnetization M and if the value of d_1 at $T = 78^oK$ is assumed to be near the value of d_1 at $T = 0^oK$, an approximate value for T_c can be obtained. Equation 3, when the assumptions are made, gives a value of about 425^oK for the Curie temperature. The dashed curve in the insert of Fig. 8 is a plot of the values obtained from Equation 3 for d_1 where d_1 has been assumed to be proportional to M and 425^oK has been used as the Curie temperature.

Finally we would indicate the known properties of point defects and dislocations[7]. Electrons may be liberated from the valence band into the conduction band and they may be trapped by point defects to form color centers and may be captured by dislocation lines[8]. Lidiard[9] and more recently Phariseau[10] have discussed the electrostatic potential around a dislocation line. It should be an interesting theoretical problem to investigate whether electrons captured by dislocation lines can have the magnetic properties described in this present paper.

---

7 F. Seitz, Rev. Mod. Phys. 18, 384, (1946)
8 H. Kawamera and H. Okura, J. Phys. Chem. Solids 8, 161, (1959)
9 S. D. Eshelby, C. W. A. Newey, P. L. Pratt, and A. B. Lidiard, Phil. Mag. 3, 76, (1958)
10 P. Phariseau, J. de Physique, 25, 868 (1964)

SPACE TECHNOLOGY PROJECT NO. 13

"A STUDY OF CADMIUM ABSORPTION OF RESONANCE NEUTRONS

IN VARIOUS FOIL MATERIALS"

"A STUDY OF CADMIUM ABSORPTION OF RESONANCE NEUTRONS IN VARIOUS FOIL MATERIALS"

Principal Investigators:

Dr. R. G. Cochran, Professor and Head, Nuclear Engineering Department

Mr. J. E. Powell, Graduate Assistant

Mr. Robert T. Perry, Graduate Assistant

This is a final report of the research efforts concerning "A Study of Cadmium Absorption of Resonance Neutrons in Various Foil Materials."

The project has now been carried to a successful conclusion and a final technical paper is being prepared for publication.

A review of the theoretical and experimental results indicates the high degree of validity that has apparently been obtained.

A standard technique for measuring low energy neutron fluxes is the foil activation method where thin metal foils such as indium are irradiated and then their radioactivity determined by counting, the flux is calculated from the foil's activity. The portion of the neutron spectrum to which an indium foil is sensitive can be divided into a thermal region and a resonance region by use of a cadmium filter. A bare foil gives the total flux and a cadmium covered foil yields the resonance flux so that the thermal flux is given by

$$\phi_{th} = \phi_{total} - \phi_{res}.$$

The cadmium filter in addition to absorbing all of the thermal neutrons also absorbs some of the resonance neutrons and to correct for this effect it is necessary to define a cadmium correction factor called F_{cd}. It is defined as the ratio of the activity of a foil with a zero cadmium cover thickness to the activity of a foil covered with an arbitrary thickness of cadmium.

To determine F_{cd}, a plot is made of the cadmium covered activity versus cadmium cover thickness and the resulting curve is extrapolated to the zero cover thickness activity. F_{cd} is then given by

$$F_{cd} = \frac{A_o}{A_{cc}}$$

where A_o is the zero cover activity and A_{cc} is the arbitrary cover activity. However, a plot of the resonance activity versus cadmium cover thickness does not produce a curve that can be extrapolated accurately so it is desirable to plot the resonance activity as some function of the cadmium cover thickness so that a straight line results.

For the case of an incident isotropic flux upon the cadmium covered foils Powell and Walker (1) found that the resonance activity should be plotted as a function of E_3, $(T_{cd}) - E_3(T_{cd} + T_{in})$ to get the linear plot. However, no previous attempt has been made to find the proper function for the case of an incident anisotropic flux.

To find this function it is desirable to derive a theoretical expression for F_{cd}. This is done by calculating the activity of a cadmium covered foil and then taking the limit as the cadmium thickness decreases to zero in order to obtain the zero thickness activity. The ratio of these two activities gives a theoretical expression for F_{cd}.

The cadmium covered activity is calculated by taking the incident neutron current and multiplying it by the probability that a neutron will escape capture in the cover and be absorbed in the foil. Assuming purely absorbing infinite slabs for the foils and covers the resulting expression becomes

$$A_{cd} = \int_{E_{cd}}^{\infty} de \int_{0}^{1} dyy\ 4(x_1,\ y,\ E)\ e^{-T_{ed}/y}(1-e^{-T_{in}/y}) + \int_{E_{cd}}^{\infty} de \int_{-1}^{0} dyy\ 4(x_4,\ y,\ E) e^{T_{ed}/y}\ (1-e^{T_{in}/y}) \qquad (1)$$

The T's are the foil and cover thickness in units of absorption mean free paths ad $4(x, y, E)$ in the magnitude of the vector flux. Taking the limit as T_{ed} 0 the bare activity becomes

$$A_b = \int_{E_{cd}}^{\infty} de \int_{6}^{1} dyy\ 4(x_2,\ y,\ E)\ (1-e^{-T_{in}/y}) + \int_{E_{cd}}^{\infty} de \int_{-1}^{0} dyy\ 4(x_3,\ y,\ E)\ (1-e^{T_{in}/y}) \qquad (2)$$

The various X_i are shown in fig. 1 to obtain the flux anisotropy it was aimed that a plane source of neutrons was at X=0.

Equations 1 and 2 cannot be solved until the flux is known for the geometrical system shown in fig. 1 and to obtain it the integra-differential Boltzman equation must be solved. To solve this equation

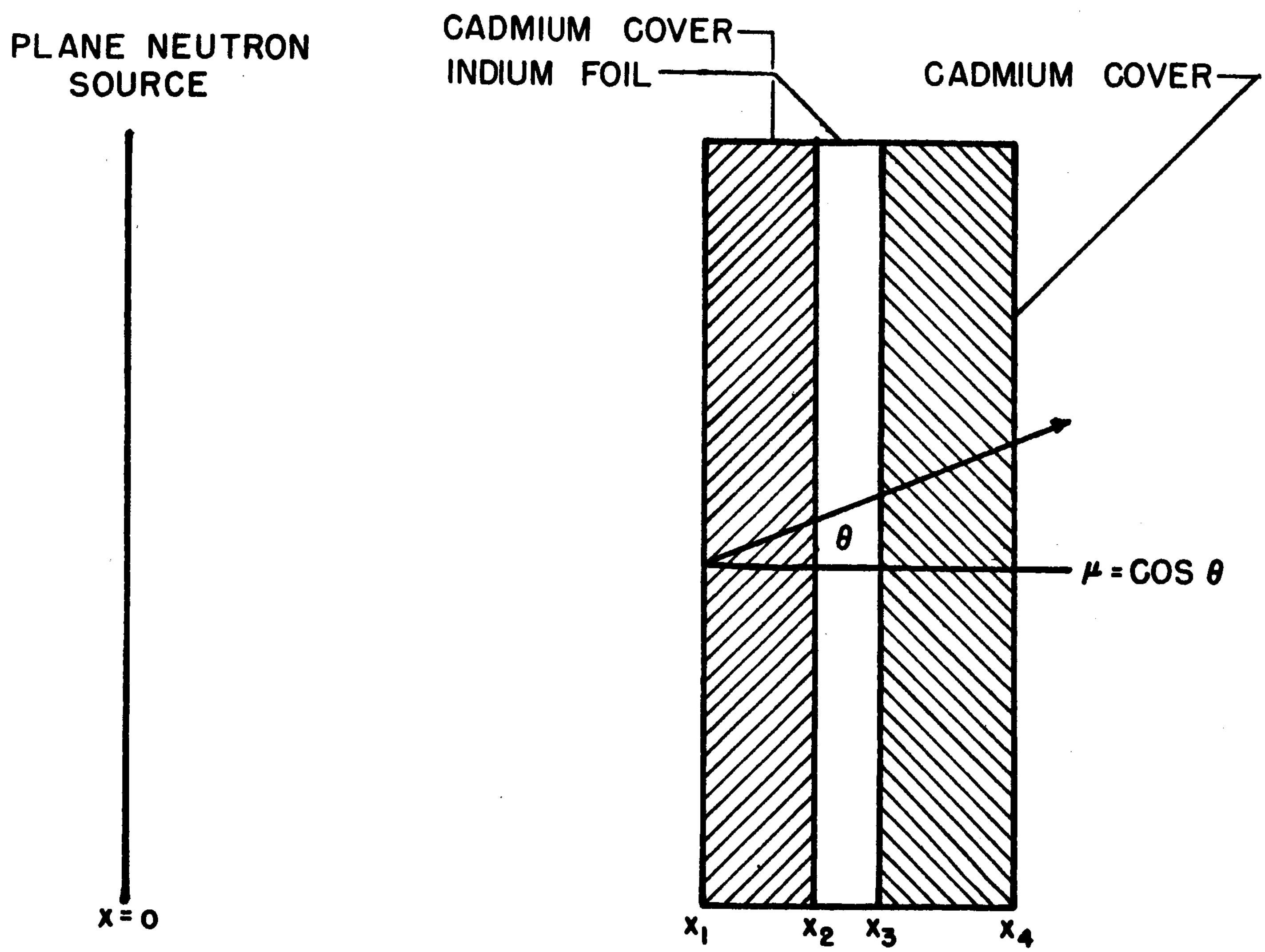
PLANE NEUTRON
SOURCE
CADMIUM COVER
INDIUM FOIL
CADMIUM COVER
θ
μ = COS θ
X = 0
X1
X2
X3
X4

Figure 1.

use was made of Spencer's and Fano's method (2) which had been used previously for x-ray transport problems but not for neutron transport. The method consists of expanding the flux in a series of Legendre polynomials and then expanding the Lengendre coefficients in a series of orthognal polynomials in the x variable. The expansions are

$$4(x,y,E) = \sum_{2} \frac{2\ 1+1}{2} N_e(x,E)\ P_e\ (y) \tag{3}$$

$$N_e\ (x,E) = e^{-\gamma(x)} \sum_{n} A_{en} U_n(\gamma)(X) \qquad 1 \text{ even} \tag{4}$$

$$= \gamma(x)\ e^{-\gamma(x)} \sum_{n} A_{en} V_n\ (\gamma)(X)\ 1 \text{ add} \tag{5}$$

The A_{en} are found by calculating the spatial movements of the Legendre coefficients. These moments are defined by

$$b_{en} = \int_{-\infty}^{\infty} x^n N_e\ (x,E)\ dx \tag{6}$$

and the A_{en} are related to the b_{en} by

$$A_{en}^{(E)} = \sum_{v=0}^{m} \binom{m}{v} \frac{(-1)^v}{2v!} \quad b_{1'}{}^{(E)}_{\gamma v} \qquad 1 \text{ even} \tag{7}$$

$$A_{en}^{(E)} = \sum_{v=1}^{m+1} \binom{m+1}{v} \frac{(-1)^{v-1}}{(2v-1)!} \qquad b_{1'}{}^{(E)}_{\gamma v-1} \quad 1 \text{ add} \tag{8}$$

To calculate the moments equation 3, is put into the Boltzman equation and after simplification a set of integral equations for the b_{en} results. These equations are solved numerically and the A_{en} are calculated from equations 7 and 8. After the A_{en} are found the N_e are known and equations 1 and 2 can be solved numerically. The experimental data is then plotted as a function of A_{cd} given by equation 1. It was found that by fitting the data in this moment a linear plot was obtained and an accurate value of F_{cd} could be obtained.

The experimental data was obtained by irradiating cadmium covered indium foils 2 cm in diameter with thicknesses varying from 2 mils to 8 mils. The cadmium covers were 1 in. in diameter and were .031 in., .042 in., .051 in., and .062 inches in thickness. The foils were irradiated at .25 in., .75 in., 1.25 in., 1.75 in., 2.25 in., 2.75 in., and 3.25 in. out from a Pu-Be neutron source. A foil positioning device was constructed out of lucite to accurately reposition the foils. This device is shown in fig. 2. Figure 3 shows the positioning device with cadmium covered foil in place and the source assembly. The foils were counted with a gamma scintillation spectrometer which was equipped with a 3 in. by 3 in. sodium iodide well crystal. The spectrometer is shown in fig. 4. The foils were mounted in the well crystal by use of a lucite ring which held the foils in exactly the same position on the floor of the well. The positioning ring is shown in fig. 5 which is a top view of the

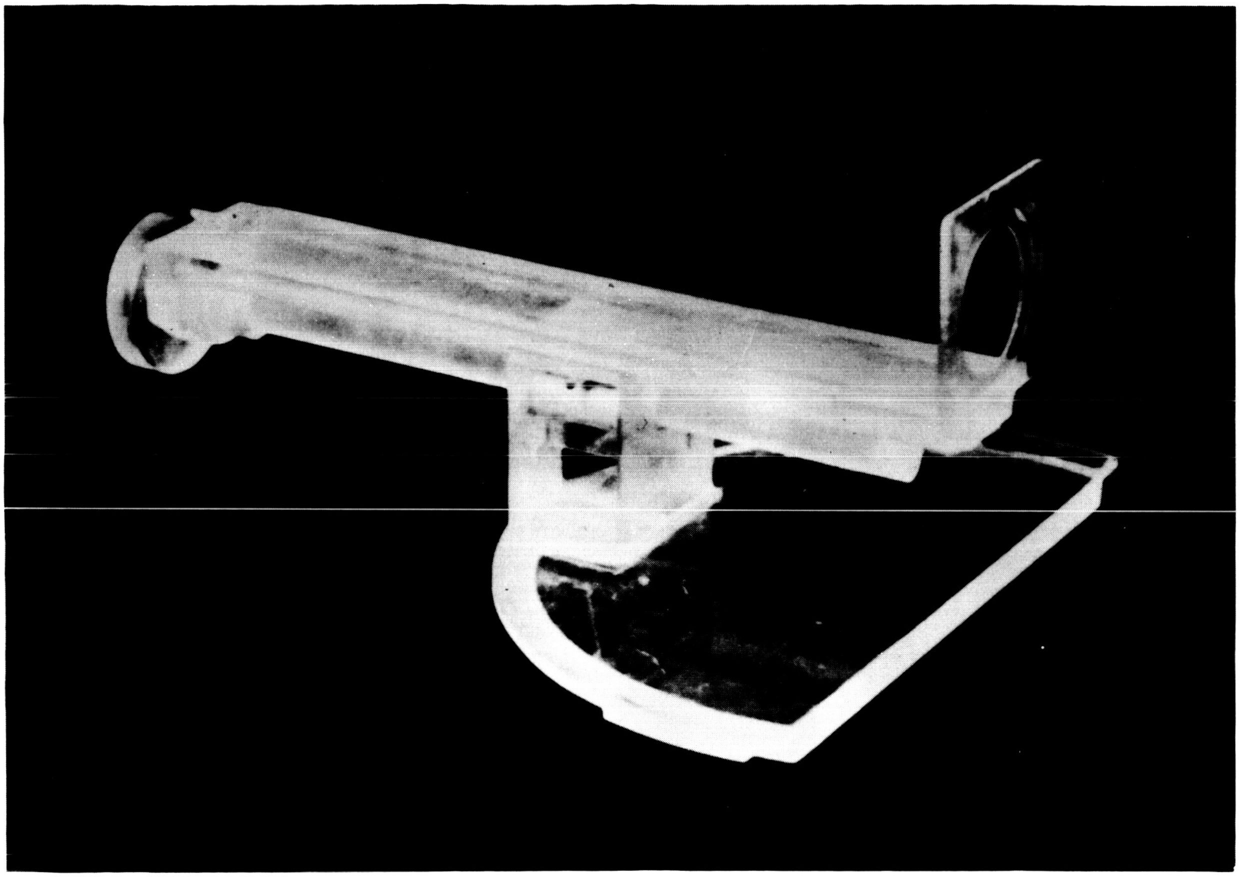

Figure 2. Foil Positioning Device

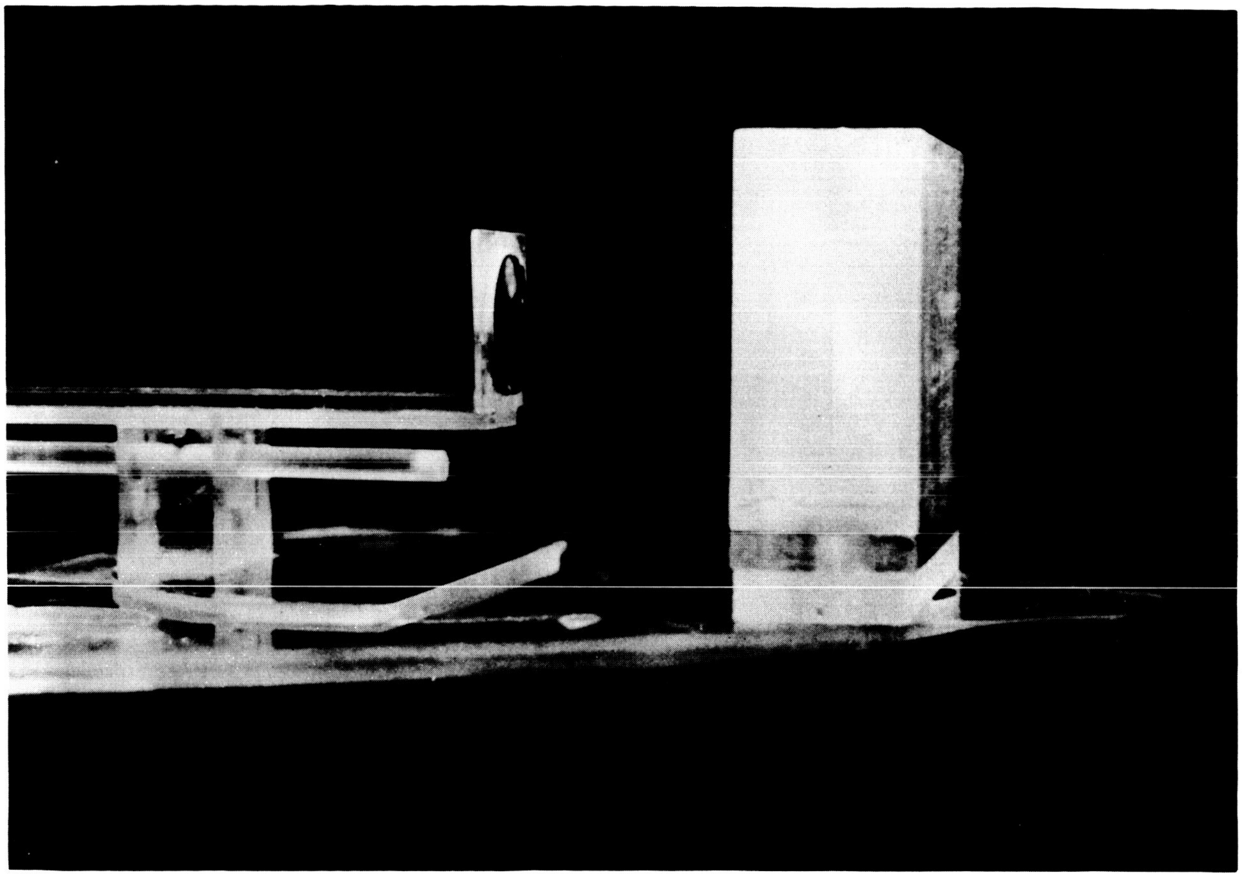

Figure 3. Foil Positioning Device with Mounted Cadimum Covered Foil 2 inches from the Source.

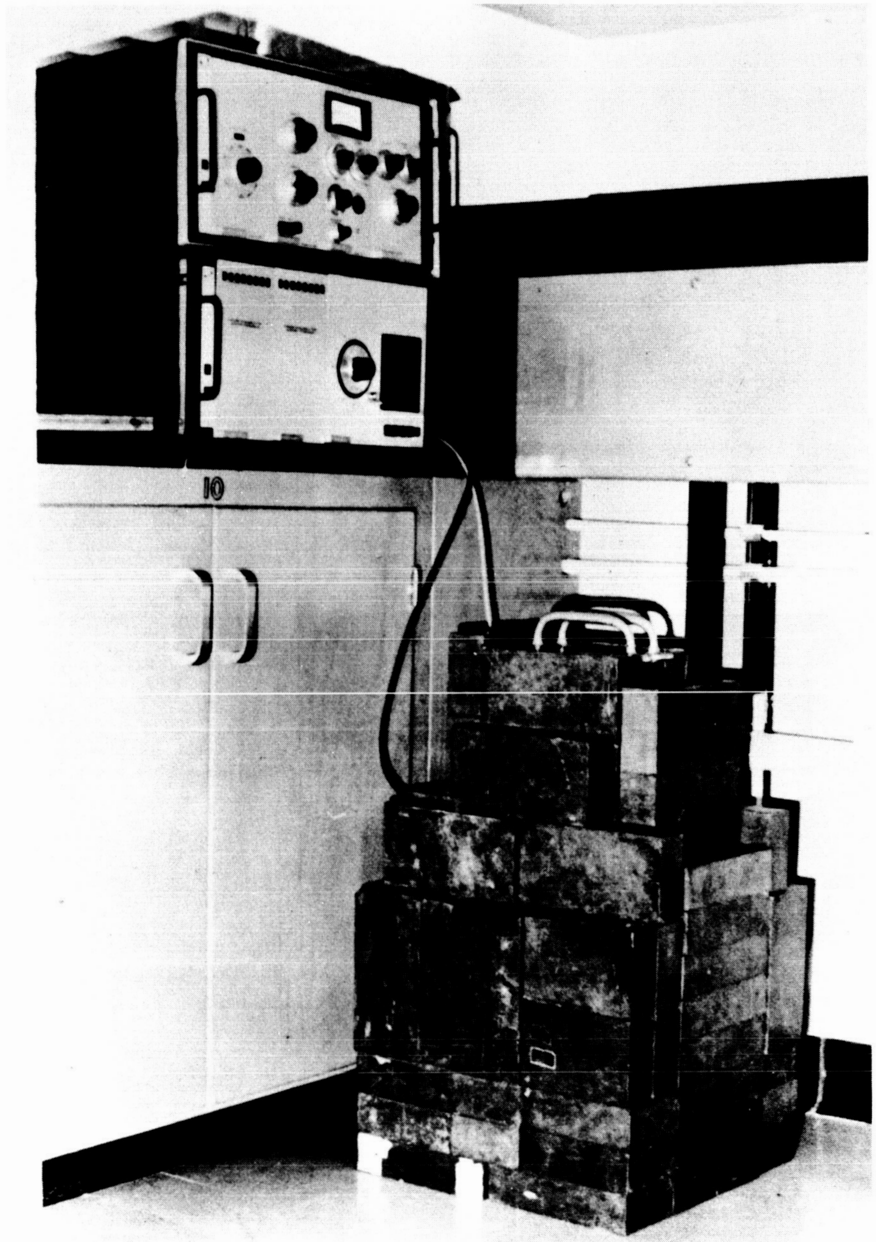

Figure 4. Gamma Scintillation Spectrometer Showing Shielded Well Crystal.

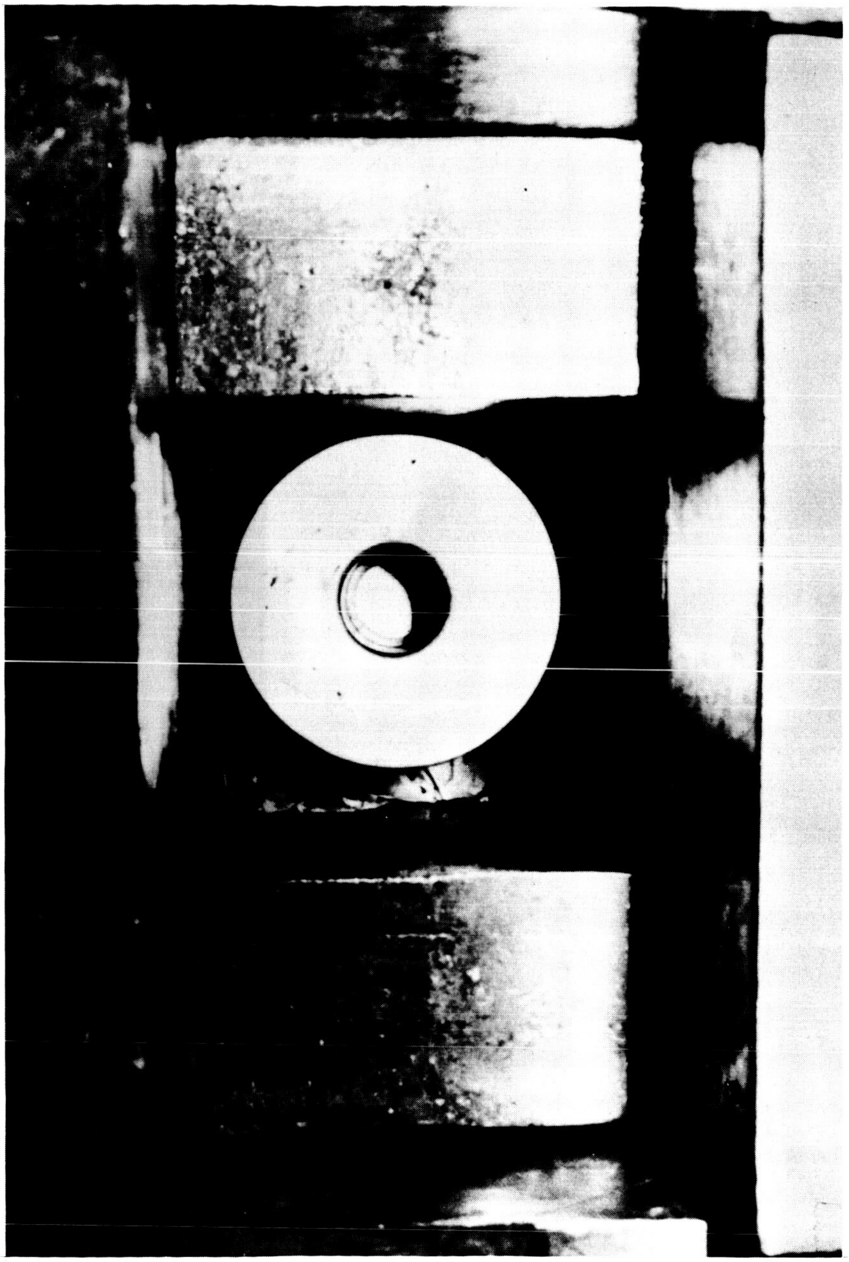

Figure 5. Top View of Well Crystal Showing Foil Positioning Ring.

well crystal.

After the data was taken it was plotted as a function of A_{cd} (equation 1) and a least squares fit was performed on the resulting data. The results of the determination of F_{cd} are shown in figure 6-12 where F_{cd} is plotted as a function of foil thickness for various distances from the source. It can be seen from these curves that substantial agreement has been obtained between theory and experiment except near the source where the two deviate by approximately 4%. It can also be seen from figures 6-12 that F_{cd} is essentially independent of foil thickness in the region near the source but that it varies slightly with foil thickness as the distance between the source and detector increases. F_{cd} for a given foil thickness decreases in value as the distance from the source increases.

These results will be of considerable assistance for experimentors making neutron flux measurements in arisotropic media such as nuclear reactor cores. The results of this research are being submitted for publication in <u>Nuclear Science and Engineering</u>.

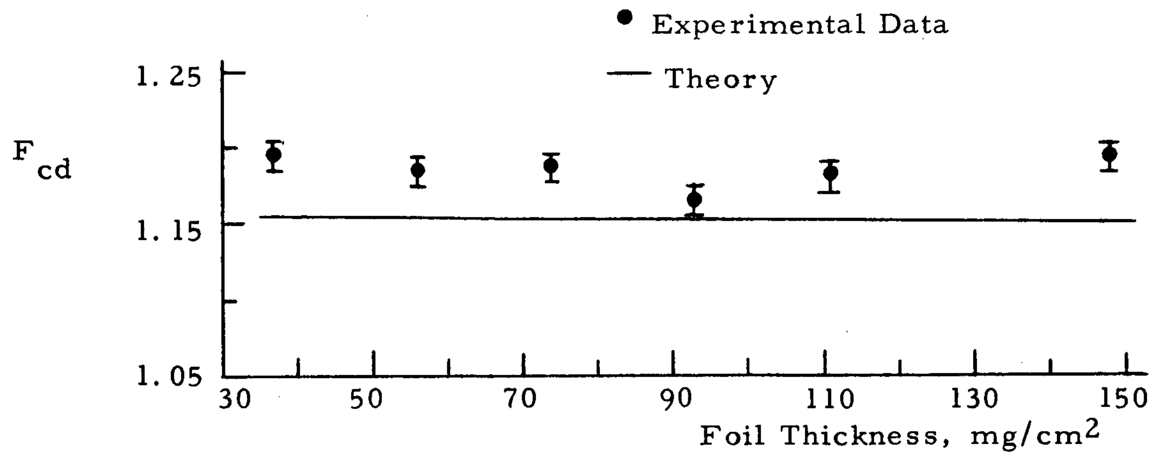

Fig. 6 Comparison of Experimental Values of F_{cd} with Theoretical Values for x = 0.25 in.

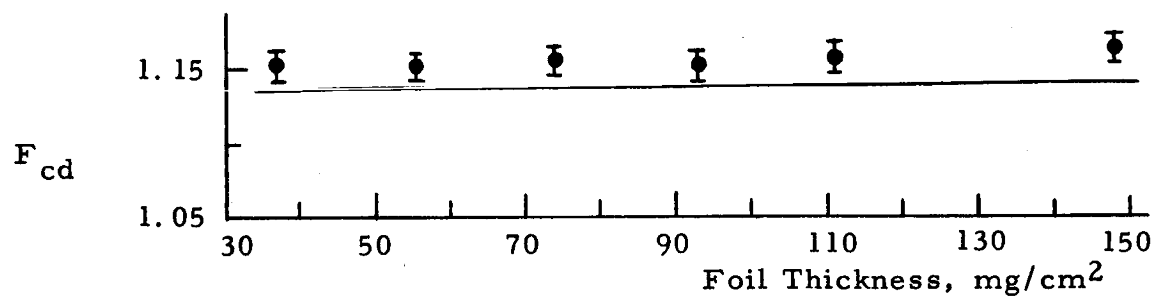

Fig. 7 Comparison of Experimental Values of F_{cd} with Theoretical Values for x = 0.75 in.

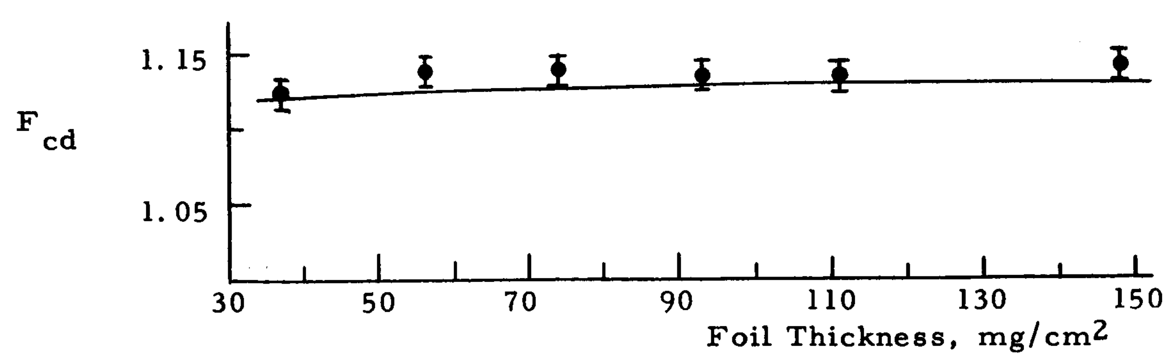

Fig. 8 Comparison of Experimental Values of F_{cd} with Theoretical Values for x = 1.25 in.

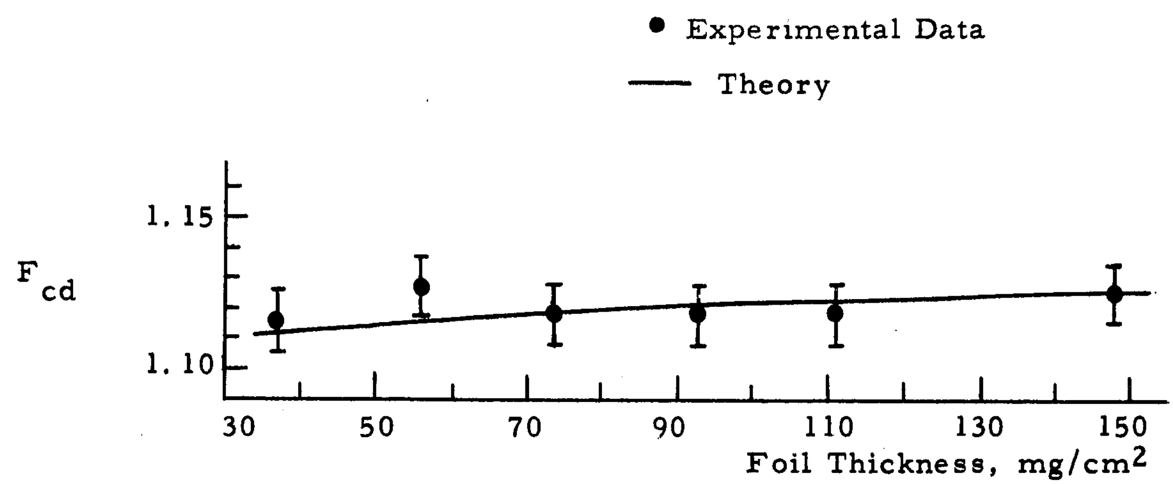

Fig. 9 Comparison of Experimental Values of F_{cd} with Theoretical Values for x = 1.75 in.

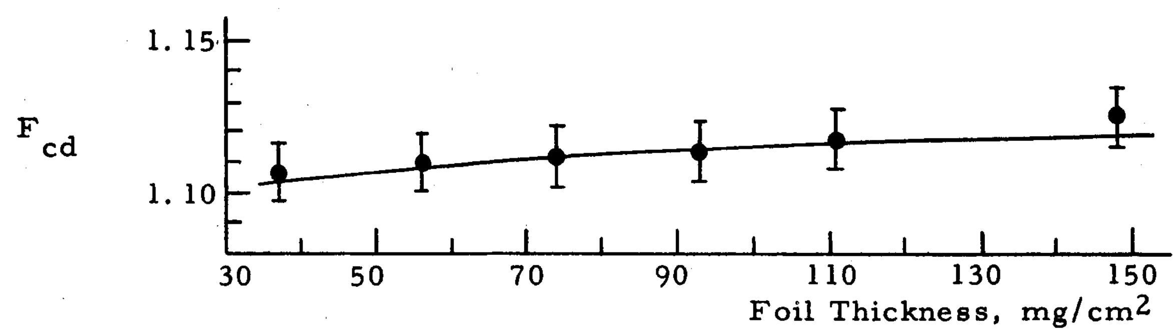

Fig. 10 Comparison of Experimental Values of F_{cd} with Theoretical Values for x = 2.25 in.

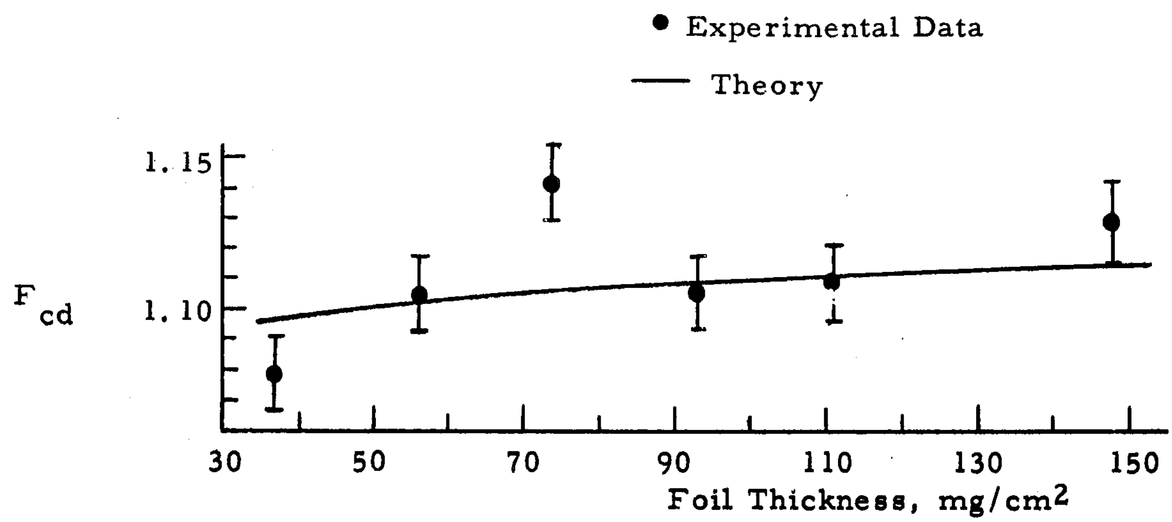

Fig. 11 Comparison of Experimental Values of F_{cd} with Theoretical Values for x = 2.75 in.

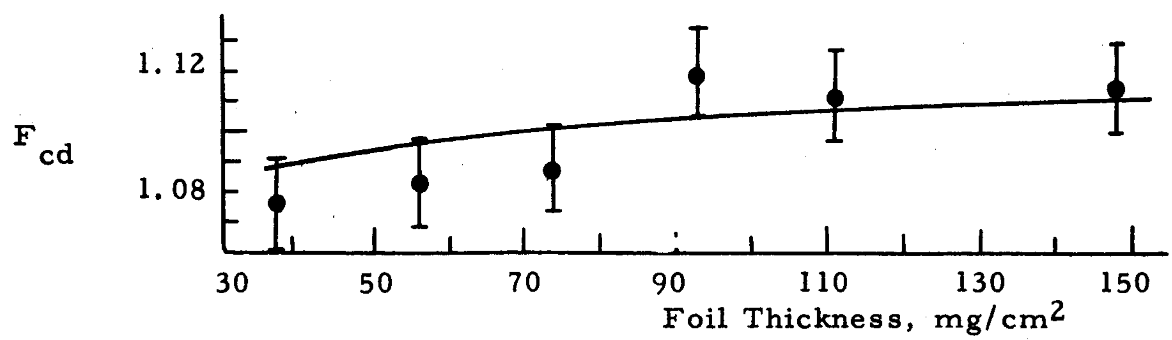

Fig. 12 Comparison of Experimental Values of F_{cd} with Theoretical Values for x = 3.25 in.

SPACE TECHNOLOGY PROJECT NO. 14

GAS DYNAMIC STUDIES IN

AN ARC-DRIVEN SHOCK TUBE

N65-33665

GAS DYNAMIC STUDIES IN

AN ARC-DRIVEN SHOCK TUBE

Project Investigators

Richard E. Thomas, Associate Professor of Aerospace Engineering

George Lee Huebner, Jr., Associate Professor of Oceanography and Meteorology and Senior Research Scientist

I. Summary

The design of the Texas A&M University (TAMU) arc-driven shock tube is presently 60 per cent complete. The performance estimates based on the selected configuration are finalized and the hardware design has been specified. Acquisition of components is expected to begin the first of August, 1965, and the operation of the system is expected in December, 1965.

II. Discussion

The configuration of the TAMU arc-driven shock tube was selected to provide an aerodynamic test facility with maximum operating range and flexibility consistent with budgetary limitations. The system is intended for the study of fundamental gas kinetics and vehicle aerodynamic problems encounted in high speed flight, especially at high altitudes.

The facility will have the wave system shown schematically in Figure 1 and is to be powered by a 20,000 volt, 200,000 joule capacitor bank which will discharge into a driver unit, filled

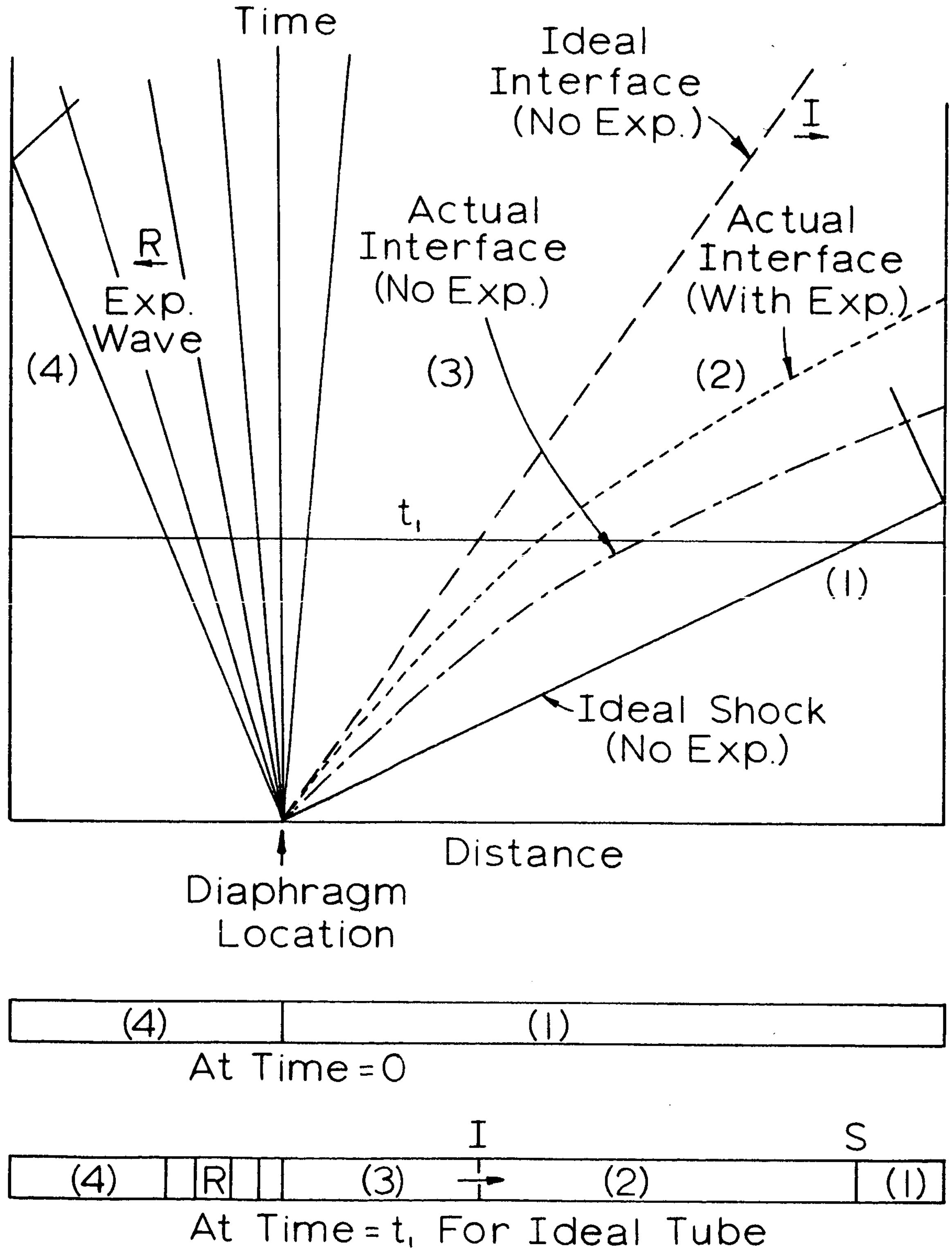

Figure 1. The wave system and flow pattern in a shock tube.

with helium and having a diameter of 6.35 cm (2.5 inches) and a maximum length of 61 cm. (24 inches). The driver is to be fitted with inserts which can decrease the length to 25.4 cm (10 inches) increasing the energy density to provide higher shock Mach numbers.

To minimize the effects of boundary layer and contact surface turbulence which is heavily dependent on the diaphragm opening process, the driven gas will expand in the TAMU facility into a 30.5 cm (nominal 12 inches) diameter driven tube, 12.2m (40 feet) long. The general layout of the facility is shown in Figure 2.

The vacuum system will consist of a 16 inch diffusion pump and a mechanical roughing pump of 61 liters per second (140 ft^3 per minute) capacity. Based on the pumping capacity of the system and the mechanization of the diaphragm holding system (lead screw operated Gray-loc flange) it is estimated that the facility could be operated every 30 minutes if desired. Most generally longer times are required to assure proper control of gas conditions in the driven tube.

Using the physical characteristics described above the performance of the facility has been estimated, a summary of which is presented in Figure 2. These estimates were based on the theory of the ideal shock tube (1) as modified by the experience of others (2), (3), (4) who have constructed similar devices.

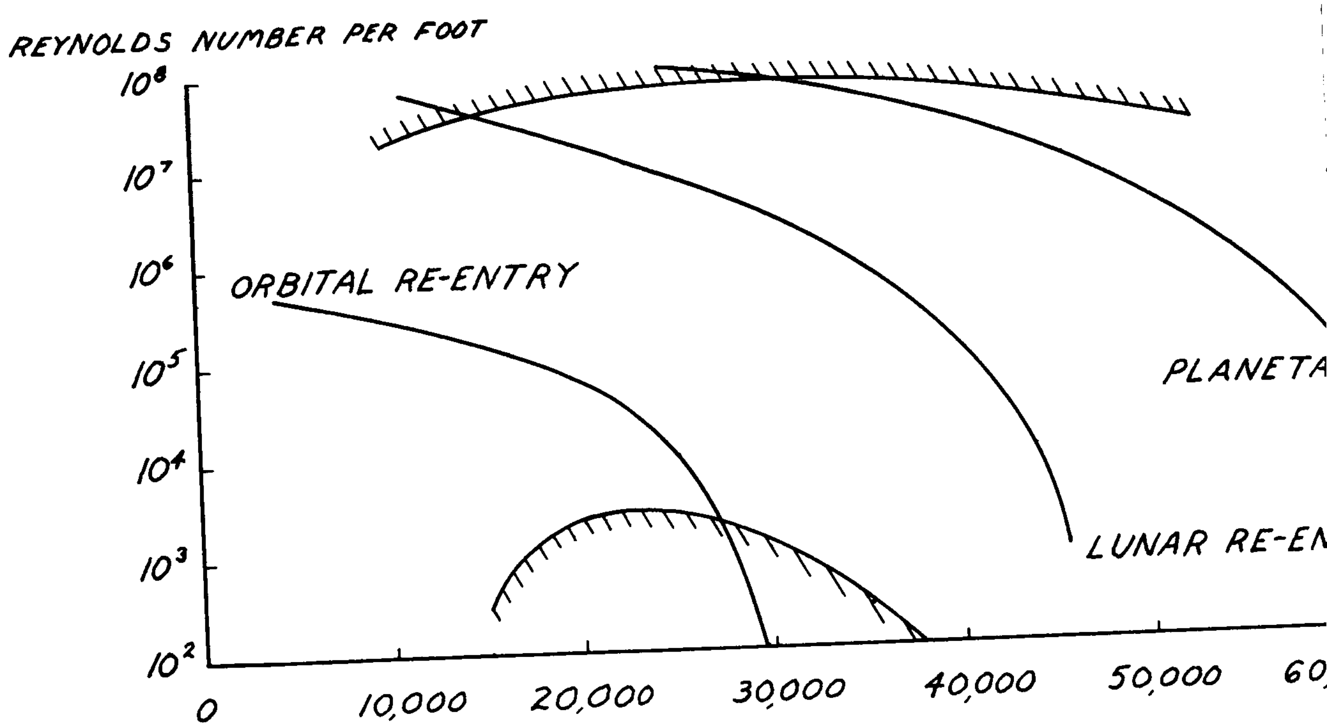
REYNOLDS NUMBER PER FOOT
10^8
10^7
10^6
10^5
10^4
10^3
10^2
ORBITAL RE-ENTRY
PLANETA
LUNAR RE-EN
0
10,000
20,000
30,000
40,000
50,000
60

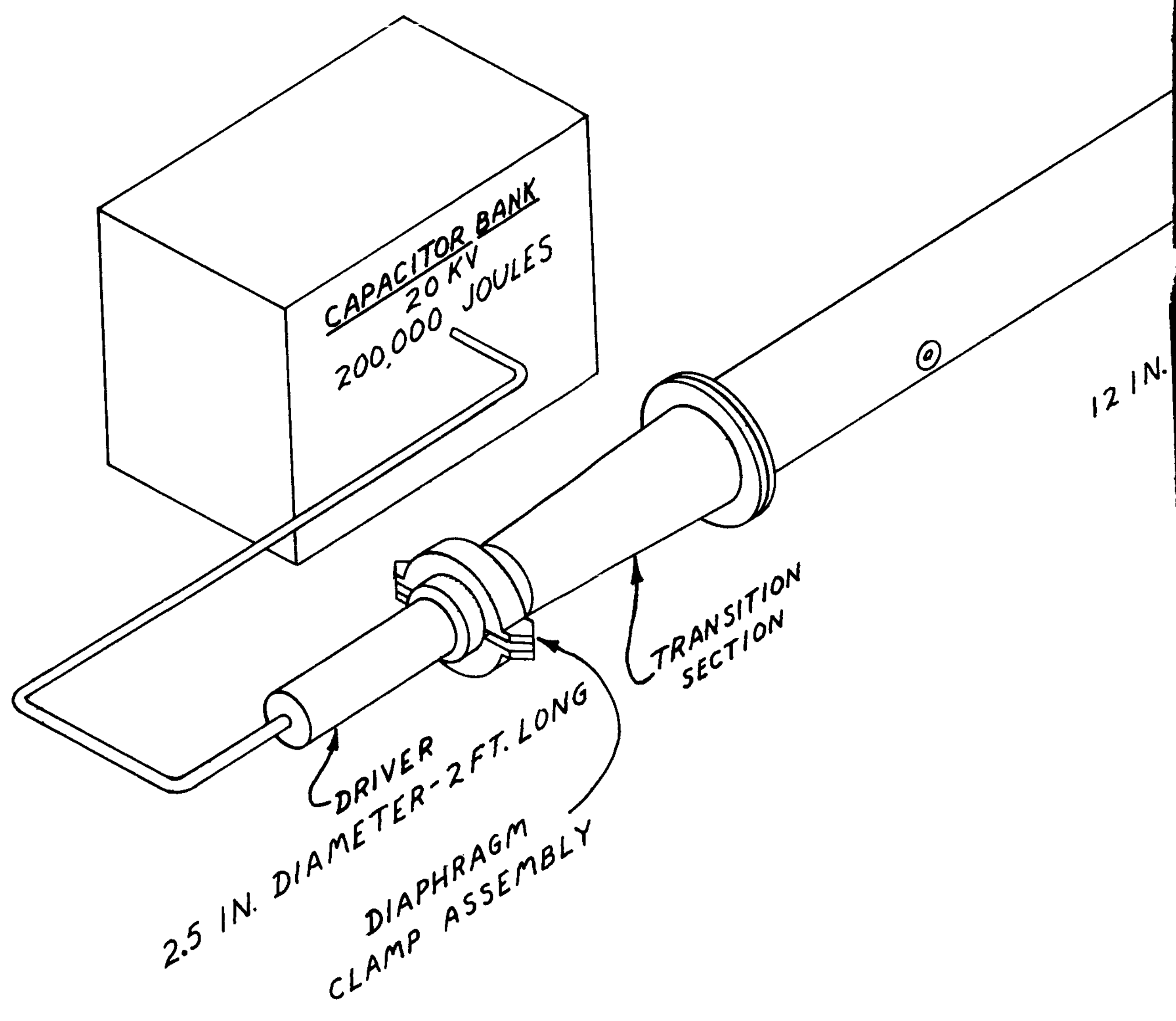
CAPACITOR BANK
20 KV
200,000 JOULES
12 IN.
TRANSITION
SECTION
DRIVER
2.5 IN. DIAMETER-2 FT. LONG
DIAPHRAGM
CLAMP ASSEMBLY

RY RE-ENTRY
TRY
VELOCITY, FPS
000

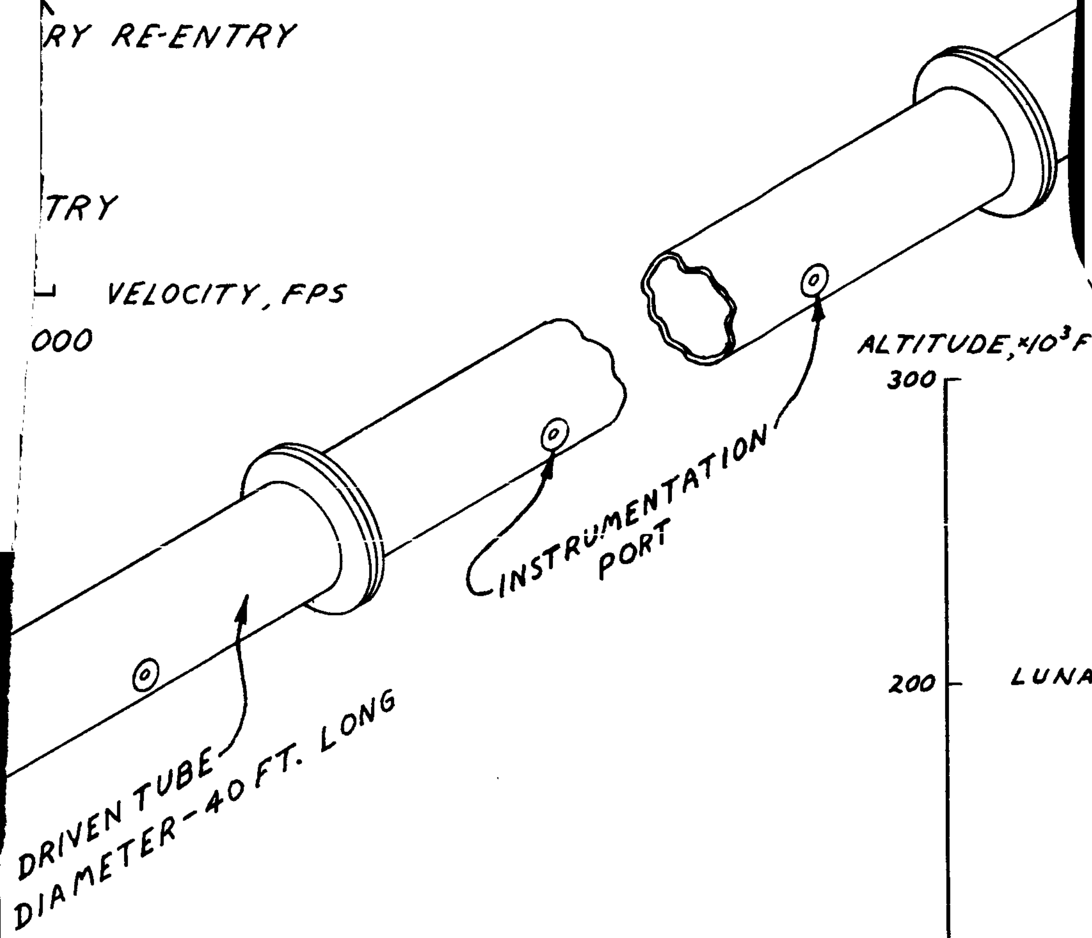

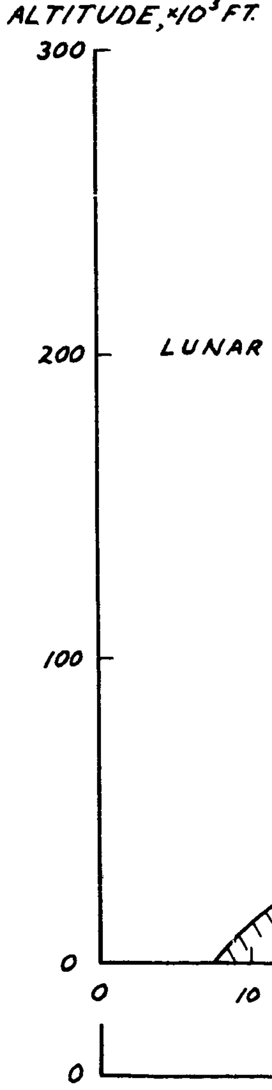

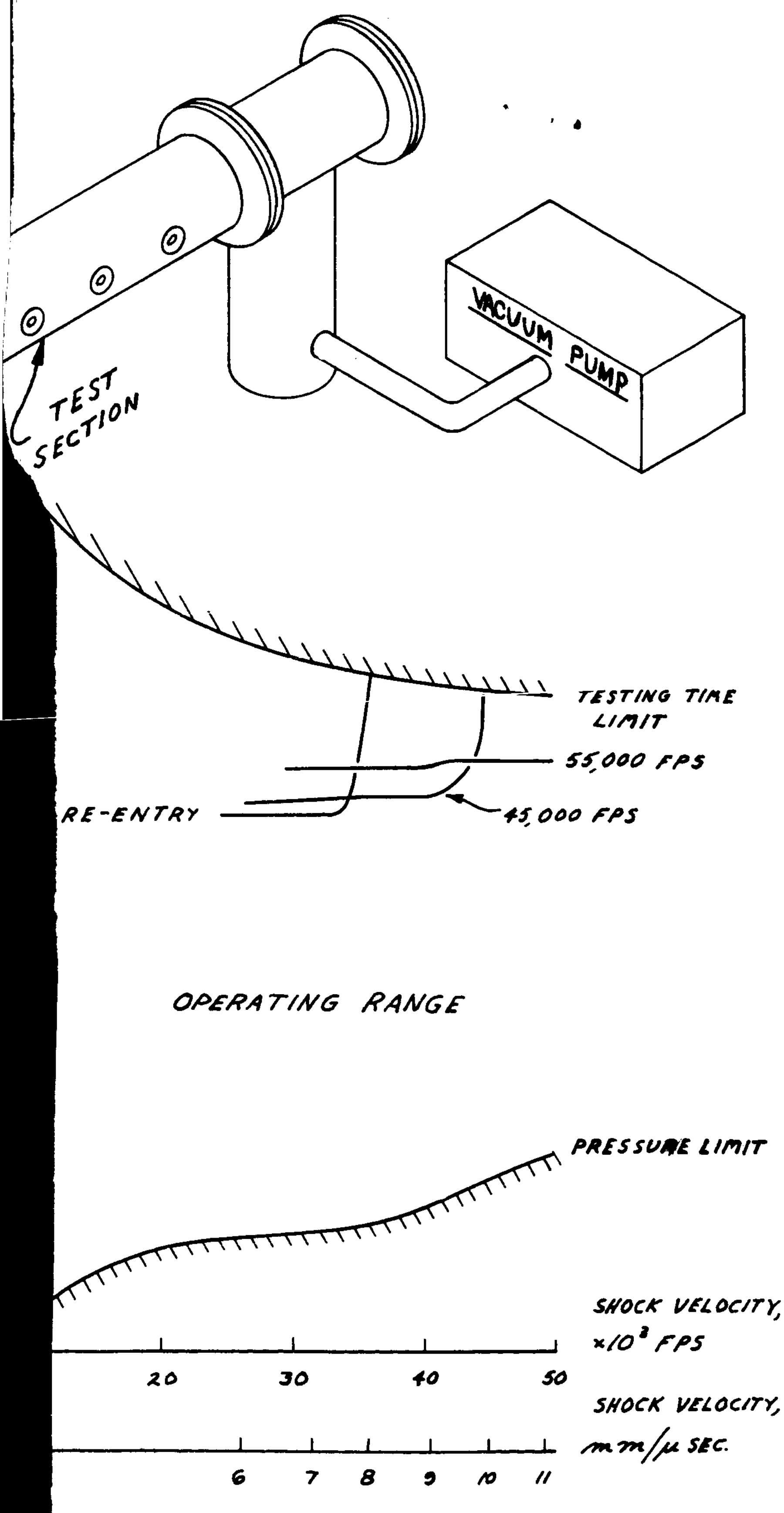

TEXAS A&M UNIVERSITY
ARC-DRIVEN SHOCK TUBE

Thus, the estimates include the efficiencies typical for this kind of system. Testing time estimates were based on Mirels theory.[5] It can be seen that the facility will be capable of producing a wide range of test conditions, including duplication of the conditions in the entry corridors of superorbital vehicles.

At the present time the design of the driver and diaphragm system is essentially complete, as is the design of the supporting structure for the facility. The entire design i.e. drawings of all components, should be completed by 1 August 1965 and hardware should begin to appear at about the same time. Assembly of the system should be completed and shakedown tests started in December of 1965.

A building at the Texas A&M Research Annex has been allocated to house the facility until such time as space is available in the Space Research Center.

First tests will be arranged to evaluate uniformity and repeatability of the flow and the operational ranges of the facility. The first model tests will include heat transfer measurements for comparison with results from other facilities.

The instrumentation system and the proposed initial research studies in the facility are being carefully considered so as to maximize the probability of research support outside of the current grant. The utilization of such devices as lasers and electron beams is being examined along with the more standard instrumentation techniques. It is considered likely that the first study will involve the examination of thermodynamic and chemical non-equilibrium zones downstream of shock waves.

References

1. Nagamatsu, H. T., Shock Tube Technology and Design, Report No. 58-RL-2107, General Electric Co., Schenectady, New York, November, 1958.

2. Camm, John C., and Rose, Peter H., Electric Shock Tube For High Velocity Simulation, Research Report No. 136, Avco-Everett Research Laboratory, Everett, Mass., July 1962.

3. Warren, W. R., Rogers, D. A., Harris, C. J., The Development of An Electrically Heated Shock Driven Test Facility, Report R625D37, Space Sciences Laboratory, General Electric Co., Philadelphis, Pa., April, 1962.

4. Lee, John D., and Nerem, Robert M., Theory and Performance of a Shock Tube Having An Arc-Heated Driver, RF Project 1021-18, The Ohio State University Research Foundation, Columbus, Ohio, June, 1962.

5. Mirels, Harold, "Test Time in Low-Pressure Shock Tubes" The Physics of Fluids, V. 6, No. 9, September 1963.

SPACE TECHNOLOGY PROJECT NO. 15

RESEARCH IN ELECTRICAL ENGINEERING

RESEARCH IN ELECTRICAL ENGINEERING

Project Investigators:

Dr. M. G. Rekoff, Jr., Department of Electrical Engineering

Mr. Donald F. Sellers, Graduate Assistant

Very limited support has been provided for research on a Vibrating Momentum Exchange Device. This device is described below.

The Vibrating Momentum Exchange Device is a device used to develop a torque through the mechanism of a changing momentum for the purpose of positioning artificial satellites in space. Since in space there is nothing to push against, attitude correction of the vehicle is generally accomplished by some form of momentum exchange. The inertia wheel and the twin gyro are well known examples of such devices.

The VMED as currently being developed in the Department of Electrical Engineering enjoys some advantages over the two aforementioned devices. Most importantly, there are no sliding surfaces in the device. This fact infers that the device can be operated in a hard vacuum without a special container. This further implies that the supporting structure for the device can be the vehicle frame itself.

The VMED consists of a mechanical tuned circuit with velocity and position pick offs which are used to excite the electromagnetic forcers that drive the unit. A rough sketch of the device and its allied electronics is shown in figure 1.

The tuned mechanical circuit is a slender rod having a relatively large mass on the end opposite the point of attachment of the rod to the vehicle frame. In figure 1, the x-axis of this device forms a tuning fork oscillator where the frequency of oscillation is determined by the spring and mass of the mechanical circuit. This arrangement is necessary because slight changes in temperature caused significant changes in the circuit resonant frequency. Mechanical resonant circuits have very high Q and a difference of 1% between driving frequency and resonant frequency causes the mechanical circuit to drop completely out of resonance. With this scheme the driving frequency and the resonant frequency are always the same.

The output axis of the VMED is the Z-axis where a torque will be obtained if the center of the mass moves in a spiral, resulting in a rate of change (increasing) in angular momentum in the Z-axis. Rotation in one direction will give a torque out of the mass and rotation in the opposite direction yields a torque into the mass. A decrease in angular acceleration will yield forces in the opposite directions.

The role of the Y-axis forcer is to provide displacements

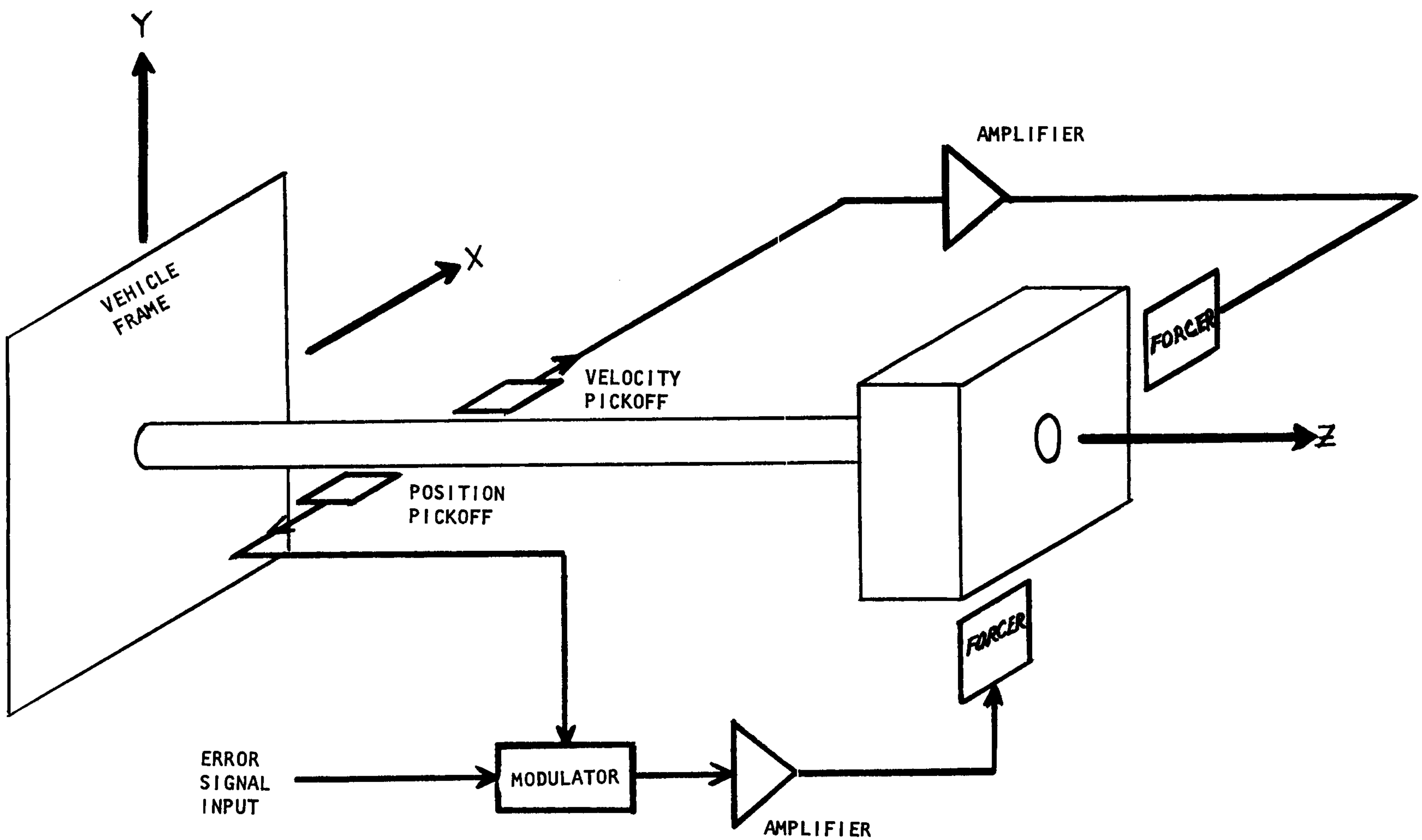
Y
X
VEHICLE FRAME
AMPLIFIER
VELOCITY PICKOFF
FORCER
Z
POSITION PICKOFF
FORCER
ERROR SIGNAL INPUT
MODULATOR
AMPLIFIER

FIGURE 1

of the mass in the Y direction which dependent on an error signal coming from a sensor determining the attitude of the vehicle. Since a spiral motion is required there must be a difference in the phase of the signals driving the X and Y axis. Using a velocity pick off for one axis and a position pick off for the other insures a perfect 90^{o} displacement in phase of there two signals. Thus the strength of the Y axis forcer is determined by the error signal and the time that the force is applied is determined by the VMED itself. Having the two forces displaced 90^{o} in space and 90^{o} in time causes the mass to move in a circular motion, much in the same fashion as the flux rotates in a polyphase a-c machine.

The final design details are being worked out and testing is currently under way.

This apparatus is being tested on an airbearing table obtained on loan LTV Military Electronics Division of Ling-Temco-Vought Inc. An optical pick off is on loan from Ames Research Center, National Aeronautics and Space Administration which is used to measure minute angular deflections of the air bearing table.

Figure 2 is a photograph of the apparatus showing the table, VMED, vernier balancing equipment, and optical pick off.

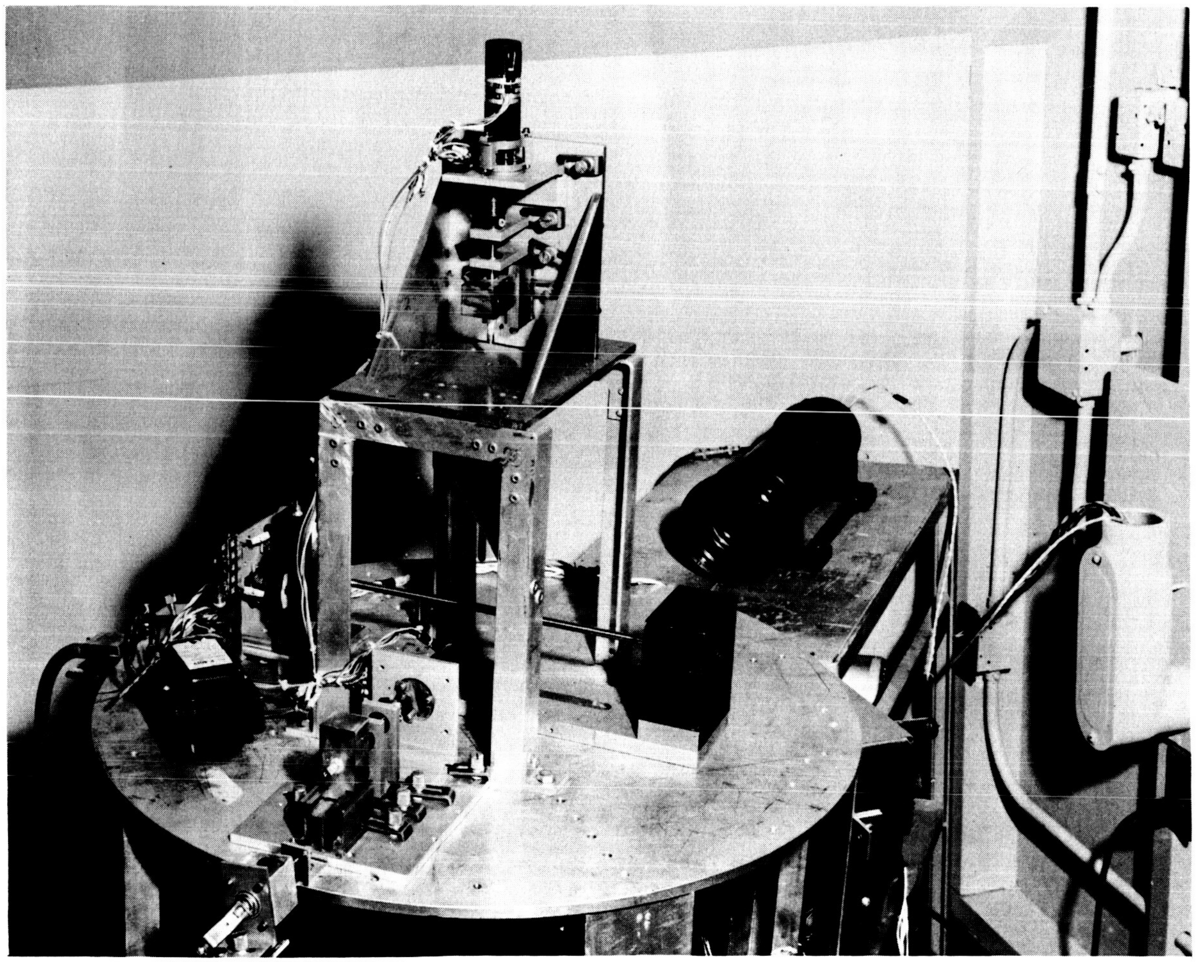

FIGURE 2